ISOLATION AND ANALYSIS OF COMPOUNDS WITH ANTI-TRYPANOSOMAL AND ANTI-CANCER ACTIVITY

by

Anuradha Liyana Pathiranage

A Dissertation Submitted in Partial Fulfillment of the Requirements for the Degree of Doctor of Philosophy in Molecular Bioscience

Middle Tennessee State University

August 2016

Dissertation committee:

Dr. Norma K Dunlap, Chair

Dr. Scott Handy

Dr. Keying Ding

Dr. Elliot Altman

Dr. Mary Farone

ACKNOWLEDGEMENTS

First and foremost, I want to thank my advisor Dr. Norma Dunlap for the continuous support of my studies, for her patience, motivation, and immense knowledge. This dissertation could not have been completed without the great support that I have received from her. She is not only the best research advisor but also the best supporter during my studies at MTSU even during tough times in the Ph.D. pursuit. Her mentorship was paramount in providing a well-rounded experience consistent my long term career goals. Thank you so much for everything you've done and everything you continue to do.

I would like to thanks my thesis committee: Dr. Scott Handy, Dr. Keying Ding, Dr. Elliot Altman and Dr. Mary Farone for their insightful comments and encouragement. I like to take this moment to thank all faculty and staff members at MTSU chemistry department. I would like to thank my friend, Dr. Leah Martin for supporting me spiritually throughout my time at MTSU.

Lastly, I would like to thank my family for all their love and encouragement. I am extremely grateful to my father Ariyasena Liyanapathirana and my mother Ariyawathi Gunathilaka who raised me and taught me to study hard and to give priority in my life to the quest for knowledge. Most of all I would like to thank my husband Vajira Manatunga and my daughter Tharushi for always being there for me and encouraging me to pursue this degree.

ABSTRACT

Project 1

Synthesis and evaluation of ether-linked demethylepipodophyllotoxin dimers.

A series of novel ether-linked dimers of demethylepipodophyllotoxin are topoisomerase II poisons that exhibit higher levels of double-stranded versus single-stranded DNA cleavage than their corresponding monomers. The dimers also have higher levels of tumor cell cytotoxicity than the monomers, lending support to the two-drug model for interaction of demethylepipodophyllotoxins with human topoisomerase IIα.

Project 2

Antitrypanosomal activity of iridals from *Iris domestica.*

The petroleum ether extract of *Iris domestica (Belamcanda chinensis)* has been evaluated for activity against *Trypanosoma brucei*. Bioassay-guided fractionation led to the isolation of four known iridals as the active components. Chemical modification of these isolates afforded novel stable derivatives that maintained bioactivity. This is the first known report of the antitrypanosomal activity of these compounds.

TABLE OF CONTENTS **PAGE**

LIST OF TABLES

TABLE **PAGE**

LIST OF FIGURES

FIGURE **PAGE**

FIGURE **PAGE**

CHAPTER 1

INTRODUCTION TO MEDICINAL PLANTS AS A DRUG SOURCE

Plants synthesize an extensive array of secondary metabolites, or natural products, and many of them have significant pharmacological properties. Over the centuries, cultures around the world have learned how to use plants against illness. Historically, numerous useful drugs have been developed from compounds isolated from medicinal plants. Today, many of the most useful and curative drugs are derived from natural product sources and plant-based drugs continue to play an essential role in health care. According to the World Health Organization (WHO), more than 80% of the world's population relies on traditional medicine for their primary healthcare needs. Currently, herbal medicines are gaining renewed attention from modern pharmaceutical institutes, as scientists become aware that herbal medicine is still an important resource for drug development.

In herbal medicine, medications are prepared from entire plants, roots, barks, leaves, flowers, seeds, and aerial parts from a particular herb or many plant species. These medications contain more than hundreds of compounds but only one or a few will be medicinally important.

These medicinally important compounds have been isolated from a procedure called bioassay guided fractionation (Figure 1). In bioassay-guided fractionation, a crude extract is prepared from plant material partitioned into solvents, usually methanol or ethanol.

The crude extract is chromatographically fractionated and re-fractionated many times with different solvents. Fractions are obtained in a sequential process using different solvents, such as hexane, chloroform, ethyl acetate, butanol and water. Each time, all the fractions produced are evaluated in a bioassay system. Only active fractions are further fractionated and evaluated in a bioassay system until the active compounds are isolated.

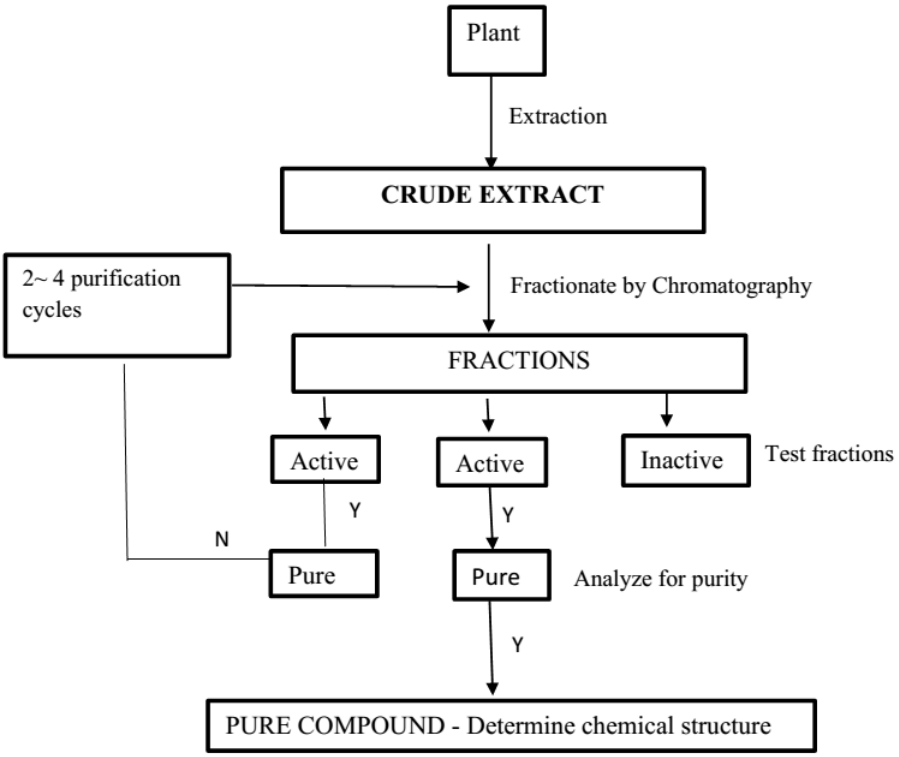

Figure 1. Bioassay guided fractionation of plant extracts.[1]

Currently many diseases are treated by drugs isolated from botanical natural products. For example, artemisinin was isolated from the plant *Artemisia annua*, and its derivatives possess activity against *Plasmodium falciparum* which causes malaria. Digoxin, extracted from *Digitalis lanata*, is used to treat various heart diseases. Morphine is a pain medication extracted from *Papaver somniferum*. Chinese herbal extracts from the Ginkgo leaf, containing mainly ginkgo lactone A, ginkgo lactone B and ginkgo lactone C, are used for preventing or treating deafness and tinnitus. Many important and existing cancer compounds have been isolated from natural plant extracts, including etoposide, derived from podophyllotoxin isolated from *Podophyllum peltatum Linnaeus*. Other examples include: camptothecin isolated from *Camptotheca acuminate*, taxol, extracted from the Yew tree and vincristine and vinblastine extracted from *Catharanthus roseus,* also known as Vinca.

Overview of cancer drugs

Cancer is a disease that kills about 8.2 million people annually throughout the world, accounting for more than 2-3% of the annual deaths recorded globally. [2] All the cells in the human body have the same DNA, which contain 23 pairs of chromosomes. During each cell division the chromosomes are copied, but sometimes mutations occur in the DNA. Most of these mutations result in apoptosis, or cell death, but if the mutant cell survives, it will pass its mutated DNA to the next generation through cell division. When these mutant DNA cells accumulate, they can affect the cell's behavior resulting in a series of molecular changes that alter the normal properties of a cell, leading to cancer. Normal cell division is precisely controlled but

cancerous cells divide repeatedly without control, and they crowd out other normal cells and function abnormally. When cancer cells grow they change the normal cell characteristics, such as changes in cell structure, immortality, decreased cell adhesion, production of new enzymes, ability to divide infinitely, and random migration. These cellular changes cause the cancer cells to divide and grow faster and spread, impair the correct function of major organs. These abnormal masses of cells are called tumors. Tumors can be malignant (cancerous) or benign (non- cancerous). Benign tumors do not spread but they grow; whereas malignant tumors spread and invade other tissues in a process known as metastasis.

Cancers can be classified according to the tissue from which they arise. Carcinomas are cancers that occur in epithelial tissues, including breast, lung and skin. Sarcomas are cancers that begin in the connective tissues such as bone, cartilage, fat, and muscle. Leukemias are cancers of the bone marrow and blood cells.

Even though many treatments are available for cancer therapy, cancer is still the second leading cause of death globally. There are many types of cancer treatments and the types of treatment depend on the specific cancer.[2] Types of cancer treatment include chemotherapy, or drugs use to kill cancer cells, and surgery, which removes tumors from the body. Radiation is also used to kill cancer cells, and immunotherapy helps the immune system to fight cancer. More recently researchers around the world have developed more advanced cancer drugs with deeper insights into the mechanisms of anticancer activity and better understanding of the molecular mechanisms involving the initiation of tumor growth and metastasis.

The first use of cancer chemotherapy began in 1940, with the use of nitrogen mustards and folic acid metabolites. Since then cancer drug development has exploded into a billion-dollar industry. According to the National Cancer Institute (NCI), more than 200 cancer drugs are available for cancer chemotherapy, with many different mechanisms of actions.[3]

Chemotherapy drugs can be divided into several groups based on mechanism and chemical structure. Major types of chemotherapy drugs include those that affect DNA, mitosis inhibitors and the newer synthetic kinase inhibitors (Figure 2).

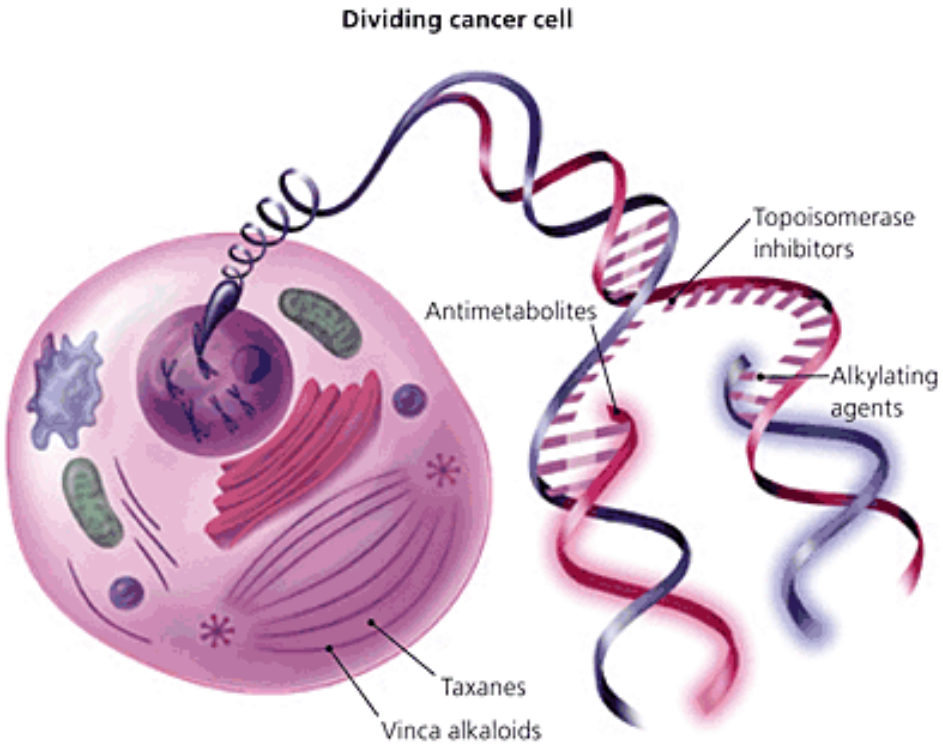

Figure 2. Mechanism of traditional chemotherapy. Printed with permission from Renee Cannon. [4]

As seen in Figure 2, drugs that affect DNA include antimetabolites, topoisomerase inhibitors and alkylating agents; drugs affecting mitosis include taxanes and vinca alkaloids. These drugs stop or slow the growth of cancer cells as well as stop or slow the growth of healthy cells that grow and divide rapidly, such as cells that line intestines and hair follicles, leading to common side effects of bone marrow suppression, nausea and hair loss.

Drugs affecting DNA

Drug molecules can interact with DNA in different ways. They can either directly bind to the DNA double helix or control transcription factors. Alkylating agents and intercalators directly bind to the DNA double helix. Alkylating agents are synthetic drugs that involve reactions with DNA. As seen in Figure 3, these drugs add methyl or other alkyl groups onto DNA bases. This in turn inhibits the correct base pairing of DNA and causes miscoding and degradation of DNA.

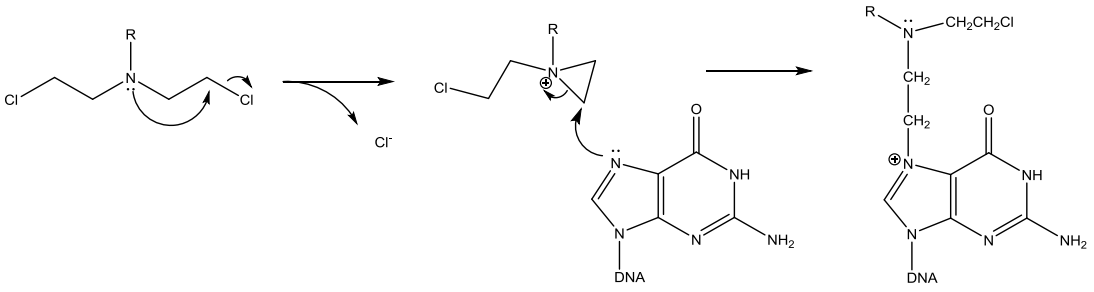

Figure 3. Mechanism of alkylation of DNA guanine. A bis (chloroethyl) amine forms an aziridinium ion that reacts with a base of guanine in DNA. [5]

Examples of alkylating agents are nitrogen mustards such as mechlorethamine and chlorambucil (Figure 4). Intercalators such as daunomycin, isolated from a natural source, *Streptomyces verticillius*, insert between the base pairs of DNA, resulting in distortion of the α- helix.

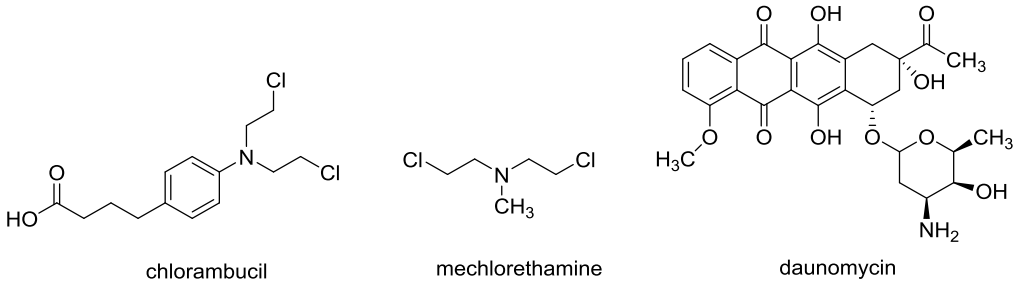

Figure 4. DNA alkylating agents and intercalators.

Antimetabolites were among the first effective chemotherapeutic agents discovered and include folic acid analogs. Antimetabolites closely resemble and substitute for this natural enzyme substrate. Folic acid is converted into tetrahydrofolic acid by the enzyme dihydrofolate reductase and tetrahydrofolic acid is a cofactor in the synthesis of nucleic acids. Methotrexate is a N-methyl analogue of folic acid so it serves as a fraudulent substrate and inhibits the conversion of tetrahydrofolate resulting in impaired synthesis of nucleic acids (Figure 5).

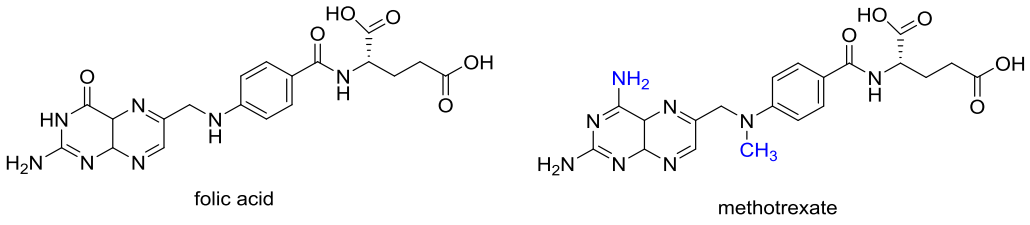

Figure 5. Antimetabolite methotrexate, N-methyl analogue of folic acid.

Topoisomerase inhibitors interfere with enzymes called topoisomerases that regulate supercoiling of DNA and maintain the proper topological state of DNA. They do this by forming a nick in the DNA, allowing one strand to pass through and then re-sealing the nick. Topoisomerase inhibitors are classified by which type of enzyme they inhibit.[6] Camptothecin is a topoisomerase I inhibitor, isolated from the tree *Camptotheca acuminate* (Happy tree), a tree native to China and used as a cancer treatment in Traditional Chinese Medicine.[7] Camptothecin itself is too insoluble to be used as a drug but several water soluble analogs, topotecan and irinotecan are used in chemotherapy. DNA topoisomerase II inhibitors include etoposide and teniposide, semisynthetic derivatives of podophyllotoxin (Figure 6).[8]

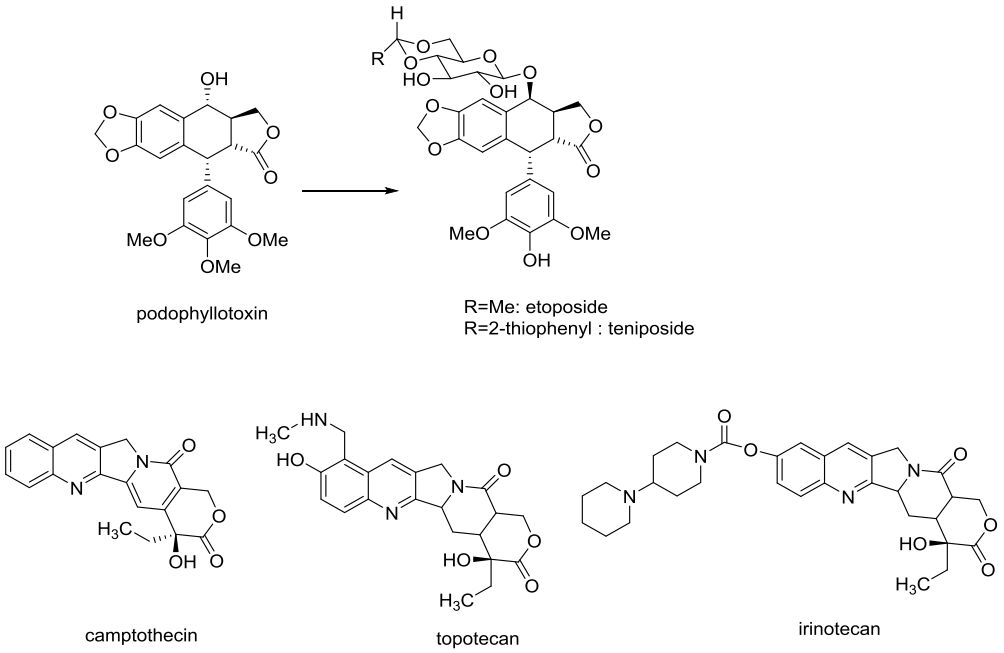

Figure 6. Examples of DNA topoisomerase I and II inhibitors.

Drugs affecting mitosis

Microtubules are the major cytoskeletal components in all eukaryotic cells. They are dynamic structures, composed of 13 filaments, important for maintenance of cell shape and forming spindles in cell division. As seen in Figure 7, new tubulin subunits are added to the plus end of the microtubule, whereas degradation occurs on the minus end.

Vinca alkaloids, vincristine and vinblastine, bind to the plus end of tubulin, thereby preventing them from being incorporated in growing microtubules. Taxanes, interact with the minus end of tubulin and prevent disassembly. As a result, the balance between assembly and disassembly of the microtubule is destroyed (Figure 7).

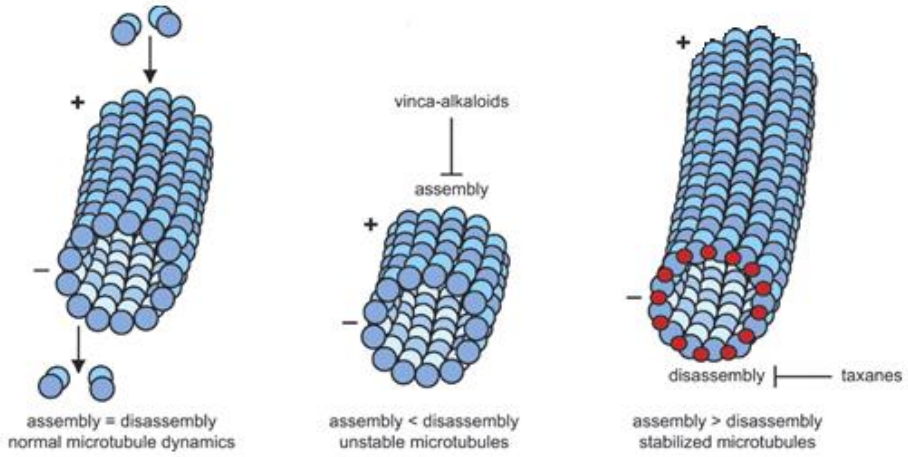

Figure 7. Mechanisms of vinca alkaloids and taxanes on microtubules.[9] Printed with permission from Cold Spring Harbor Lab Press.

Botanical based anticancer drugs

Many active components have been discovered from medicinal plants with anticancer activity. Many of these discoveries were the result of screening programs by the National Cancer Institute (NCI) from 1940-1980. Examples that have led to clinically useful drugs include camptotecin, taxol, vincristine, and podophylotoxin. As already mentioned these target both microtubules and topoisomerase.

The Madagascar periwinkle, *Catharanthus roseus,* a member of the Apocynaceae family, is important because of its diverse medicinal properties. It is a rich source of the indole alkaloids, vincristine and vinblastine (Figure 8).

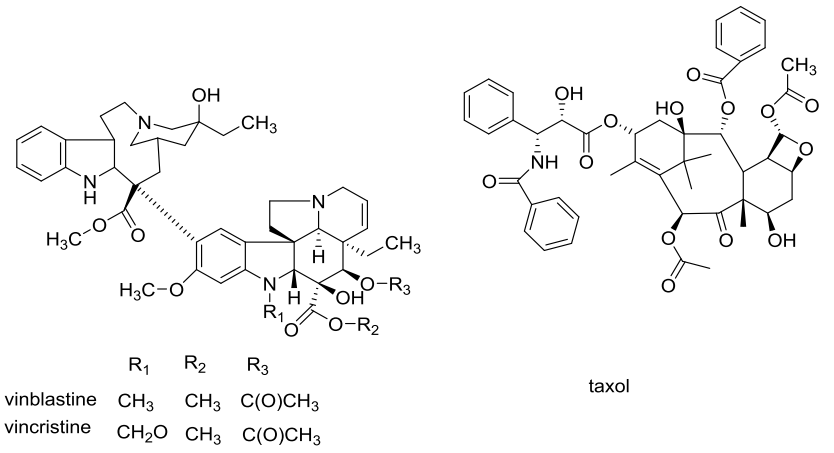

Figure 8. Structures of vincristine, vinblastine and taxol.

Low "dimeric" alkaloid contents in the plant have led to alternative production methods involving cell cultures, semi-synthesis or total chemical synthesis. Total synthesis has proved difficult due to structural complexity of the molecules and

complicated reaction steps involving stereochemistry. The amide vindesine was synthesized from vinblastine by reaction with refluxing ammonia (Figure 9), that can be used for the treatment of adenocarcinoma, lymphosarcoma and osteogen sarcoma.[10]

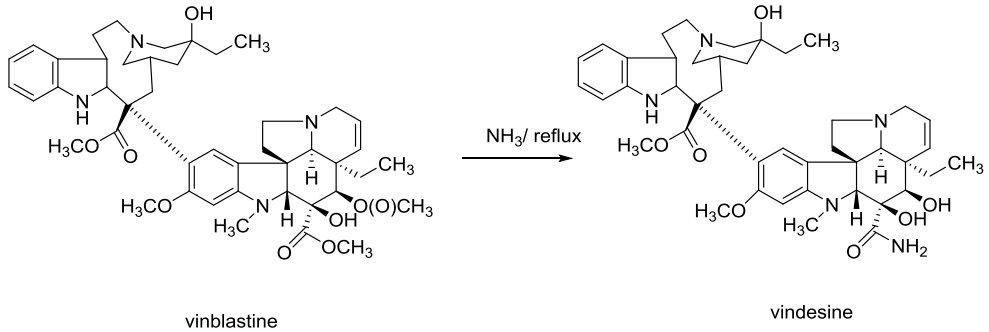

Figure 9. Synthesis of vindesine from vinblastine.[10]

One plant collected as part of the NCI program was the Pacific yew, *Taxus brevifolia.* In 1967, Monroe E. Wall and Mansukh C. Wani isolated taxol from the bark of *Taxus brevifolia* (Figure 8). [11]

Podophyllotoxin is another toxic microtubule inhibitor, isolated from *Podophyllum peltatum linnaeus,* commonly known as the Mayapple plant. It is also produced by the *Podophyllum emodi* and *Podophyllum pleianthum*, the Indian and Taiwanese species, respectively.[12]

Modifying the structure of a drug may change the nature of its molecular target. Epimerization at C-4 (4S configuration) of podophyllotoxin to give epipodophyllotoxin, and substitution at that position with various nucleophiles has led to compounds with useful antitumor activity which act as topoisomerase poisons, including etoposide and teniposide.[13]

Medicinal plants as a source of drugs to treat protozoan infections

While the anticancer activity of plants used in traditional medicine has been investigated for years, more recently other diseases have been studied. Traditional remedies for plants include treating fever, diarrhea and stomach ailments. These are symptoms of infectious organisms, including protozoan parasites. Protozoan parasitic diseases such as malaria, the trypanosomiases and leishmniases are caused by blood and tissue protozoa. These diseases are lethal and there are few modern medical treatments.

The treatment of parasitic protozoa in humans is challenging due to some reasons. The first reason is the complexity of the organisms' life cycles. During the life cycle, a protozoa generally passes through several stages that differ in structure and activity. Some protozoa have complex life cycles requiring two different host species or only a single host to complete the life cycle. The second reason is drug resistance; the rapid multiplication rate of many parasites increases the chances for mutation and makes them drug resistant.

An alternative to modern synthetic drugs is the search for plant extracts with anti-parasitic activity. A good starting point to find the anti-parasitic activity of plant extracts would be traditional medicinal plants, such as those known from Asia, Africa or America, that have been employed to treat infections. Malaria has been known in human history beginning with the oldest recordings in China approximately 5000 years ago.[14] Human malaria is caused by unicellular protozoa of the genus *Plasmodium*, which are transmitted by various mosquito vectors. The first effective treatment for malaria came from the bark of cinchona tree, which contains quinine.

For almost three centuries, quinine was the only active principal effective against *Plamodium falciparum.* After the Second World War, quinine was replaced by the development of synthetic antimalarial drugs belonging to the classes of 4- and 8-aminoquinolines, such as chloroquine and primaquine (Figure 10).

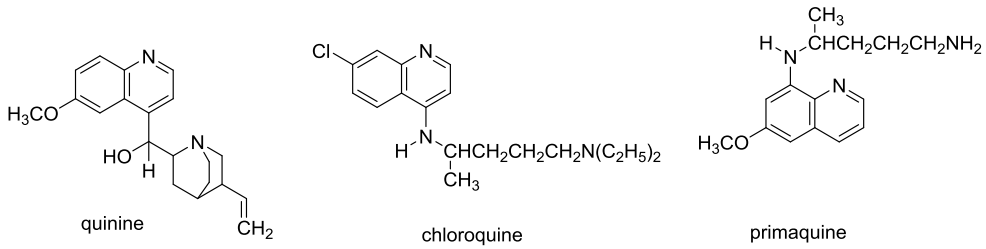

Figure 10. Structures of quinine, chloroquine and primaquine.

Over the years *P. falciparum* has become resistant to many of the synthetic drugs. A breakthrough for the development of antimalarial drugs was the identification of the artemisinin from *Artemisia annua* (Asteraceae), which can even kill multidrug resistant strains of *P. falciparum.* The discovery of the anti-malarial drug artemisinin began in 1967 in China as a response to outbreaks of quinine-resistant malaria in the North Vietnamese during the Vietnam War. A research project (project 523) was initiated by the Institute of Chinese Materia Medica (ICMM), China Academy of Traditional Chinese Medicine, joined the "Group of TCM" of Project 523.[15] They collected and screened more than 100 compound recipes from traditional Chinese medicine. Bioassay-guided screening of alcoholic extract of *Artemisia* was discovered with inhibitory activity against

P. falciparum, however the results were not reproducible in later experiments. But later Youyou Tu, who was inspired by the detailed methods of *Artemisia* usage described in ancient Ge Hong's book "*Zhou Hou Bei Ji Fang*". The book reads: "for the treatment of malaria, a handful of *Artemisia* soaked in two liter of water. Take the pressed juice." This led to the idea that the heating in the traditional extraction procedure was destroying the active component. Removal of the acidic portion of the extract led to the neutral extract, which was non-toxic and showed 100% inhibition against *P. falciparum*. Pure crystals were obtained and the structure was confirmed by X-ray crystallography in 1979 and is known as artemisinin (Figure 12).[16] The discovery of artemisinin certainly played a critical role in opening new therapeutic means and saving millions of lives from malaria disease. Several semisynthetic derivatives of artemisinin, some with greater antimalarial potency, artemether, artesunate and have been developed later (Figure 11). [16]

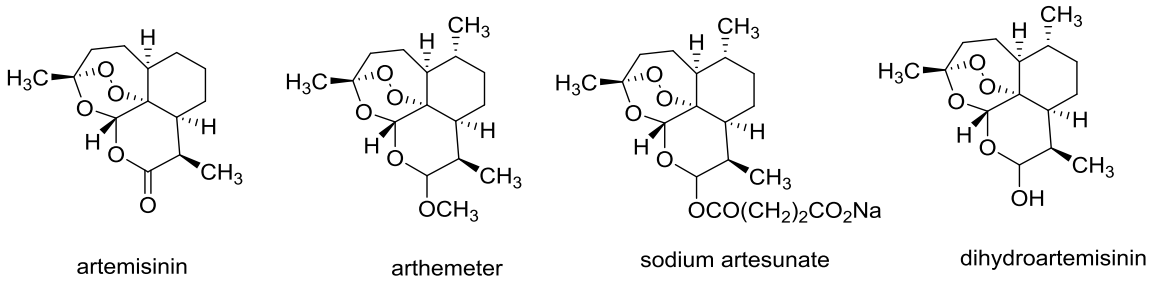

Figure 11. Structures of the artemisinin type compounds.

Several other protozoan diseases, including Chagas disease (American trypanosomiasis), human African trypanosomiasis (HAT or sleeping sickness), and the

Leishmaniases (a set of trypanosomal diseases) are caused by parasitic protozoa known as trypanosoma, which are transmitted to human and animal hosts by insect vectors.

Trypanosoma

Trypanosoma brucei, Trypanosoma cruzi and Leishmania are Kinetoplastids. Kinetoplastids are flagellated protozoans, which are unicellular eukaryotic organisms. All kinetoplastids contain a mitochondrial DNA structure, which is called kinetoplast DNA, or kDNA, organized in a unique giant network of interlocked rings.[17]

There are four main cellular forms of trypanosomatids, including the trypomastigote, amastigote, promastigote and epimastigote. They can be distinguished from each other by cell shape, flagellum presence, and position of the basal body, kinetoplast, and nucleus. In general, the epimastigote and promastigote are found in insects, and the trypomastigote and amastigote are found in the mammalian hosts.

Human African trypanosomiasis (HAT)

Human African trypanosomiasis (HAT) or sleeping sickness is a disease caused by infection with *Trypanosoma brucei gambiense* and *Trypanosoma brucei rodesiense. Trypanosoma brucei brucei* is another species that affects cattle and causes a disease called Nagana. It is often used in screening assays because this parasite does not infect humans and thus is of no health risk for the researcher. HAT causes severe and progressively fatal central nervous system impairment. The disease is endemic to the African continent. *T. brucei* are spread by the Tsetse fly. During a blood meal on the

mammalian host, an infected tsetse fly injects trypomastigotes into skin tissue (Figure 12-A).[18] Then parasites enter the lymphatic system and pass into the bloodstream, are carried to other sites throughout the body, reach other body fluids (e.g., lymph, spinal fluid) and transform into bloodstream trypomastigotes. When taking a blood meal on an infected mammalian host, bloodstream trypomastigotes are ingested by the tsetse fly. In the fly's midgut, the parasites transform and then leave the midgut, and transform into epimastigotes. The epimastigotes reach the fly's salivary glands and continue the life cycle. In the first stage of human disease or haemo- lymphatic stage, the parasites multiply in blood and lymph in human body, which causes fever, headaches and joint pains. In the second stage or neurological stage, the parasites cross the blood brain barrier and infect the central nervous system, which causes signs and symptoms of the disease such as confusion, poor coordination and disturbance of the sleep cycle.[18]

Chagas' disease

The related organism, *Trypanosoma cruzi,* causes Chagas' disease, transmitted by the kissing bug (triatomines), and is endemic in South America and has been found in the southern United States. Most infected persons remain asymptomatic for the remainder of their lives. However, approximately 30% of infected persons will progress to the chronic form of Chagas disease after 10-30 years, when cardiac and gastrointestinal damage usually results in death. *Brucei* is an extracellular parasite, *cruzi* and Leishmania are intracellular parasites. In Chagas' disease an infected insect takes a blood meal and releases metacyclic trypomastigotes in its feces near the site of the bite wound (Figure 12-B).[18] Trypomastigotes enter the host blood through the wound or through intact

mucosal membranes. Trypomastigotes spread through the blood, infecting tissue, especially tissues of the heart and the alimentary tract. In tissues they develop into intracellular amastigotes that proliferate and finally differentiate to trypomastigotes. When taking a blood meal on an infected mammalian host, bloodstream trypomastigotes are ingested into the kissing bug. In the insect's gut, the parasites transform into proliferative epimastigotes, and then leave the gut, and transform into trypomastigotes and continoue the life cycle.

Leishmaniasis is caused by protozoan parasites of the genus Leishmania, which are spread by the bite of the sandfly. The infection causes ulcerative skin lesions, permanent disfigurement, and serious disability. The sandflies inject the promastigotes into human blood. In the blood, promastigotes are phagocytosed and settle inside a phagolysosome, where they differentiate into amastigotes. Amastigotes proliferate, extending the infection, and the ones present in skin macrophages can be taken up by sandflies.[18]

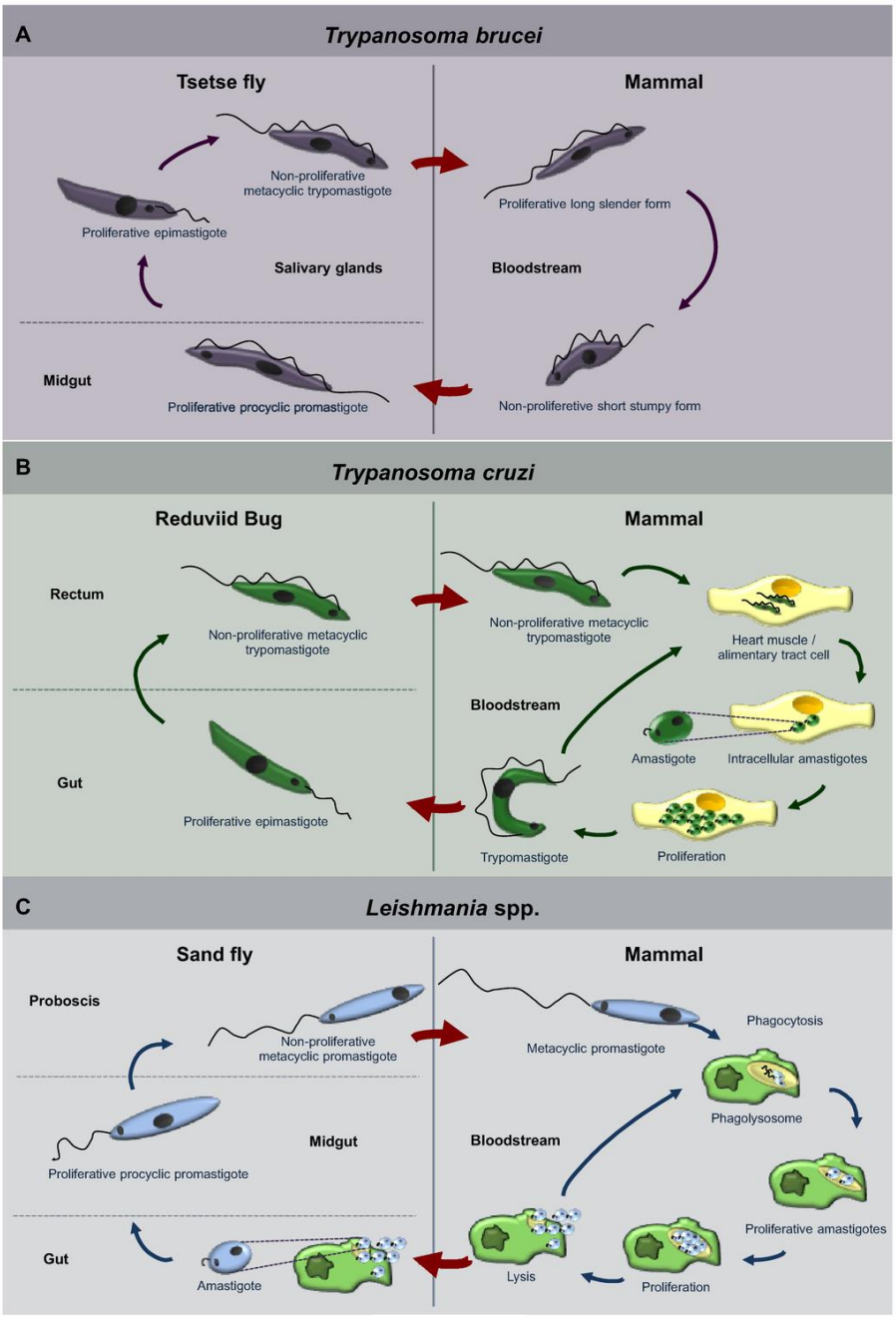

Figure 12. Diagrams of the life cycles of the three trypanosomatid parasites: *Trypanosoma brucei* (A), *Trypanosoma cruzi* (B), *Leishmania* spp. (C). [18]

Current drugs to treat HAT are based on synthetic drugs developed more than 80 years ago, such as pentamidine and suramin. These require parenteral administration and are only effective against the early haemo-lymphatic stage of the disease (Figure 13). Treatments for the second stage of HAT are more challenging to develop due to the need to cross the blood-brain barrier to be effective. The only drug currently available for the treatment of the late stage CNS infection is the trivalent arsenical melarsoprol, which requires parenteral administration and has unacceptable side effects that are similar to arsenic poisoning. Benznidazole is used to treat the initial (acute) stage of Chagas disease. Although the drug may provide some symptomatic relief or slow progression in the chronic stage, there is no known cure for Chagas' disease in the chronic stage. Although nifurtimox is still used as a mainline treatment for Chagas disease, benznidazole is the preferred treatment due to the serious side effects and contraindications of nifurtimox.[19] Leishmaniasis patients are treated with the synthetic drugs stibogluconate, meglumine and pentamidine (developed 70 years ago), which have severe side effects.[20]

Although all drugs in use are synthetic and many are toxic, recent attention has turned to plant extracts. A number of medicinal plants have been screened for anti-trypanosomal and leishmaniasis activity. Some natural products are very active in the sub-micromolar range and show good selectivity. Among these, only few have been studied in animal models, but unfortunately none of these results have proceeded into clinical practice. [21]

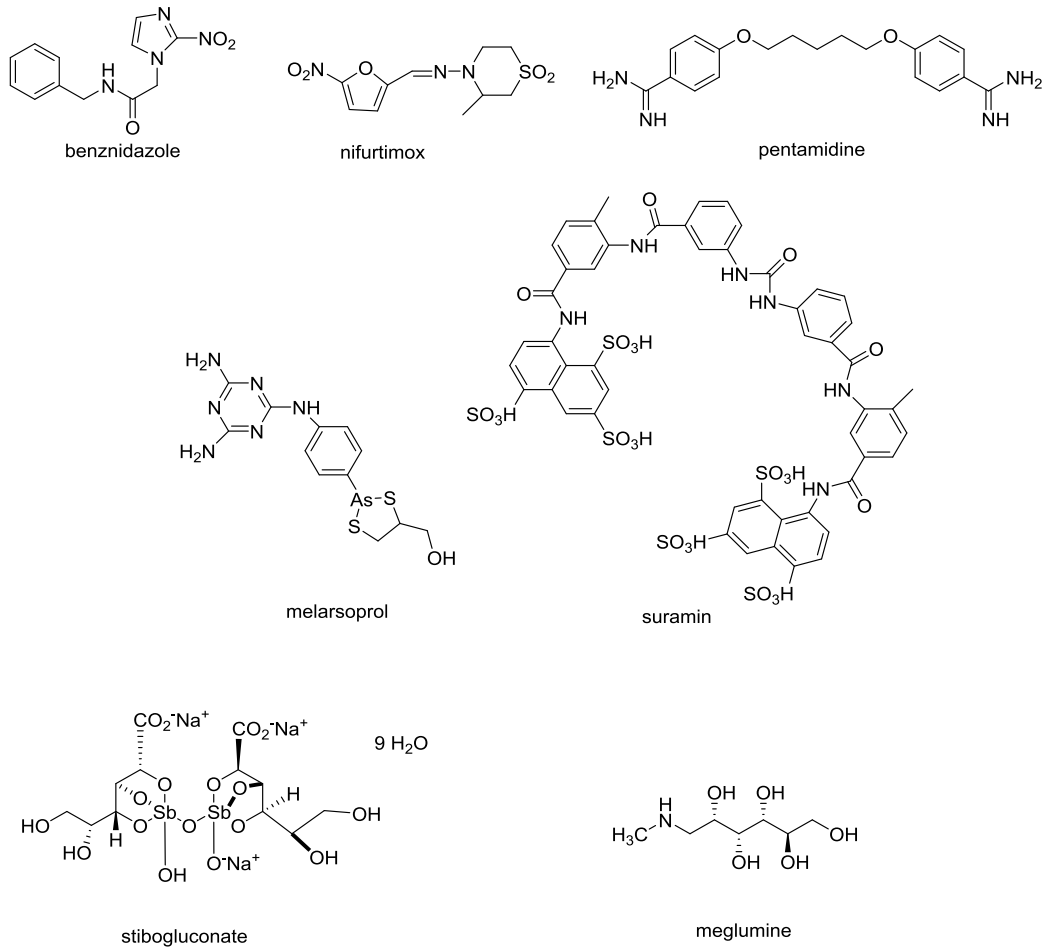

Figure 13. Chemical structures of agents currently used to treat African sleeping sickness, Chagas's disease and leishmaniasis.

Several alkaloids have been tested on *T. brucei in vitro*. For an example emetine, an isoquinoline alkaloid from *Cephaelis ipecacuanha, O*-methylmoschatoline, isolated from *Unonopsis buchtienii* (Annonaceae) was very active against *T. brucei.* Several phenolic derivatives, such as cissampeloflavone isolated from *Cissampelos pareira* (Menispermaceae), also showed good activity against *T. brucei.* It has been reported that

quinones, such as plumbagin, which can be found in *Drosera* species, are active on *T. b. brucei*. Several terpenes have also been tested, such as terpinen-4-ol, which exhibited a high trypanocidal activity with *T. brucei*. (Figure 14).[22]

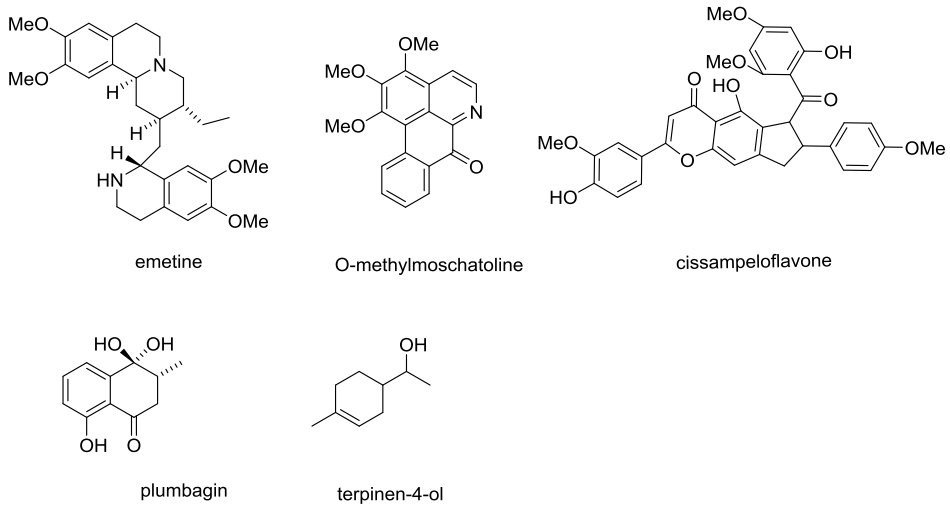

Figure 14. Natural products derived from plants with activity against *Trypanosoma brucei*.

Plant metabolites active against *T. cruzi* were extensively reviewed almost a decade ago. The potent antioxidative flavanol, gallocatechin 3, 3′-digallate and demethylpraecansone A were active against *T. cruzi* (Figure 15). Helenalin exhibited an IC_{50} value of 0.695 μM against *T. cruzi*.[22] Vinblastine and sanguinarine have substantial anti-trypanosomal activities with inhibitory IC_{50} values in the micromolar range. Many of the secondary metabolites which have been tested against *T. brucei* also affect *T. cruzi*.

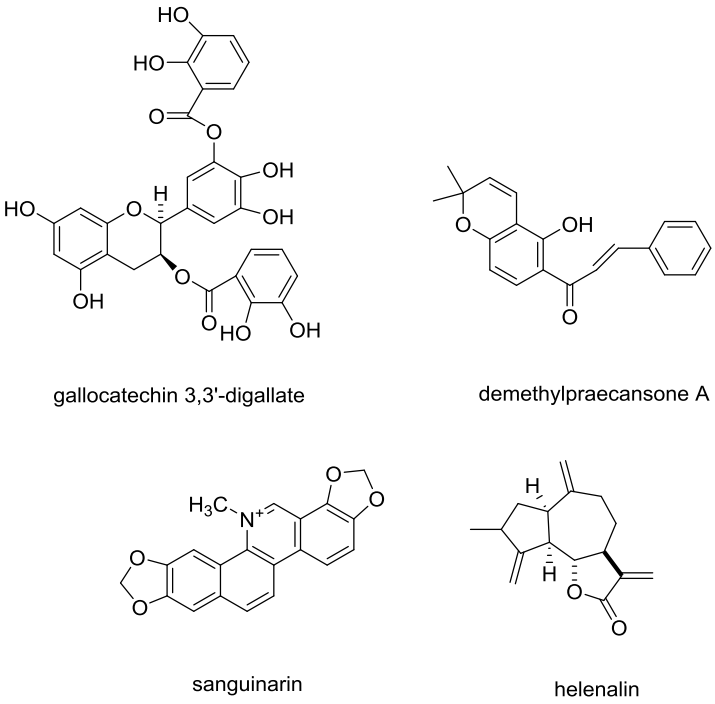

Figure 15. Natural products derived from plants against *Trypanosoma cruzi*.

Several medicinal plants have been screened for leishmaniasis activity. For example, harmine, isolated from *Peganum harmala*, displays anti- leishmanial activity (Figure 16).[23] The amide alkaloid piperine extracted from *Piper nigrum*, commonly used in traditional medicine, has been reported as having potent anti-leishmanial activity. Another glycoside with remarkable activity against *Leishmania* parasites has been isolated from the indigenous plant *Swertia chirata*. The compound amarogentin, is a secoiridoid glycoside with the capacity to inhibit DNA-topoisomerase I, an essential enzyme related to leishmania viability.[23]

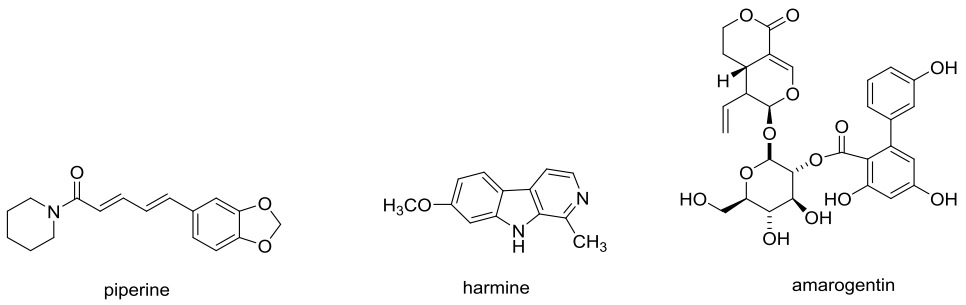

Figure 16. Natural products derived from plants with activity against leishmania.

With the recent attention to botanical extracts as potential antitrypanosomal agents, new drugs may be available in the future.

The focus of the research described here is on both anti-tumor and anti-trypanosomal agents derived from plant sources.

CHAPTER 2

SYNTHESIS AND EVALUATION OF ETHER-LINKED DEMETHYLEPIPODOPHYLLOTOXIN DIMERS

Introduction

Podophyllotoxin is a toxic microtubule inhibitor, isolated from *Podophyllum peltatum linnaeus*, commonly known as the Mayapple plant (Figure 17).[24-26] The anticancer property of podophyllotoxin was identified in 1946, but the clinical application of podophyllotoxin as an anticancer agent has been limited because of its high toxicity. Extracts of plants with podophyllotoxin were widely used in the Chinese, Japanese and the Eastern world folk medicine (even today in China, as Bajiaolian) as remedies for gout, tuberculosis, gonorrhoea, syphilis, menstrual disorders, dropsy, cough, psoriasis, venereal warts, and certain tumors.[27] This remarkable biological activity makes podophyllotoxin an important compound for the development of new therapeutic agents by extensive structural modifications.

Figure 17. *Podophyllum peltatum Linnaeus.* [28]

Podophyllotoxin in its natural state (4R configuration), is a microtubule inhibitor. Podophyllotoxin not only disturbs the cytoskeleton of eukaryotic cells, but also targets tubulin polymerization during metaphase by arresting the formation of spindles, thereby preventing cell division.[29,30] The stereochemistry at C-4 determines the compound's affinity for either tubulin or DNA topoisomerase.

Epimerization at C4 of podophyllotoxin, and substitution at that position with various nucleophiles has led to the epipodophyllotoxins. Demethylation at C4' of the epipodophyllotoxins affords compounds with useful antitumor activity, which act as topoisomerase II poisons rather than microtubule inhibitors. Numerous analogs bearing amine and ether substituents at C4 have been reported, and several semi-synthetic drugs derived from podophyllotoxin, including etoposide and teniposide, are used clinically for the treatment of cancer (Figure 18).[31, 32] Others, such as the amine derivative TOP-53, have shown superior antitumor activity to etoposide and advanced to clinical trials, although TOP-53 itself was shown to have unacceptable levels of toxicity.[33]

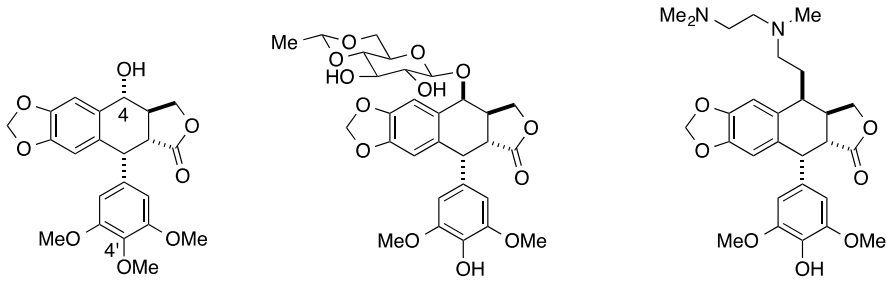

Figure 18. Structures of podophyllotoxin, etoposide and TOP-53.

DNA topoisomerase II is an essential enzyme that removes knots and tangles from DNA by generating transient double-stranded breaks in the nucleic acid backbone and maintains the proper topological state of DNA.[34] The enzyme does this by forming a nick in the DNA, allowing one strand to pass through, and then re-sealing. As seen in Figure 19, there are two classes of topoisomerases, topoisomerase I and topoisomerase II. Topoisomerase I cuts only one strand of a DNA double helix, relaxes the tension, and then reanneals the cut strands. Topoisomerase II cuts both strands of one DNA double helix, then passes another unbroken DNA helix through the enzyme, and then reanneals the cut strands.

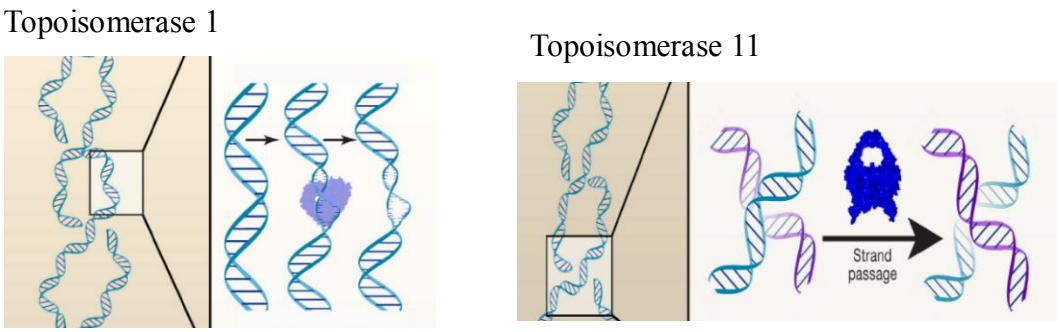

Figure 19. Two types of DNA strand cleavage and re-sealing by topoisomerase.[35]

Drugs that act as topoisomerase II poisons form a ternary drug-DNA-topoisomerase II complex and stabilize the covalent DNA cleavage complex as shown in figure 20. [36] Etoposide kills cells by increasing the concentration of topoisomerase II-DNA cleavage complexes so etoposide is referred to as a topoisomerase II poison.

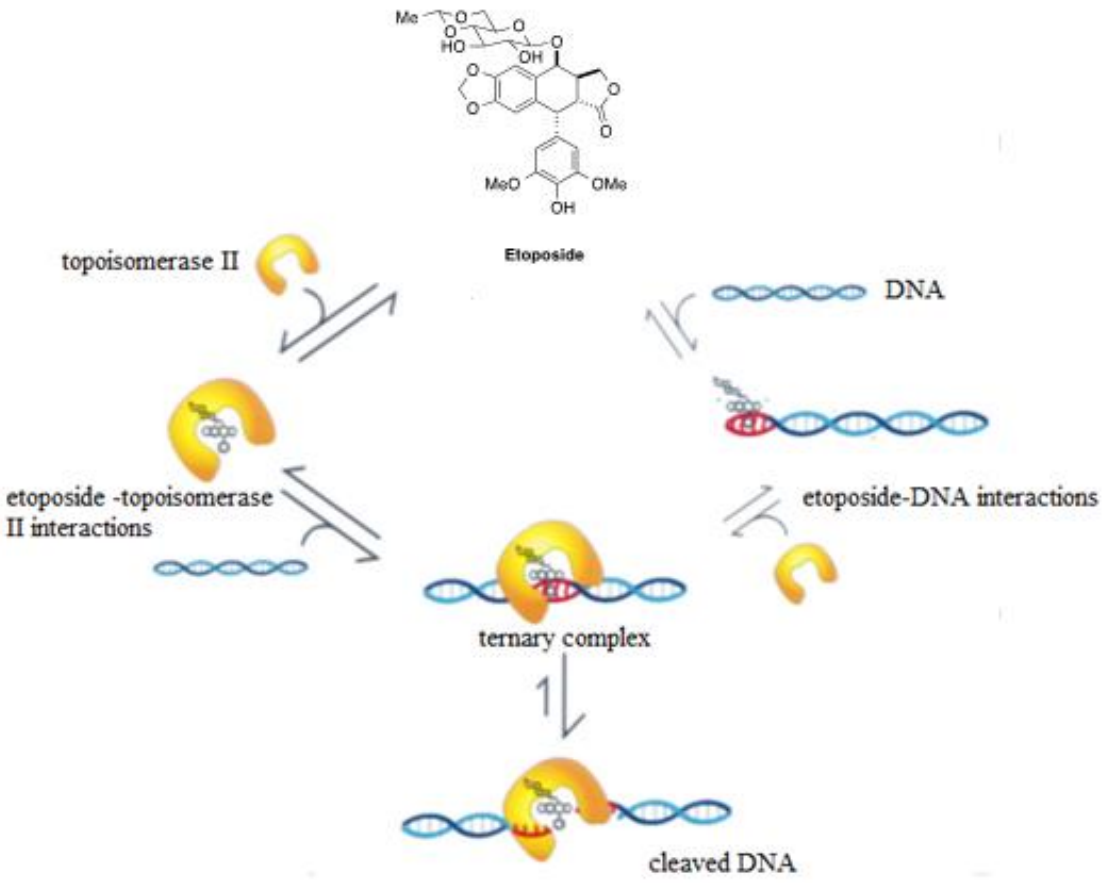

Figure 20. Pathway of etoposide-induced DNA cleavage complex formation.

The primary pathway for the formation of the noncovalent enzyme-drug-DNA ternary complex is through etoposide-topoisomerase II interactions. Etoposide may bind DNA prior to ternary complex formation. Once the ternary complex is formed it enhances cleavage complex formation. [36]

Etoposide stabilizes topoisomerase II-associated double-stranded DNA breaks by inhibiting the ability of the enzyme to ligate cleaved nucleic acid molecules. The mechanism of action of the demethylepipodophyllotoxin analogs involves an increase in topoisomerase II-mediated DNA breaks, and etoposide inhibits the ability of topoisomerase II to ligate the cleaved DNA.[37] It has been suggested that the activity of etoposide depends on one molecule of etoposide binding at the scissile bond on each strand of DNA to effect double-stranded cleavage, requiring two drugs per event.[37]

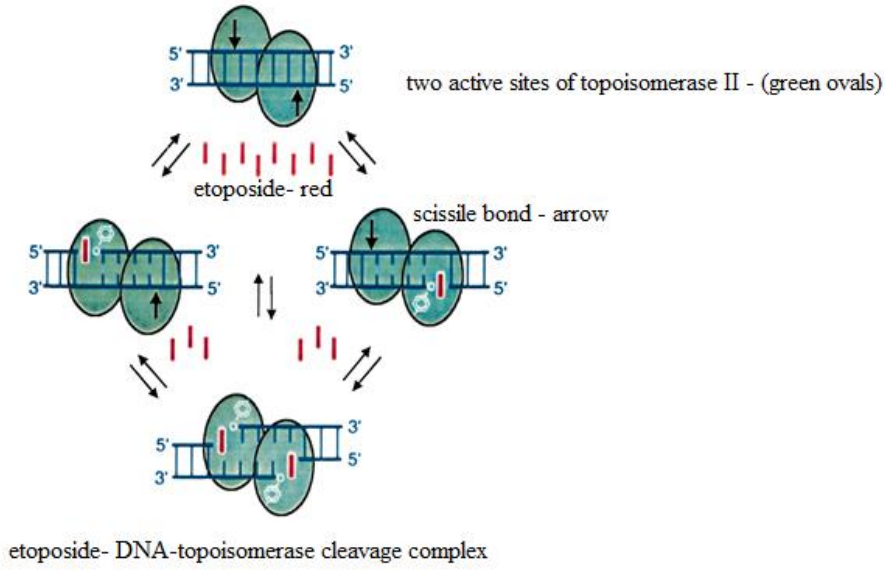

Figure 21. Two-drug model for etoposide action against human topoisomerase IIα.

To induce double stranded DNA breaks, etoposide interactions are required at both scissile bonds of topoisomerase II. Etoposide action in one scissile bond stabilizes the strand specific nick rather than a double-stranded break. Evidence suggests that the two drugs act independently of each other with human topoisomerase II.

Results and discussion

One implication for drug design is that covalently linked dimers of demethylepipodophyllotoxin analogs might show increased levels of double-stranded cleavage, and may display increased cytotoxicity as compared to the monomers. Although many C4 substituted demethylepipodophyllotoxins have been reported, there is only one report of demethylepipodophyllotoxin dimers, which were linked by rigid aryl diamines.[38] Linking groups included phenyl, naphthyl, biphenyl, and fluorenyl diamines, with some of the dimers having useful tumor cytotoxicity as seen in Figure 22.

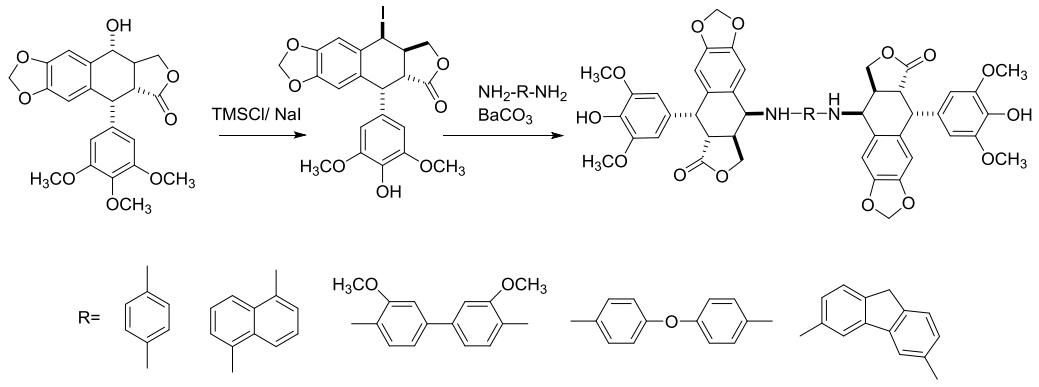

Figure 22. Synthesis of demethylepipodophyllotoxin dimers, linked by rigid aryl diamines.[38]

Syntheses of several novel, flexible, ether-linked dimers are reported here, including assays for the DNA cleavage activity and cytotoxicity of these compounds. These linked demethylepipodophyllotoxin analogs provide further insight into the two-drug model and may potentially provide novel antitumor agents.

The dimers of 4'-*O*-demethylepipodophyllotoxin were prepared *via* a one-pot synthesis. Treatment of podophyllotoxin with iodotrimethylsilane, followed by addition of the appropriate diol, afforded the ether-linked dimers **1-3** as shown in Figure 23. In a similar fashion, the corresponding monomers (**4-6**) were prepared in order to provide comparison to the dimers.

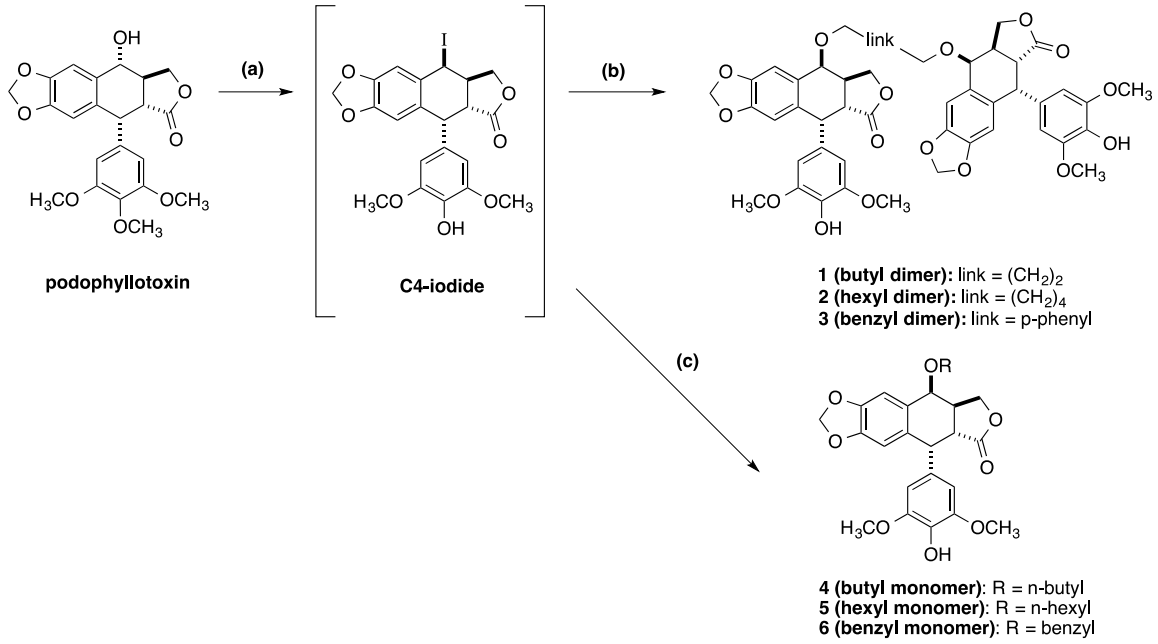

Figure 23: Synthesis of dimers and monomers.

Reagents and conditions: (a) TMSI, CH_2Cl_2, 0^0C, 2h (b) Ba_2CO_3, HO-$(CH_2)_n$-OH, 25˚C, CH_2Cl_2, 18h (c) Ba_2CO_3, ROH, 25˚C, CH_2Cl_2, 18h

The dimers and monomers, as well as etoposide, were assayed for their DNA cleavage activity and cytotoxicity. DNA cleavage was observed in the presence of human topoisomerase IIα. In addition to DNA cleavage, the dimers and monomers were tested for cytotoxicity in an adenocarcinoma cell line, and for cytotoxicity in normal cells.

The dimers and monomers, as well as etoposide, were assayed for their DNA cleavage activity and cytotoxicity. DNA cleavage was observed in the presence of human topoisomerase IIα and all dimers induced high levels of double-stranded DNA cleavage with very low levels of single-stranded cleavage (Figure 24). While the benzyl ether monomer **6** displayed a similar pattern to dimers, the alkyl ether monomers **4** and **5** induced very little DNA cleavage. A summary of the relative amounts of double-stranded vs. single-stranded DNA cleavage by the analogs at 100 μM also is shown. Comparing alkyl dimers (**1**-**3**) to monomers (**4**-**6**) there is a pattern of a higher ratio of double-strand to single-strand cleavage for the dimers over the monomers, although the difference is not as pronounced for the more rigid benzyl ethers.

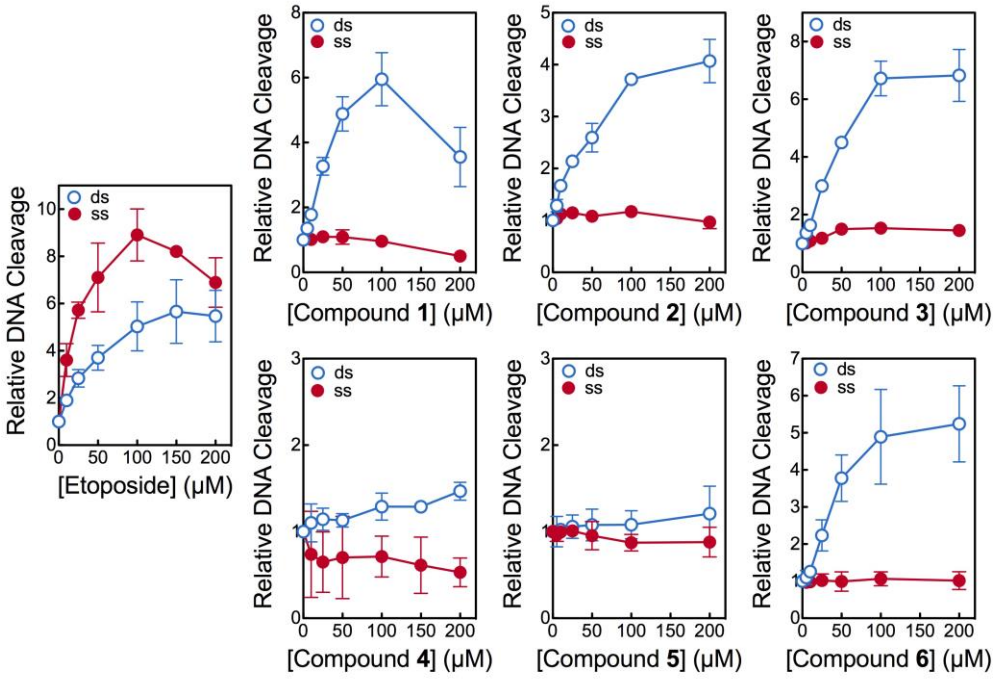

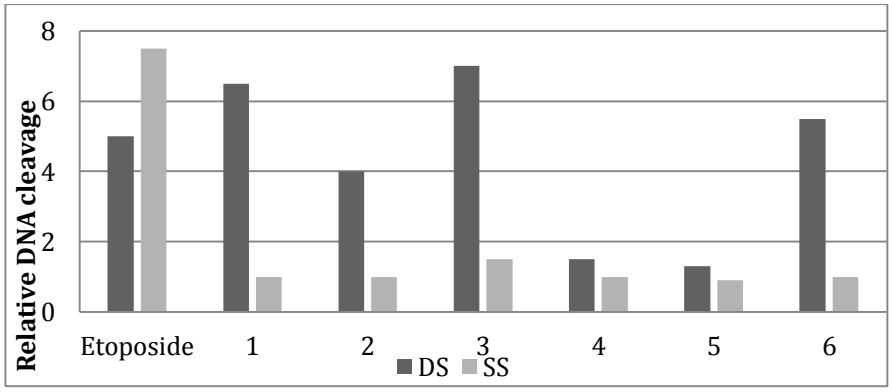

Figure 24. Results of DNA cleavage assay (top), and comparison of double-strand vs. single-strand DNA cleavage (bottom) at 100μM.

In addition to DNA cleavage, the dimers and monomers were tested for cytotoxicity in an adenocarcinoma cell line, and for cytotoxicity in normal cells. In all cases, the dimers (**1-3**) were more cytotoxic to cancer cells than both the monomers (**4-6**) and etoposide. Furthermore, they exhibited a higher selectivity ratio (Table 1).

Table 1. Cytotoxicity of compounds **1-6** in cancer cells (A549) and normal cells (L6).

Compound	IC_{50} values[a] (μM)		
	A549	L6	selectivity[b]
1	0.07 ± 0.02	0.30 ± 0.18	4.3
2	0.12 ± 0.03	0.30 ± 0.07	2.5
3	0.36 ± 0.14	0.60 ± 0.51	1.7
4	2.87 ± 1.05	4.62 ± 0.29	1.6
5	5.97 ± 2.60	4.55 ± 1.31	0.76
6	3.86 ± 0.86	4.55 ± 0.01	1.2
etoposide	2.87 ± 0.90	18.99 ± 4.37	6.7

[a] Values reported are from average of three trials. A549 is an adenocarcinoma cell line; L6 is a normal rat skeletal muscle cell line.

[b] Ratio of IC_{50} for L6/A549.

In conclusion, several flexible ether-linked dimers of demethylepipodophyllotoxin were synthesized and compared to their corresponding monomeric ethers. As predicted, all dimers induced higher levels of double-stranded DNA cleavage than the monomers in

the presence of human topoisomerase IIα. This observation lends credence to the two-drug model for demethylepipodophyllotoxin-induced DNA cleavage by topoisomerase II.[9] In addition, all dimers were more cytotoxic against tumor cells than the corresponding monomers and displayed better selectivity for tumor cells vs. normal cells.

General experimental procedures

The NMR data were obtained on either a 500 MHz FT-NMR model ECA-500 JEOL or a 300MHz FT-NMR model ECA-300 JEOL (Peabody, MA) purchased with funding provided by the National Science Foundation. Coupling constants (J values) are recorded in hertz (Hz). All signal assignments are based on COSY, HMQC and DEPT. IR spectra were recorded using a Varian 7000 FT-IR spectrometer (Varian Inc., Palo Alto, California). High resolution ESI-MS was performed at Notre Dame University, Notre Dame, Indiana. All solvents used for synthetic reactions were anhydrous reagent grade.

Synthesis

The numbering system used for the 4'-demethylepipodophyllotoxins is shown below:

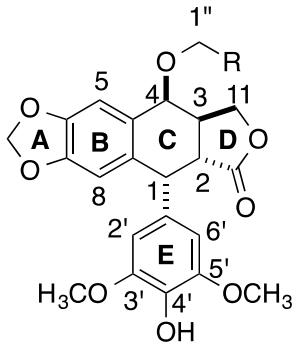

1",4"-[Bis-(4'-*O*-demethyl-4β-*O*-4-desoxypodophyllotoxin)]butanediol (1)

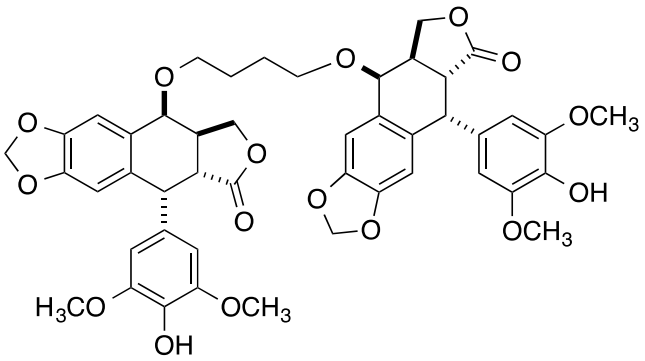

Podophyllotoxin (100 mg, 0.242 mmol) was dissolved in 2 mL methylene chloride and cooled to 0 °C under an argon atmosphere. TMSI (121 μL, 0.604 mmol) was added and the resulting solution was stirred at 0 °C for two hours, at which point barium carbonate (143 mg, 0.725 mmol) and 1, 4-butanediol (54 μL, 0.604 mmol) were added. The resulting mixture was stirred overnight at room temperature, then dissolved in 20 mL methylene chloride and washed with aqueous sodium thiosulfate. The organic layer was washed further with brine, dried over anhydrous magnesium sulfate, filtered and evaporated. The crude product was chromatographed on 15 x 120 mm silica gel eluting successively with methylene chloride, 50:1 methylene chloride-acetone, 30:1, 20:1, 15:1, 10:1, 5:1, 2:1, 1:1, and pure acetone to afford 26.1 mg of the dimer (**1**) (25.3%). Rf 0.11 [methylene chloride-acetone 9:1]; ^{1}H NMR (300 MHz, d_6-acetone): δ 6.95 (s, 2H, 5-CH), 6.53 (s, 2H, 8-CH), 6.29 (s, 4H, 2', 6'- CH), 5.98 (s, 4H, acetal OCH_2O), 5.60 (s, 2H, OH), 4.57 (t, J = 8.94, 4H, 1, 4-CH), 4.35 (t, J = 7.91 Hz, 4H, 11-CH_2), 4.28-4.28 (m, 2H, 3-CH), 3.66 (s, 12H, 3', 5'-OCH_3), 3.54-3.50 (m, 4H, 1", 4"-CH_2), 3.30 (dd, J = 14.10, 5.50 Hz, 2H, 2-CH), 1.70-1.50 (m, 4H, 2", 3"-CH_2); ^{13}C NMR (500 MHz, d_6-acetone): δ

174.58 (C=O), 148.11-130.58 (all 4° aryl C's), 109.70 (C-5, 8), 108.77 (C-2', 6'), 101.49 (acetal CH_2), 74.28 (C-4'), 70.18 (C-1), 67.39 (C-1", 4"), 61.45 (lactone CH_2), 55.81 (methoxy OCH_3), 43.76 (C-4), 41.03 (C-2), 38.50 (C-3), 26.61 (C-2", 3"); mass spectrum (FAB) *m/z* ($C_{46}H_{46}O_{16}$) calculated for (M+1) 855.2864, found 855.2936.

1",6"-[Bis-(4'-*O*-demethyl-4β-*O*-4-desoxypodophyllotoxin)]hexanediol (2)

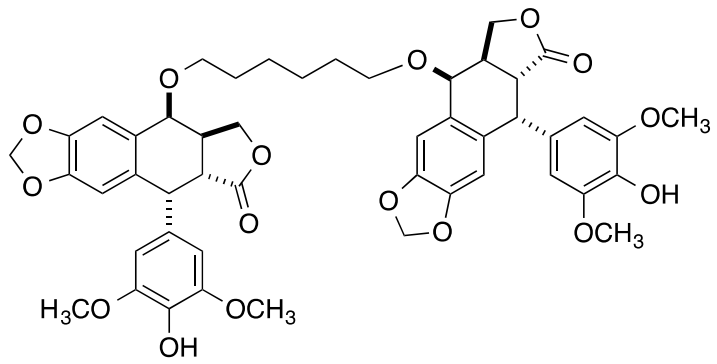

Podophyllotoxin (75 mg, 0.181 mmol) was dissolved in 1.5 mL methylene chloride and cooled to 0 °C under an argon atmosphere. TMSI (75 μL, 0.375 mmol) was added and the resulting solution was stirred at 0 °C for two hours, at which point barium carbonate (107.1 mg, 0.543 mmol) and 1,6-hexanediol (10.7 mg, 0.091 mmol) were added. The resulting mixture was stirred overnight at room temperature, then dissolved in 10 mL methylene chloride and washed with aqueous sodium thiosulfate. The organic layer was washed further with brine, dried over anhydrous magnesium sulfate, filtered and evaporated. The filtrate resulted in 21 mg of the (**2**) (26.3%). FT-IR 2952 cm^{-1} (methoxy CH_3 stretch), 2927 (asym CH_2 stretch), 2859 (sym CH_2 stretch), 1769 (lactone C=O), 1589, 1478, and 1461 (aromatic C=C ring stretch), 1228 (alcohol C-O stretch), 1118 (aromatic C-H bend); ^1H NMR (500 MHz, d_6-acetone): δ 6.92 (s, 2H, 5-CH), 6.49 (s, 2H,

8-CH), 6.31 (dd, J = 9.16, 16.32 Hz, 4H, 2', 6'- CH), 5.96 (s, 4H, acetal OCH_2O), 4.88 (s, 2H, OH), 4.58-4.53 (m, 2H, 4-CH), 4.30-4.28 (m, 2H, 1-CH), 3.99-4.04 (m, 4H, 11-CH_2), 3.66 (s, 12H, 3', 5'-OCH_3), 3.63-3.61 (m, 4H, 1", 6"-CH_2), 3.28 (dd, J = 1.72, 5.44 Hz, 2H, 2-CH), 3.00-2.86 (m, 2H, 3-CH), 1.43-1.35 (m, 4H, 3", 4"-CH_2), 1.18-1.15 (m, 4H, 2", 5"-CH_2); ^{13}C NMR (500 MHz, d_6-acetone): δ 174.87 (C=O), 152.69-130.76 (all 4° aryl C's), 109.69 (C-5, 8), 108.76 (C-2', 6'), 101.45 (acetal CH_2), 79.21 (C-4'), 74.29 (C-1), 70.16 (C-1", 6"), 67.55 (lactone CH_2), 55.80 (methoxy OCH_3), 43.80 (C-4), 40.38 (C-2), 38.60 (C-3), 29.95 (C-2", 5"), 25.99 (C3", 4"); mass spectrum (MALDI) *m/z* ($C_{48}H_{50}O_{16}$) calculated for (Na+ adducts) 905.2996, found 905.3018.

1",6"-[Bis-(4'-*O*-demethyl-4β-*O*-4-desoxypodophyllotoxin)]-*p*-benzene-dimethanol (3)

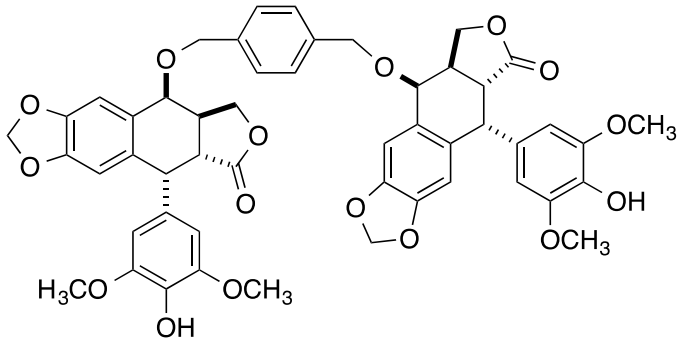

Podophyllotoxin (52 mg, 0.126 mmol) was dissolved in 1 mL methylene chloride and cooled to 0 °C under an argon atmosphere. TMSI (50 μL, 0.25 mmol) was added and the resulting solution was stirred at 0 °C for two hours, at which point barium carbonate (74.2 mg, 0.377 mmol) and 1,4-benzenedimethanol (8.7 mg, 0.063 mmol) were added. The resulting mixture was stirred overnight at room temperature, then dissolved in 10 mL methylene chloride and washed with aqueous sodium thiosulfate. The organic layer was

washed further with brine, dried over anhydrous magnesium sulfate, filtered and evaporated. The crude product was chromatographed on 15 x 120 mm silica gel eluting successively with methylene chloride, 50:1 methylene chloride-acetone, 25:1, 10:1, 5:1, 1:1, and pure acetone to afford 17.4 mg of the dimer (**3**) (30.6%). Rf 0.40 [methylene chloride-acetone 9:1]; FT-IR 2958 cm^{-1} (methoxy CH_3 stretch), 2925 (CH_2 stretch), 1771 (lactone C=O), 1591, 1481, and 1460 (aromatic C=C ring stretch), 1230 (alcohol C-O stretch), 1120 (aromatic C-H bend); ^1H NMR (500 MHz, d_6-acetone): δ 7.39 (s, 2H, aryl CH), 7.34 (s, 2H, aryl CH), 7.05 (s, 2H, OH), 6.93-6.86 (m, 2H, 5-CH), 6.53 (s, 2H, 8-CH), 6.29 (s, 4H, 2', 6'- CH), 6.00-5.96 (m, 4H, acetal OCH_2O), 4.75 (d, J = 2.29, 2H, 4-CH), 4.73-4.67 (m, 4H, 1", 6"-CH_2), 4.58 (d, J = 5.73, 2H, 1-CH), 4.38-4.27 (m, 4H, 11-CH_2), 3.65 (s, 12H, 3', 5'-OCH_3), 3.27 (dd, J = 14.32, 5.15 Hz, 2H, 2-CH), 3.05-2.97 (m, 2H, 3-CH); ^{13}C NMR (500 MHz, d_6-acetone): δ 174.48 (C=O), 147.09-130.15 (all 4° aryl C's), 126.58-128.01 (C-3", 4", 7", 8"), 109.70 (C-5, 8), 108.74 (C-2', 6'), 101.53 (acetal CH_2), 73.75 (C-1), 71.54 (C-1", 6"), 67.41 (lactone CH_2), 63.61 (C-4'), 55.80 (methoxy OCH_3), 43.78 (C-4), 41.02 (C-2), 38.45 (C-3); mass spectrum (MALDI) *m/z* ($C_{50}H_{46}O_{16}$) calculated for (Na+ adducts) 925.2683, found 925.2673.

4'-*O*-demethyl-4β-*O*-(butyl)-4-desoxypodophyllotoxin (4)

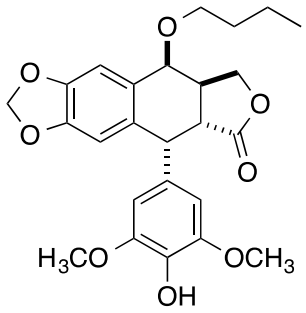

Podophyllotoxin, (125 mg, 0.302 mmol) was dissolved in 2 mL methylene chloride and cooled to 0 °C under an argon atmosphere. TMSI (151 μL, 0.755 mmol) was added and the resulting solution was stirred at 0 °C for two hours, at which point barium carbonate (178 mg, 0.906 mmol) and 1-butanol (165 μL, 1.8 mmol) were added. The resulting mixture was stirred overnight at room temperature, then dissolved in 20 mL methylene chloride and washed with aqueous sodium thiosulfate. The organic layer was washed further with brine, dried over anhydrous magnesium sulfate, filtered and evaporated. The crude product was chromatographed on 15 x 120 mm silica gel eluting successively with methylene chloride, 50:1 methylene chloride-acetone, 30:1, 20:1, 15:1, 1:1, and pure acetone to afford 40.9 mg of the monomer (**5**) (28.8%). Rf 0.64 [methylene chloride-acetone 9:1]; ^{1}H NMR (500 MHz, d_6-acetone): δ 6.90 (s, 1H, 5-CH), 6.49(s, 1H, OH), 6.26 (s, 1H, 8-CH), 5.56 (s, 2H, 2', 6'-CH), 4.52 (s, 2H, acetal OCH_2O), 4.22-4.31 (m, 2H, 1-4-CH), 4.19-4.21 (t, 1H, 11α-CH_2), 3.62-3.63 (m, 1H, 11β-CH_2), 3.61 (s, 6H, 3', 5' –OCH_2), 1.98-1.99 (m, 2H, 1"-CH_2), 1.49-1.51 (m, 4H, 3"-CH_2), 1.32-1.34 (m, 2H, 2"-CH_2), 0.86 (t, 2H, 4"-CH_2); ^{13}C NMR (500 MHz, d_6-acetone): δ 174.55 (C=O), 148.10-130.60 (all 4° aryl C's), 110.21 (C-5, 8), 109.67 (C-2', 6'), 108.78 (acetal CH_2), 101.48 (C1, 4), 74.28 (C-1"), 69.391 (C11 CH_2), 55.81 (OCH_3), 29.48 (C-2"), 19.28 (C-3"), 13.37 (C4"); mass spectrum (FAB) *m/z* ($C_{25}H_{28}O_8$) calculated for (*m/z*) 456.1784, found 456.1768.

4'-*O*-demethyl-4β-*O*-(hexyl)-4-desoxypodophyllotoxin (5)

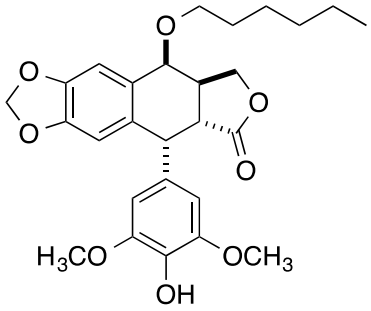

4'-*O*-demethyl-*epi*-podophyllotoxin , (100 mg, 0.250 mmol) was dissolved in 2 mL methylene chloride and cooled to 0 °C under an argon atmosphere. TMSI (125 μL, 0.625 mmol) was added and the resulting solution was stirred at 0 °C for two hours, at which point barium carbonate (148 mg, 0.750 mmol) and 1-hexanol (153 μL, 1.5 mmol) were added. The resulting mixture was stirred overnight at room temperature, then dissolved in 20 mL methylene chloride and washed with aqueous sodium thiosulfate. The organic layer was washed further with brine, dried over anhydrous magnesium sulfate, filtered and evaporated. The crude product was chromatographed on 15 x 120 mm silica gel eluting successively with methylene chloride, 50:1 methylene chloride-acetone, 30:1, 20:1, 15:1, 1:1, and pure acetone to afford 30.9 mg of the monomer (**4**) (25.5%). Rf 0.75 [methylene chloride-acetone 9:1]; ^{1}H NMR (500 MHz, d_6-acetone): δ 7.07 (s, 1H, 5-CH), 6.89 (s, 1H, OH), 6.48 (s, 1H, 8-CH), 6.24 (s, 2H, 2', 6'- CH), 5.93 (s, 2H, acetal OCH_2O), 4.52-4.50 (m, 2H, 1, 4-CH), 4.31 (t, J = 8.02 Hz, 1H, 11α-CH_2), 4.21-4.17 (m, 1H, 11β-CH_2), 3.61 (s, 6H, 3', 5'-OCH_3), 3.54-3.49 (m, 2H, 1''-CH_2), 3.25 (dd, J = 14.03, 5.15 Hz, 1H, 2-CH), 2.94-2.88 (m, 1H, 3-CH), 1.54-1.49 (m, 4H, 2'', 3''-CH_2), 1.24-1.19 (m, 4H, 4'', 5''-CH_2), 0.80 (t, J = 6.87 Hz, 2H, 6''-CH_2); ^{13}C NMR (500 MHz, d_6-acetone): δ 174.65 (C=O), 148.89-147.10 (all 4° aryl C's), 110.21 (C-5, 8), 108.75 (C-2', 6'),

101.48 (acetal CH_2), 74.27 (C-1, 4), 70.18 (C-1"), 67.35 (lactone CH_2), 55.79 (methoxy OCH_3), 41.01 (C-2), 38.48 (C-3), 31.58 (C-2"), 29.94 (C-3"), 25.83 (C-4"), 22.45 (C-5"), 13.50 (C-6"); mass spectrum (FAB) *m/z* ($C_{27}H_{32}O_8$) calculated for (*m/z*) 484.2097, found 484.2108.

4'-*O*-demethyl-4β-*O*-(methylbenzyl)-4-desoxypodophyllotoxin(6)

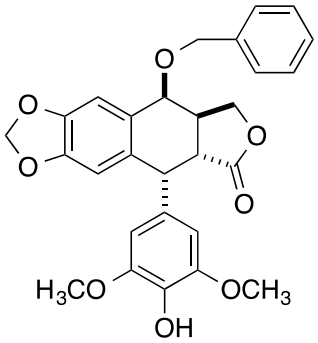

4'-*O*-Demethyl-*epi*-podophyllotoxin , (100 mg, 0.250 mmol) was dissolved in 2 mL methylene chloride and cooled to 0 °C under an argon atmosphere. TMSI (125 μL, 0.625 mmol) was added and the resulting solution was stirred at 0 °C for two hours, at which point barium carbonate (148 mg, 0.750 mmol) and benzyl alcohol (162 μL, 1.5 mmol) were added. The resulting mixture was stirred overnight at room temperature, then dissolved in 20 mL methylene chloride and washed with aqueous sodium thiosulfate. The organic layer was washed further with brine, dried over anhydrous magnesium sulfate, filtered and evaporated. The crude product was chromatographed on 15 x 120 mm silica gel eluting successively with methylene chloride, 50:1 methylene chloride-acetone, 30:1, 20:1, 15:1, 1:1, and pure acetone to afford 28.5 mg of the monomer (**6**) (21.8%). Rf 0.70 [methylene chloride-acetone 9:1]; ^{1}H NMR (500 MHz, d_6-acetone): δ 7.53-7.29 (m, 5H, aryl CH), 6.88 (s, 1H, 5-CH), 6.53 (s, 1H, 8-CH), 6.30 (s, 1H, OH), 5.97 (s, 2H, 2', 6'- CH) , 4.88-4.86 (m, 1H, 11α-CH_2), 4.74 (m, 1H, 11β-CH_2), 4.59 (m,

2H, 1-4-CH), 4.37 ((m, 1H, 1"-CH_2), 3.64 (s, 6H, 3', 5' –OCH_3), 3.37-3.36 (m, 1H, 3-CH), 2.o6-1.64 ((m, 1H, 2-CH); ^{13}C NMR (500 MHz, d_6-acetone): δ 174.51 (C=O), 148.21-127.62 (all 4° aryl C's), 110.30-109.76 (C-3", 4", 7", 8"), 108.75 (C-5, 8), 101.63 (C-2', 6'), 101.52 (acetal CH_2), 73.87 (C-1), 71.79 (C-1", 6"), 67.41 (lactone CH_2), 55.86 (methoxy OCH_3), 55.79 (C-4') 43.77 (C-4), 41.02 (C-2), 38.45 (C-3); mass spectrum (FAB) *m/z* ($C_{28}H_{26}O_8$) calculated for (*m/z*) 490.1628, found 490.1649.

Biological testing

A549 cells

The A549 (ATCC® CCL-185), human lung cancer cell line, was obtained from American Type Culture Collection (ATCC) (Manassas, VA.) RPMI 1640, Phosphate Buffered Saline (PBS) and Trypsin (porcine) (0.25%, - Ca^{2+} - Mg^{2+} + EDTA in HBSS) were obtained from HyClone Laboratories (Logan, UT). Fetal Bovine Serum (FBS) was obtained from Atlanta Biologicals (Atlanta, GA). Penicillin-Streptomycin (P/S) (Penicillin, 5000 U/ml – Streptomycin, 5 mg/ml) was purchased from Sigma (St. Louis, MO). Etoposide (Sigma, St. Louis, MO) was dissolved in dimethyl sulfoxide (DMSO) (Sigma, St. Louis, MO) to concentrations of 10 mM. The resazurin-based metabolic indicator, AlamarBlue, was purchased from Invitrogen (Frederick, MD.) Black wall, clear and flat-bottom, tissue culture treated 96 well micrototiter plates were purchased from Corning, NY.

A549 cells were cultured in RPMI 1640 containing 10% heat inactivated FBS and 1% penicillin-streptomycin. Subconfluent cells were passaged every 3–4 days and

maintained in a 37°C humidified incubator in an atmosphere of 5% CO_2. Cells were detached using trypsin, counted using a Neubauer hemocytometer, and adjusted using fresh media to a density that would deliver 2 $\times 10^3$ cells per well (90 uL) in a 96-well microtiter plate. After 24 h incubation, compounds diluted in culture medium were added (10μL) to each well with different concentrations with a minimum of three wells for each concentration. Each trial was then repeated for a minimum of three replicates. For the control experiments, wells with medium only (blank), positive control (Etoposide 10μM) and DMSO 1% were also included in each plates.

Following incubation for 48 h, 10 μL of AlamarBlue was added into each well. Relative fluorescence (RFU) readings were obtained 10 h later using excitation/emission setting of 555/ 570 nm, using a SpectraMax M2 fluorescent plate reader (Molecular Devices, Sunnyvale, CA). The percentage of cell inhibition was calculated using the formula:

$$\%\ inhibition = 1 - \frac{[\text{Treated sample RFU} - \text{Medium only RFU}}{[\text{Untreated RFU} - \text{Medium only RFU}]}\ \text{X } 100$$

L6 cells

The rat skeletal muscle cell line, L6 (ATCC® CRL-1458) was obtained from ATCC for a non-cancerous cell line comparison. In addition to the cell culture and testing materials described for A549, DMEM was obtained from HyClone Laboratories (Logan, UT). Podophyllotoxin (Sigma, St. Louis, MO) was dissolved in DMSO (Sigma, St. Louis, MO) to a concentrations of 100 ug/mL. The resazurin-based metabolic indicator, PrestoBlue, was purchased from Invitrogen (Frederick, MD.)

L6 cells were cultured in DMEM containing 10% heat inactivated FBS and 1% P/S. Subconfluent cells were passaged every 3–4 days and maintained in a 37°C humidified incubator in an atmosphere of 5% CO_2. Cells were detached using trypsin, counted using a Neubauer hemocytometer, and adjusted using fresh media to a density that would deliver 5×10^3 cells per well (90 uL) in a 96-well microtiter plate. After 3 h incubation, compounds diluted in culture medium were added (10μL) to each well with different concentrations with a minimum of three wells for each concentration. Each trial was then repeated for a minimum of three replicates. For the control experiments, wells with medium only (blank), positive control (podophyllotoxin) and DMSO 1% were also included in each plate.

Following incubation for 71.5 h, 11 μL of PrestoBlue was added into each well. RFU readings were obtained 30 m later using excitation/emission settings of 560/590 on the fluorescent plate reader, and percent inhibition calculated as previously described.

High concentrations of all compounds produced complete cell lysis, as no intact cells were observable by microscopy. Low level doses appeared to produce blebbing which may be indicative of apoptosis. Inhibition data were analyzed using Graph Pad Prism 4.0 using a four parameter nonlinear regression and 50% inhibitory concentrations (IC_{50}) were derived from each inhibition curve.

DNA Cleavage Assay

DNA cleavage reactions were performed as described by Fortune and Osheroff. *(Fortune, J. M., and Osheroff, N. (1998) Merbarone inhibits the catalytic activity of human topoisomerase IIα by blocking DNA cleavage. J. Biol. Chem. 273, 17643-17650.)* Reaction mixtures contained 150 nM human topoisomerase IIα, 10

nM negatively supercoiled pBR322 DNA, and 0–200 μM demethylepipodophyllotoxin derivatives in 20 μL of cleavage buffer [10 mM Tris-HCl (pH 7.9), 5 mM $MgCl_2$, 100 mM KCl, 0.1 mM EDTA, and 2.5% (v/v) glycerol]. Reactions were incubated for 6 min at 37 °C, and enzyme-DNA cleavage complexes were trapped by adding 2 μL of 5% SDS followed by 2 μL of 250 mM EDTA (pH 8.0). Proteinase K was added (2 μL of a 0.8 mg/mL solution), and reaction mixtures were incubated for 30 min at 45 °C to digest topoisomerase IIa. Samples were mixed with 2 μL of agarose loading dye [60% sucrose in 10 mM Tris-HCl (pH 7.9), 0.5% bromophenol blue; and 0.5% xylene cyanol FF], heated for 2 min at 45 °C, and subjected to electrophoresis in 1% agarose gels in 40 mM Tris-acetate (pH 8.3) and 2 mM EDTA containing 0.5 μg/mL ethidium bromide. DNA cleavage was monitored by the conversion of the negatively supercoiled plasmid to linear molecules. DNA bands were visualized by ultraviolet light and quantified using an Alpha Innotech digital imaging system.

CHAPTER 3

ANTITRYPANOSOMAL COMPOUNDS ISOLATED FROM IRIS DOMESTICA (BELAMCANDA CHINENSIS)

Introduction

Iris domestica is a member of the *Iridaceae* family and was formerly known as *Belamcanda chinensis*. The common name of *Iris domestica* is Blackberry Lily, sometimes called Leopard flower (Figure 25). The rhizome of this plant has been used in Traditional Chinese Medicine for hundreds of years as a treatment for curing pulmonary diseases, asthma, liver complaints and cancer. [39]

Figure 25. *Iris domestica* (printed from Wikipedia)

Many compounds have been isolated from *Iris domestica* in the last few decades, including flavonoids, quinones, and terpenoids. According to the literature, most of the compounds reported belong to the flavonoid family, including tectorigenin, iridin, irigenin, isisflorentin, hispidulin, isorhamnetin, isoiridin and isotectorin (Figure 26).[40] They have a broad

spectrum of biological and pharmacological activities, such as antimutagenic and antioxidant, antibacterial, hypoglycemic and anticancer effects.[41]

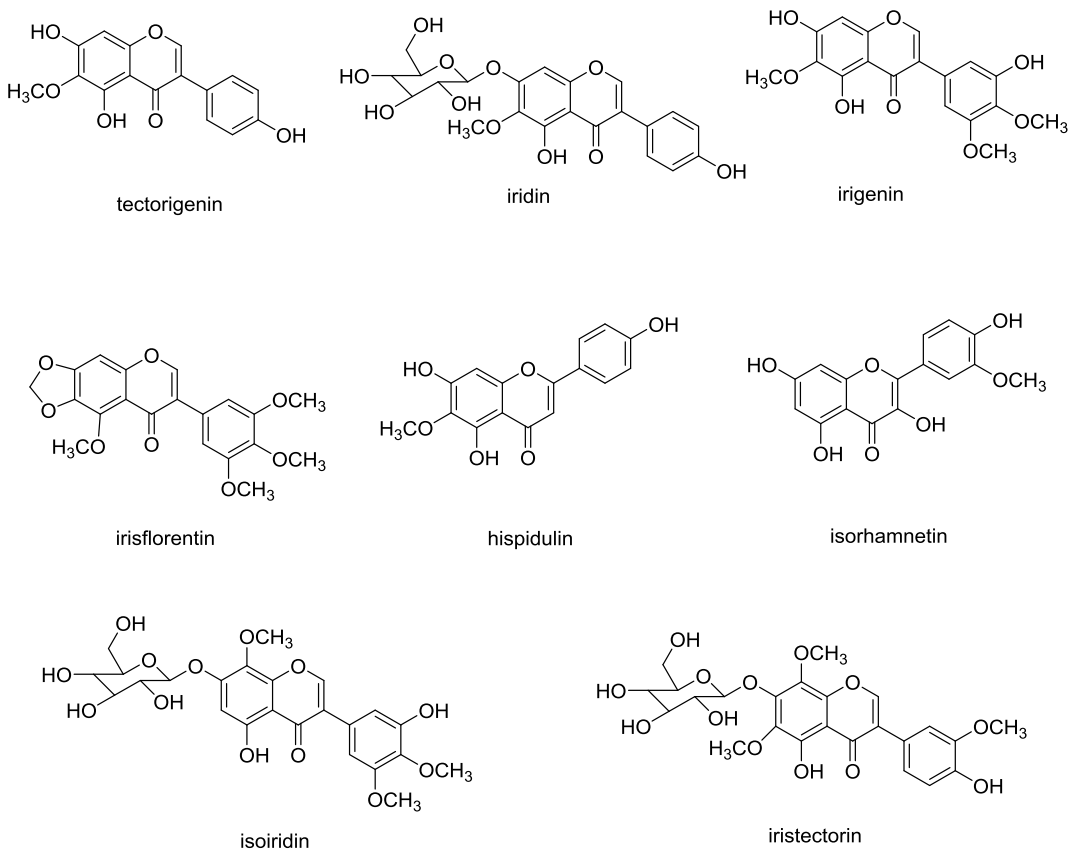

Figure 26. Structures of flavonoids isolated from *Iris domestica*.

Quinones and phenols were also isolated from *Iris domestica*, including belamcandones A–D, ardisianone A and belamcandols (Figure 27).[42]

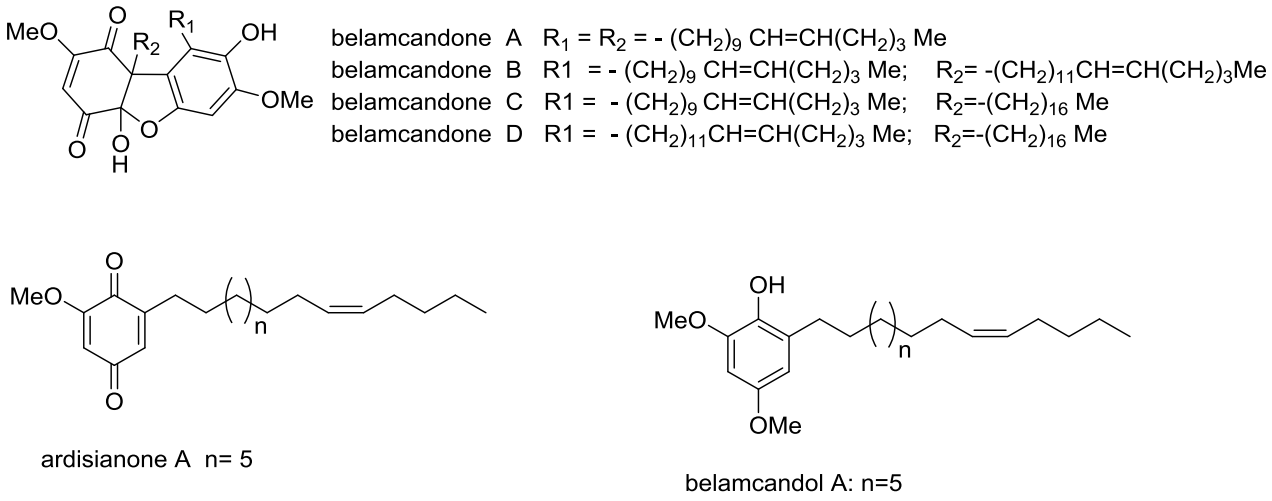

Figure 27. Structures of quinones and phenols isolated from *Iris domestica*.

One of the most common terpenoids isolated from *Iris domestica* are iridals. These are found in the rhizomes of many Iris species and are unique to irises. Up to now more than 40 different iridals have been isolated from various Iris species. Most of these iridals have been isolated as esters at the hydroxypropyl side chain of C3 (Figure 28). Iridals are characterized by some common features. A multi-substituted cyclohexane ring is found with a prenylated side chain at C 11. An acrolein group at C-7 and hydroxypropyl chain at C-6 are typical fragments of a seco A-ring of triterpenoids. These compounds are extremely sensitive and decompose rapidly on contact with air.

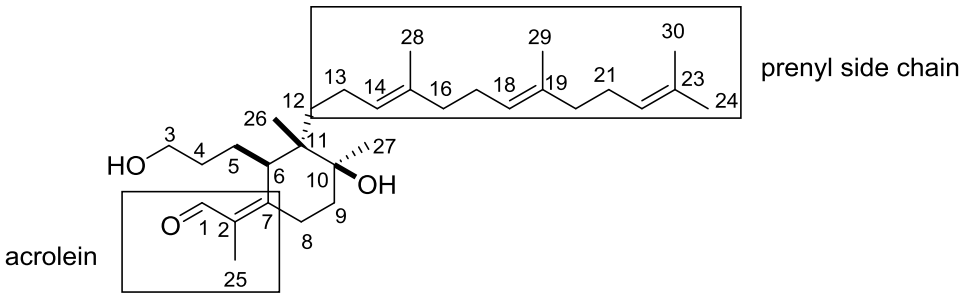

Figure 28. Iridals example showing basic structure skeleton which is numbered as shown.

Iridals were discovered in the 1970's by Marner et al, who were studying the characteristic violet-like smelling compounds of the essential oil of rhizomes of *Iris sp*. Irises have been cultivated since ancient times to prepare perfumes and cosmetics with the fragrance of sweet violet.[43] These violet-like smelling compounds have long been known to be the three isomeric irones as seen in Figure 29. These ketones do not occur in freshly harvested iris plants. These irones are formed over years by a slow process of oxidative degradation of parent molecules. α-Irone and γ-irones were isolated by Marner and workers from *Iris pallida* and *Iris florentina*, and for the first time they isolated the parent molecules responsible for α-irone and γ-irone as iridals , iripallidal and iriflorental.

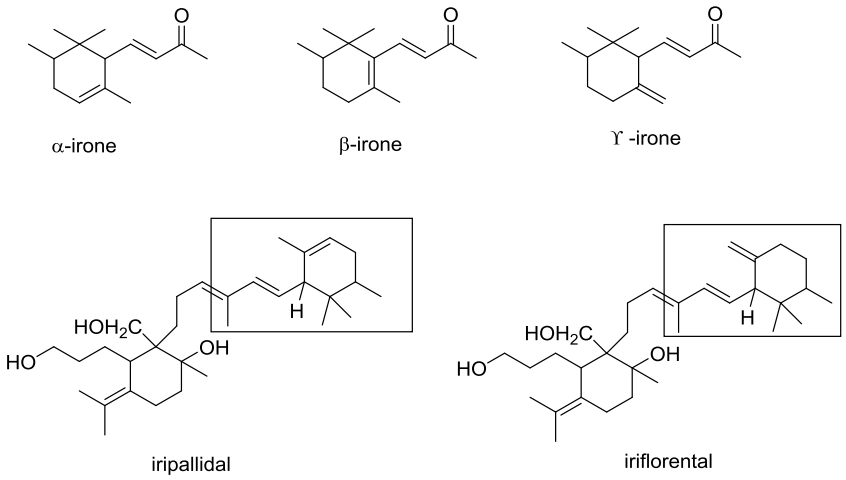

Figure 29. Structures of α-irone, β-irone and γ-irone with the parent molecules, iripallidal and iriflorental.[43]

They investigated the biosynthesis of iridal triterpenoids and proposed iridal biosynthesis, by observing key metabolites developed in cell cultures of *Iris pseudacorus*. The basic iridal

skeleton is derived from *trans* squalene (Figure 30).[44] Epoxidation and subsequent cyclization leads to an intermediate which rearranges to form compound **7**. All of the iridals differ from each other by oxidation pattern and positions of double bonds and number of rings. For example, oxidation of compound **7** at C (21) results 10-desoxy-21-hydroxy-iridal **8**; oxidation of compound **7** at C(10) results compound **9** . Oxidation of compound **9** at C (21) gives 21-hydroxy-iridal **10**. Compound **9** act as an accepter of an activated methyl group and the side chain cyclizes to give product **11**. Further hydroxylation of compound **9** results in 16-hydroxy iridal **12**. Dehydration of the side chain of **12** and subsequent oxidation at 26 results in 26-acetylated derivatives of iridals **13**. According to this proposed pathway there are many possibilities for the iridal structure.

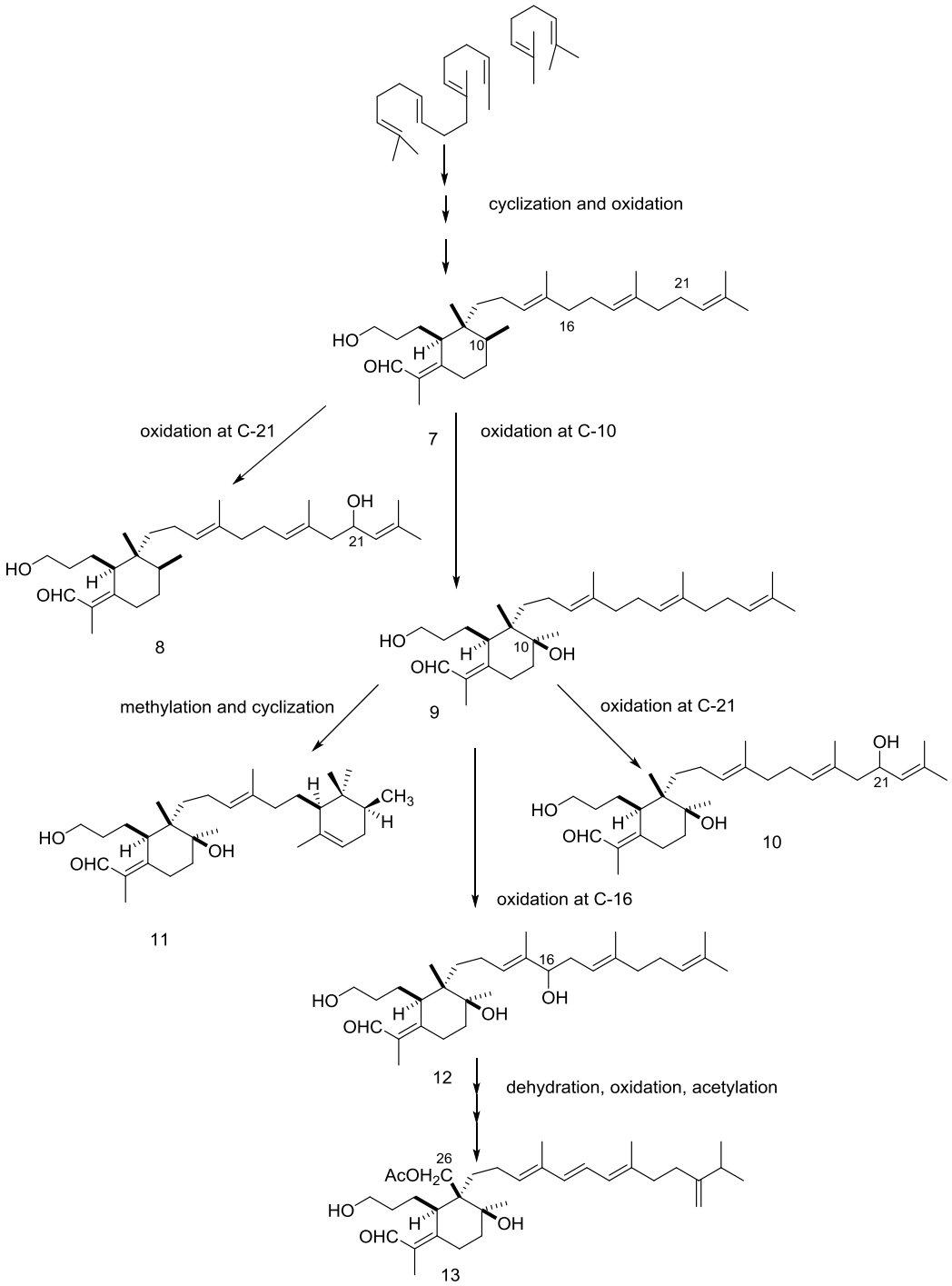

Figure 30. Proposed biosynthetic pathway of iridals from squalene. [44]

Iridals can be classified into four broad groups: simple iridals, spiroiridals, cycloiridals and oxaspiroiridals as seen in Figure 31.

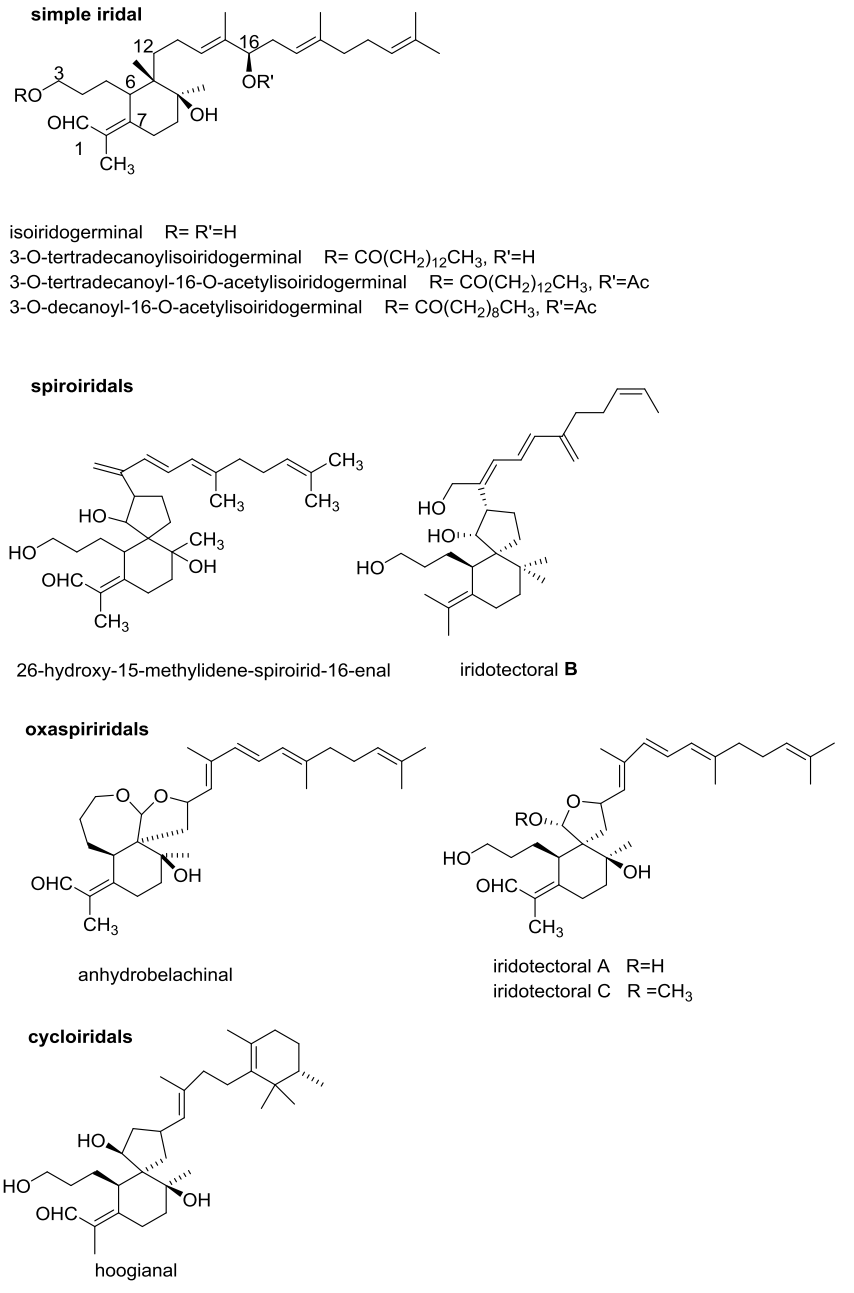

Figure 31. Iridal classification. [45]

Iridals can be classified into four broad groups: simple iridals, spiroiridals, cycloiridals based on number of ring, spiro ring system, presence of oxygen in the spiro rings and functional groups attachment to the prenylated side chain. (Figure 31) [45] Isoiridogermanal and its esters are some examples of simple iridals, that have been isolated from *Iris domestica*, *Iris.tectorum* and *Iris germanica*. These simple iridals showed ichthytoxic activity as well as exhibit cytotoxicity toward the A2780 ovarian and K562 leukemic human tumor cell lines.[46]

Isoiridogermanal was first isolated in 1983 and the absolute configuration has been established by means of chemical and physical analysis.[43] Isoiridogermanal synthesis starts from squalene and epoxidation at C 2-3 of squalene and subsequent cyclization leads to a bicyclic ionic intermediate. This undergoes ring cleavage and rearranges to form aldehyde intermediate. After several biological reactions, including reduction, oxidation and hydration isoiridogemanal is synthesized (Figure 32).

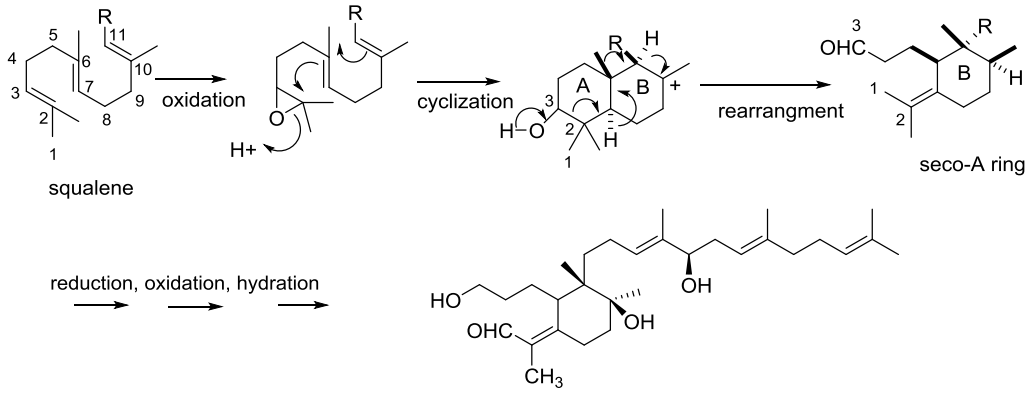

Figure 32. Possible biosynthetic pathway for isoiridogermanal.

Marner and Jaenicke proposed pathways for formation of the spiro and oxaspiroiridals from simple iridals. Iridotectoral B and 28-hydroxy-15-methylidene-spiroirid-16-enal are some examples of spiroiridals isolated from *Iris tectorum* and *Iris domestica* with ichthyotoxic activity, tumor-promoting activity and Protein Kinase C Activation. In spiroiridals two rings are fused at one common carbon, C-11. 23, 28-Hydroxy-15-methylidene-spiroirid-16-enal is formed as depicted in Figure 33.

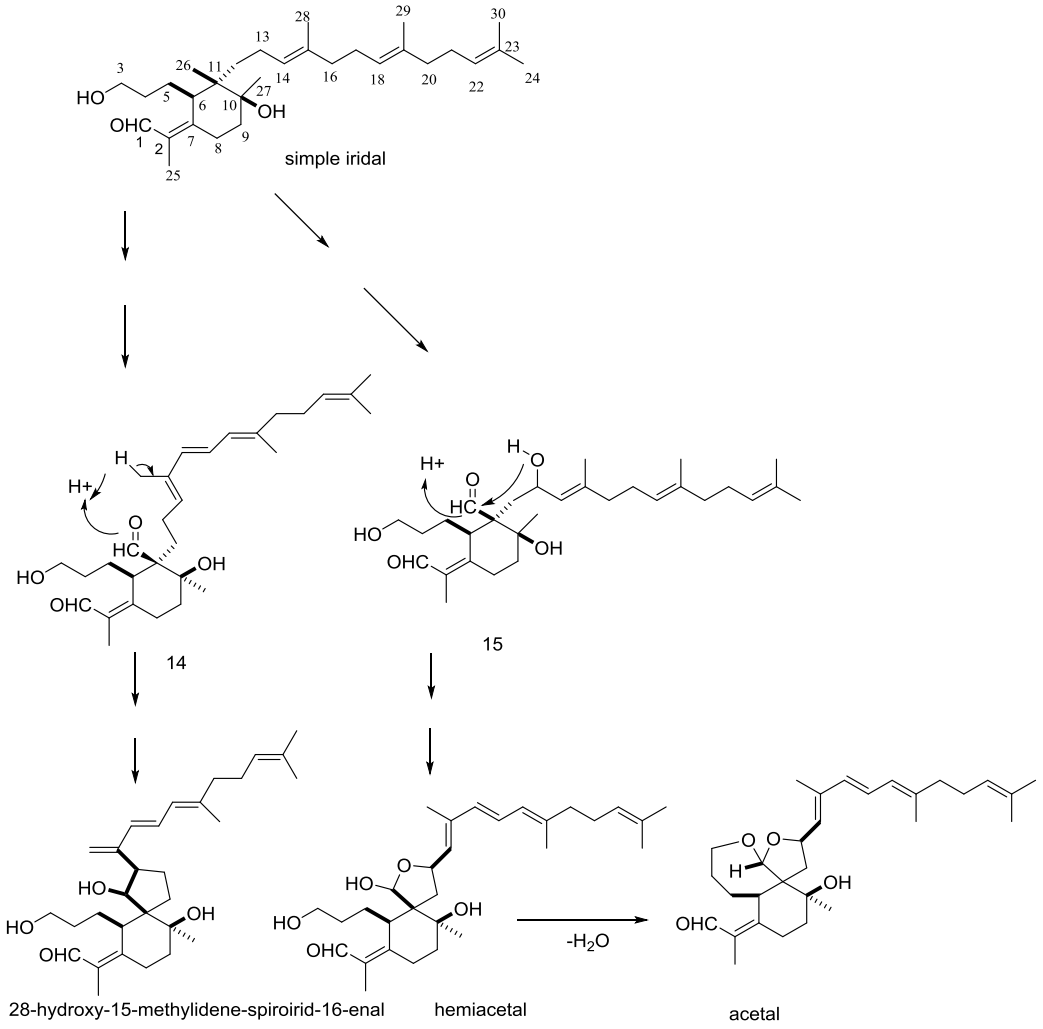

Figure 33. Possible biosynthetic pathways to the spiroiridals.

An additional unsaturation is introduced at C 15, 28 of the prenyl side chain of a simple iridal and oxidation at C-26 result in an aldehyde **14**. The spiroiridal, 28-hydroxy-15-methylidene-spiroirid-16-enal is formed by acid catalyzed addition of C-14 to the aldehyde.

The spirobicyclic hemiacetal, 26-hydroxy-15-methylidene-spiroirid-16-enal and anhydrobelachinal belong to a group of oxaspiriridals isolated from *Iris domestica* and showed ichthyotoxic activity. [45] In the synthesis of hemiacetal C-13 is hydroxylate as well as C-26 , leading to a hydroxyl aldehyde **15**. This then cyclizes to give the cyclic hemiacetal. Dehydration at C-26 and addition of the C-3 OH of hemiacetal result anhydrobelachinal as seen in Figure 33.

In the presence of second ring formed by cyclization of the farnesyl side chain result bi-cyclic iridals, called cycloiridals. Hoogianal from *Iris hoogiana* is an example of cycloiridal.[47] The oxidative degradation of hoogianal yielded β-irone, a compound of interest in perfumery due to its violet aroma. Cycloiridals are considered to be derived from iridals. It has been suggested that the biosynthesis of hoogianal proceeds via the corresponding iridals, which suffer a S-adenosylmethioninemediated monocyclization initiated on the terminal double bond of the farnesyl side chain (Figure 34).

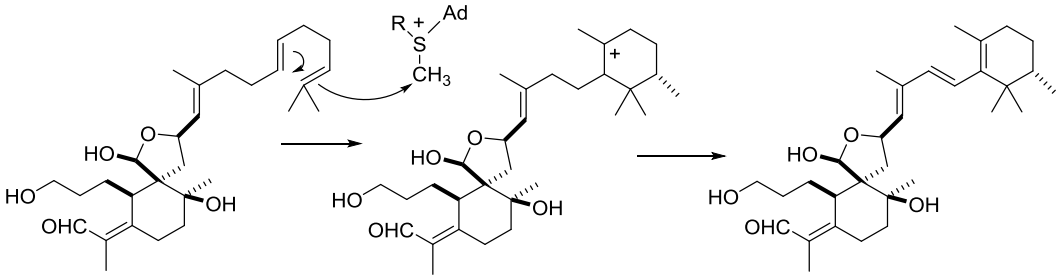

Figure 34. Proposed biosynthesis of cycloiridals.

All of these iridals display a wide range of biological properties including ichthyotoxicity, cytotoxicity, tumor-promoting activity, antiplasmodial activity, neuroprotective activity and PKC activation. [47- 51] Their unique structures as well as diverse biological properties make iridals attractive targets for isolation and chemical synthesis.

The complete assignment of proton and carbon, and hence structure elucidation of iridals were facilitated by the measurements of ^{1}C NMR, ^{1}H NMR, HMQC, HMBC and ^{1}H-^{1}H COSY spectra in the present study.

Results and discussion

In an attempt to identify novel compounds with antitrypanosomal activity, *in vitro* high throughput screening assays were conducted using TCM plant extracts. The crude petrol extract of *I. domestica* was selected for further study based on the high antitrypanosomal activity and low toxicity to a mammalian cell line at 50 µg/mL. Bioassay-guided fractionation of the extract afforded four fractions with pronounced activity against *T. brucei* (FIII-FVI). ^{1}H-NMR analysis of all four fractions showed aldehyde signals (δ 9-10) as well as alkenes (δ 5-6), indicating the presence of iridals. Two of the fractions (FIV and FVI) were purified further to afford the myristate ester of isoiridogermanal (**16**) and free anhydrobelachinal (**17**), respectively as seen in Figure 35.

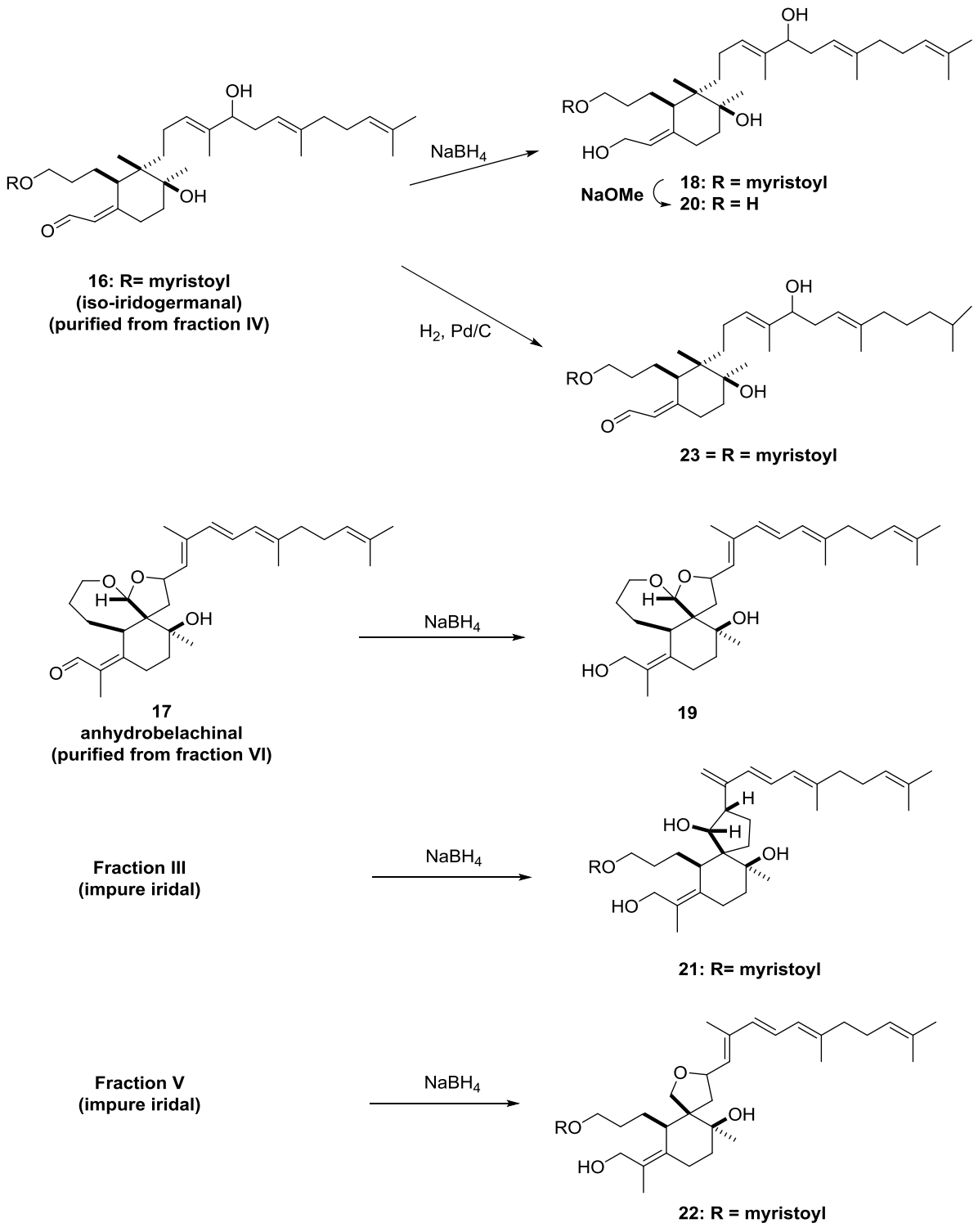

Figure 35. Structures of isolated iridals and semi-synthetic analogs.

Key features indicating the isoiridogermanal structure included the aldehyde signals (^{1}H-NMR δ10.25; ^{13}C-NMR δ 198) and the C16 hydroxyl (^{1}H-NMR δ3.98; ^{13}C-NMR δ 75). Key features indicating the anhydrobelachinal structure included the aldehyde signals (^{1}H-NMR δ10.28; ^{13}C-NMR δ 190) and the C26 acetal (^{1}H-NMR δ5.44; ^{13}C-NMR δ 111.1), as well as the presence of five vinyl CH's as seen in Figure 36.

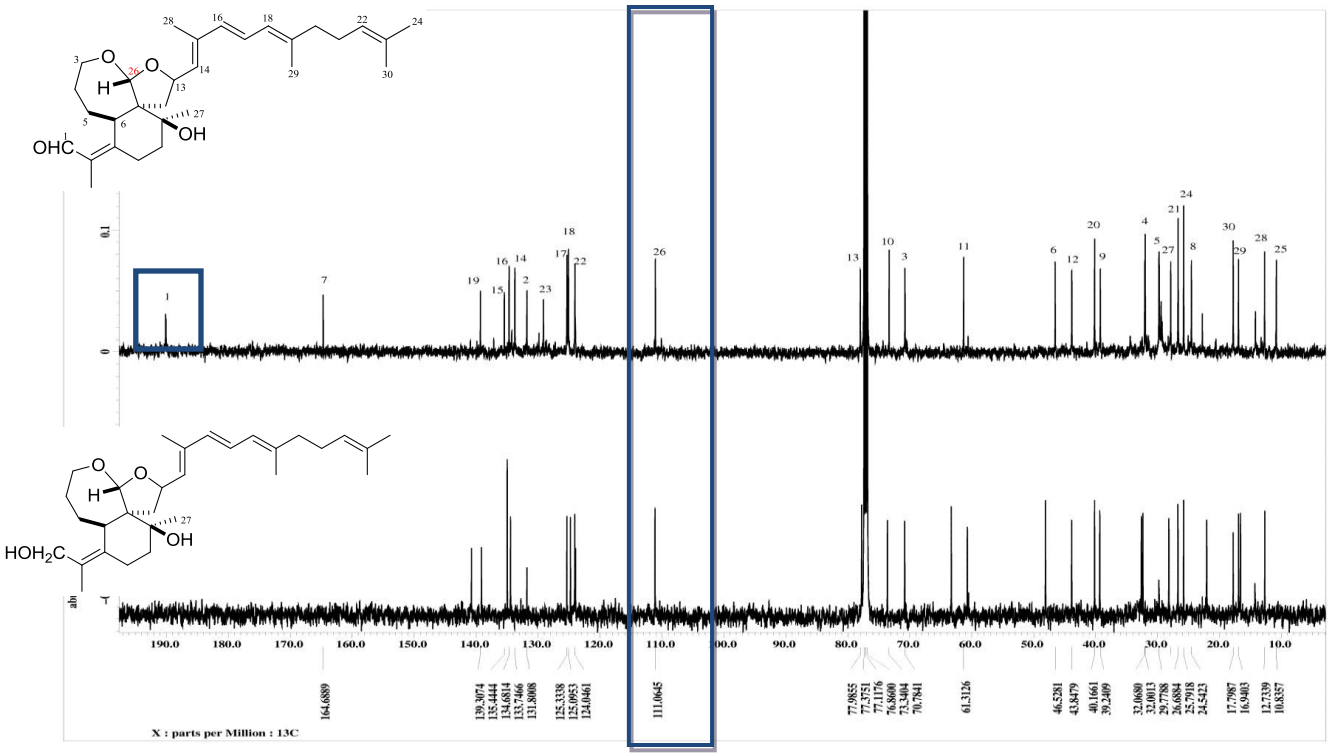

Figure 36. Overlay of ^{13}C NMR of anhydrobelachinal and reduced anhydrobelachinal.

The spectra were identical to that previously reported for both of these compounds, with further confirmation by HRMS. As previously reported, these known aldehydes are unstable, explaining the difficulties encountered in purification and storage. [45, 46] In an attempt to improve

stability, the isoiridogermanal and anhydrobelachinal were reduced to the corresponding novel allylic alcohols **18** and **19** respectively**,** which retained bioactivity. Saponification of the myristoyl ester of compound **18** afforded the isoiridogermanal analog **20** (Figure 35). Key features indicating the presence of eight vinyl arbons and 4 alcohol peaks in ^{13}C NMR as seen in figure 37.

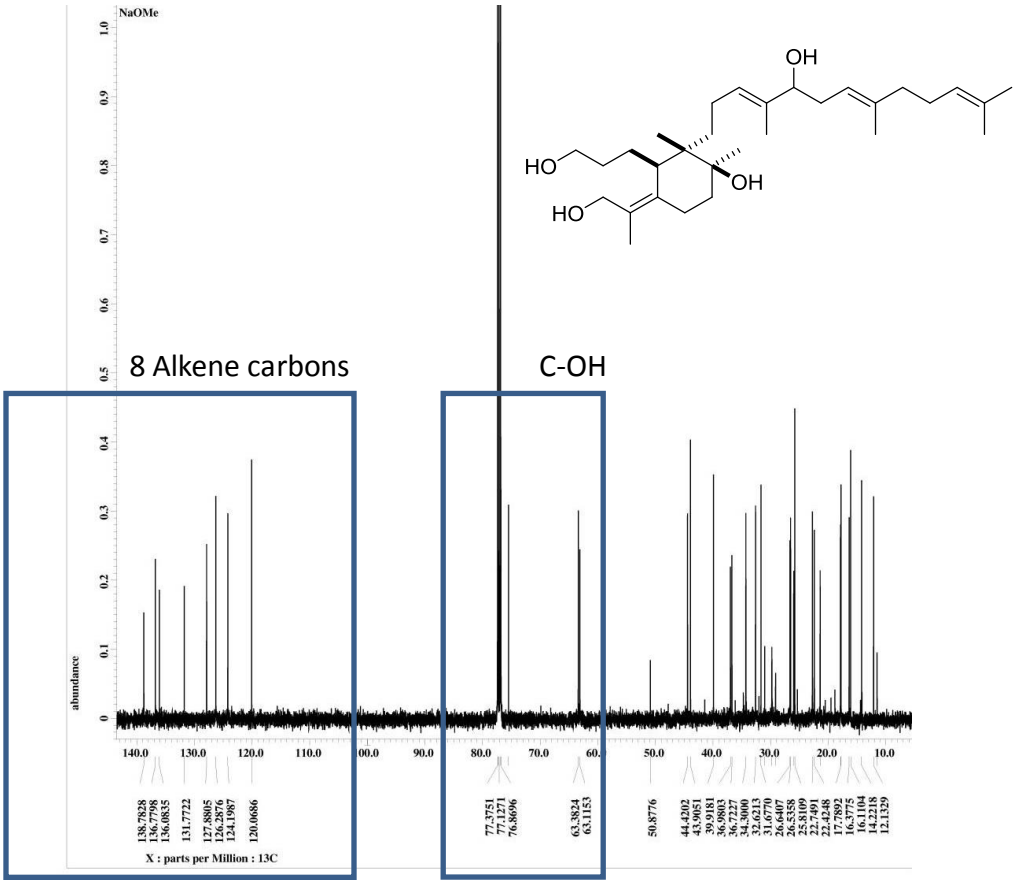

Figure 37. ^{13}C NMR of isoiridogermanal analog **20**.

The reduction of compounds **16** and **17** increased stability with only minor changes in bioactivity. Since it was difficult to obtain pure iridals from the active Fractions III and V, the impure fractions were reduced directly and two additional allylic alcohols were isolated from the mixtures, affording compounds **21** and **22**, respectively. Based on the NMR analysis, the alcohol **21** is the reduced analog of the known iridal 26-hydroxy-15-methylidene-spiroirid-16-enal.[43, 46] Key features included the vinyl CH_2 (^{1}H-NMR δ5.0, 5.28; ^{13}C-NMR and $DEPT_{135}$ δ117) and the hydroxyl at C26 (^{1}H-NMR δ5.46; ^{13}C-NMR δ 73) as seen in figure 38. Analysis by HMBC placed the vinyl CH_2 at C28, with correlations to C14 and C16.

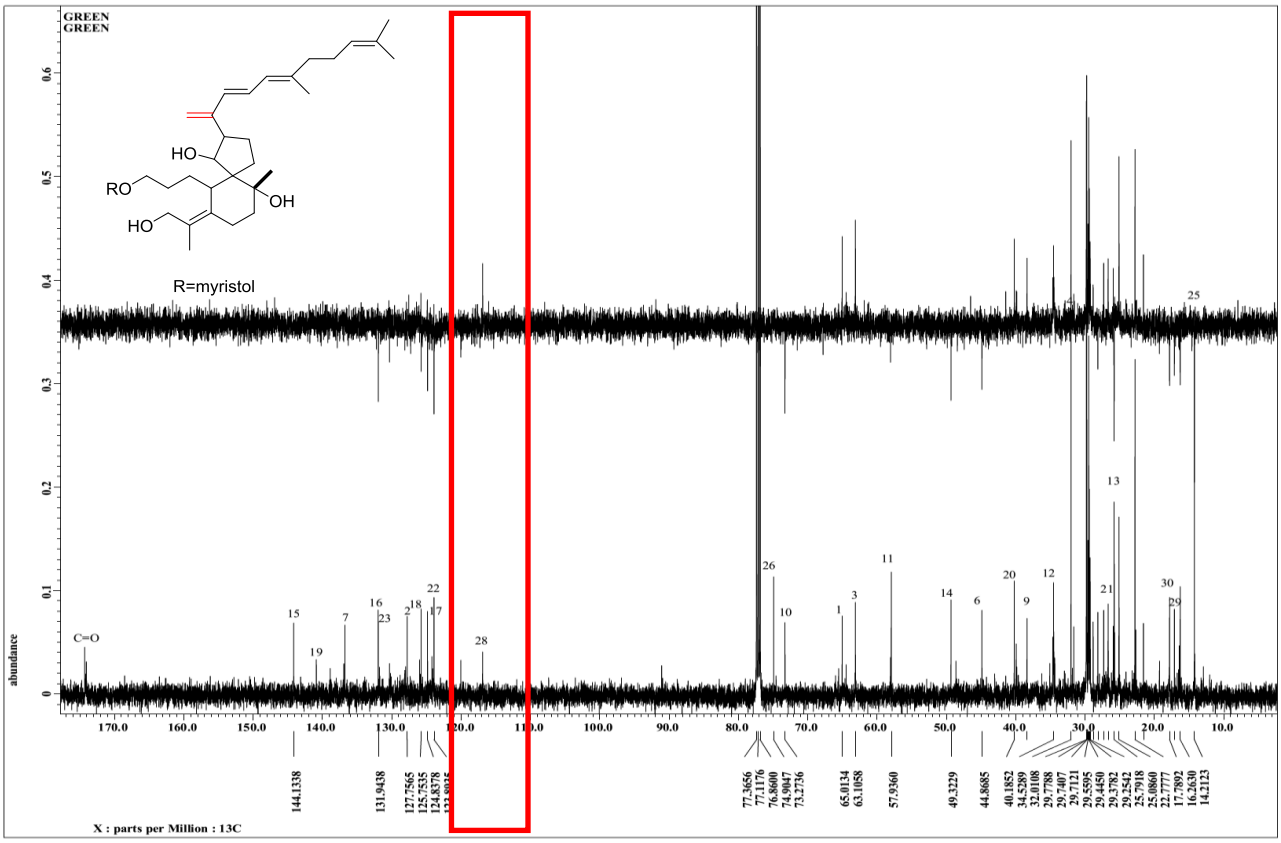

Figure 38. ^{13}C NMR analysis, the alcohol **21,** the reduced analog of the known iridal 26-hydroxy-15-methylidene-spiroirid-16-enal.

Key features included the vinyl CH_2 (^{13}C-NMR (bottom) and $DEPT_{135}$ (top) at δ117)

The alcohol **22** is the reduced analog of the known iridotectoral C that has previously been isolated from *I. domestica*.[43] Key features included the C26 acetal (^{1}H-NMR δ4.9, ^{13}C-NMR δ106) and the methoxy (^{1}H-NMRδ3.36; ^{13}C-NMR δ 54), as well as the presence of five vinyl CH signals as seen in Figure 39.

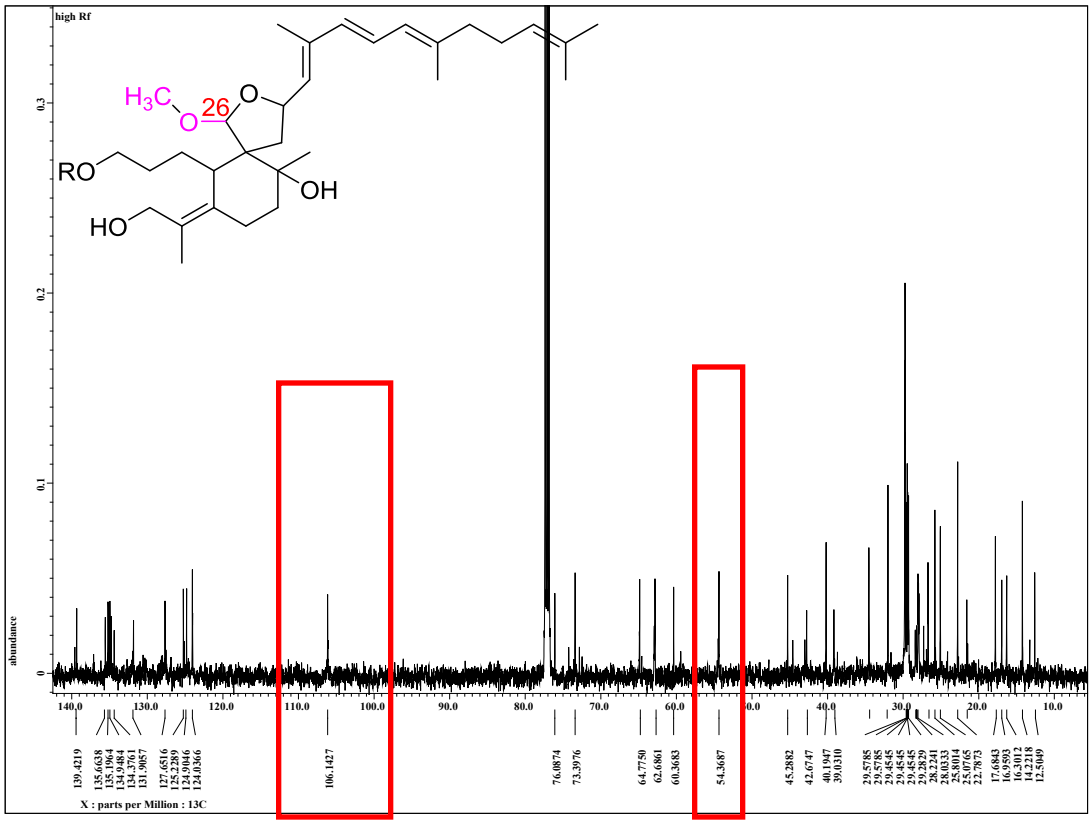

Figure 39. ^{13}C NMR of reduced analog of the known iridotectoral C.

Key features included the C26 acetal (^{13}C-NMR δ106) and the methoxy (^{13}C-NMR δ 54).

Table 2: ^{1}H-NMR data (500 MHz, $CDCl_3$); (J value in Hz in parentheses)

	18	**19**	**20**	**21**	**22**	**23**
1	4.11 t (6.6)	4.18 br s	4.08, 4.16 ABq (11.7)	4.0 m, 4.22 m	4.18, 4.22 m	4.13 m
2	--	--	--	--	--	--
3	4.01 t (6.6)	3.51 dt, 4.18 m	3.56 t (13.2)	4.20 br s	3.98, 4.08 m	4.01 m
4	1.24,1.33 m	1.6-1.8 m	1.3 m	1.6 m	1.28 m	1.3 m
5	2.01 m	2.8-3.0 m	1.9 m	1.5 m	1.80 m	1.7 m
6	2.5 m	2.30 m	2.54 m	2.79 m	2.9 m	2.6 m
7	--	--	--	--	--	--
8	2.27 m	2.27 m	2.54 m	2.35 m	2.35 m	2.3 m
9	1.68 m	1.6-1.8 m	1.75 m	1.45 m	1.67 m	1.4 m
10	--	--	--	--	--	--
11	--	--	--	--	--	--
12	1.25 m	1.4 dd, 2.0 m	1.3 m	2.2 m	1.3 m	1.3 m
13	1.95 m	4.86 q (8.02)	1.95 m	1.6 m	4.83 m	2.0 m
14	5.07 m	5.62 d (8.54)	5.07 m	3.0 m	5.5 d (8.6)	5.06 m
15	--	--	--	--	--	--
16	3.98 dd (5.1)	6.17 d (15.5)	3.93 t (13.9)	6.2 d (16)	6.1 d (7.4)	3.92 m
17	2.25 m	6.38 dd (10.9, 15.5)	2.3 m	6.39 dd (10.9, 15.5)	6.40 dd (4.0, 6.3)	2.26 t (7.5)
18	5.28 t (6.9)	5.87 d (10.9)	5.24 t (6.9)	5.88 d (10.9)	5.88 d (11.5)	5.29 m
19	--	--	--	--	--	--
20	2.03 m	2.08 m	2.03 m	2.11 m	2.09 m	2.03 m
21	2.05 m	2.09 m	2.07 m	1.4-1.6 m	2.08 m	
22	5.09 m	5.09 m	5.06 m	5.09 m	5.09 m	5.05 m
23	--	--	--	--	--	--
24	2.03 s	1.68 s	1.67 s	1.68 s	1.67 s	1.61 d (13.1)
25	1.33 s	1.77 s	1.83 s	1.80 s	1.81 s	1.61 s
26	1.09 s	5.39 s	1.09 s	4.33 d (4.0)	5.0 s	1.10 s
27	1.00 s	1.28 s	1.00 s	0.91 s	1.24 s	1.00 s
28	1.61 s	1.77 s	1.61 s	5.02 s, 5.26 s	1.79 s	1.67 s
29	1.64 s	1.77 s	1.60 s	1.79 s	1.77 s	1.61 s
30	1.62 s	1.60 s	1.58 s	1.66 s	1.60 s	1.61 d (13.1)
2'-13'	2.3,1.2-1.3	--	--	2.3,1.2-1.3	2.3,1.2-1.3	2.3,1.2-1.3
14'	0.87 t (7.2)	--	--	0.87 m	0.87 m	0.87 m
CH3O	--	--	--	--	3.34 s	--

Table 3**:** ^{13}C-NMR data (125 MHz, $CDCl_3$); (multiplicity from DEPT in parentheses)

C	**18**	**19**	**20**	**21**	**22**	**23**
1	63.6 (CH2)	63.3 (CH2)	63.1 (CH2)	65.0 (CH2)	64.9 (CH2)	63.2 (CH2)
2	135.9 (C)	139.1 (C)	136.1 (C)	137.9 (C)	139.4 (C)	135.6 (C)
3	64.8 (CH2)	70.8 (CH2)	63.4 (CH2)	63.1 (CH2)	62.8 (CH2)	64.9 (CH2)
4	34.3 (CH2)	32.4 (CH2)	32.7 (CH2)	32.0 (CH2)	34.5 (CH2)	32.0 (CH2)
5	22.8 (CH2)	32.8 (CH2)	26.6 (CH2)	29.5 (CH2)	29.3 (CH2)	26.1 (CH2)
6	44.3 (CH)	48.1 (CH)	44.0 (CH)	44.9 (CH)	45.3 (CH)	44.3 (CH)
7	128.2 (C)	124.0 (C)	127.9 (C)	127.5 (C)	127.6 (C)	128.2 (C)
8	21.4 (CH2)	22.1 (CH2)	22.4 (CH2)	22.8 (CH2)	25.1 (CH2)	21.4 (CH2)
9	39.9 (CH2)	39.3 (CH2)	36.7 (CH2)	38.3 (CH2)	38.7 (CH2)	38.2 (CH2)
10	76.9 (C)	73.6 (C)	76.9 (C)	74.9 (C)	73.4 (C)	75.0 (C)
11	43.9 (C)	60.7 (C)	44.3 (C)	57.9 (C)	60.4 (C)	43.9 (C)
12	36.7 (CH2)	43.9 (CH2)	37.1 (CH2)	34.5 (CH2)	42.8 (CH2)	37.0 (CH2)
13	22.4 (CH2)	77.8 (CH)	22.8 (CH2)	25.1 (CH2)	76.1 (CH)	22.4 (CH2)
14	126.3 (CH)	124.4 (CH)	126.3 (CH)	49.3 (CH)	125.2 (CH)	128.6 (CH)
15	138.9 (C)	140.7 (C)	136.8 (C)	144.1 (C)	134.8 (C)	141.0 (C)
16	75.4 (CH)	135.0 (CH)	75.4 (CH)	131.9 (CH)	135.2 (CH)	77.3 (CH)
17	34.5 (CH2)	124.8 (CH)	34.3 (CH2)	124.8 (CH)	134.9 (CH)	34.5 (CH2)
18	120.1 (CH)	125.4 (CH)	120.1 (CH)	125.7 (CH)	135.2 (CH)	120.0 (CH)
19	136.9 (C)	139.1 (C)	138.8 (C)	141.0 (C)	135.6 (C)	136.0 (C)
20	37.1 (CH2)	40.2 (CH2)	39.9 (CH2)	40.2 (CH2)	40.2 (CH2)	37.1 (CH2)
21	25.1 (CH2)	26.7 (CH2)	25.3 (CH2)	26.6 (CH2)	26.7 (CH2)	25.1 (CH2)
22	124.2 (CH)	124.1 (CH)	124.2 (CH)	123.9 (CH)	124.0 (CH)	22.8 (CH2)
23	131.8 (C)	131.8 (C)	131.8 (C)	131.9 (C)	131.8 (C)	26.1 (CH)
24	25.8 (CH3)	25.8 (CH3)	25.8 (CH3)	25.8 (CH3)	25.8 (CH3)	14.2 (CH3)
25	16.1 (CH3)	16.6 (CH3)	16.1 (CH3)	14.2 (CH3)	16.3 (CH3)	17.9 (CH3)
26	26.6 (CH3)	111.1 (CH)	26.6 (CH3)	73.3 (CH)	106.2 (CH)	26.6 (CH3)
27	17.8 (CH3)	28.2 (CH3)	17.8 (CH3)	27.8 (CH3)	16.9 (CH3)	17.9 (CH3)
28	12.1 (CH3)	12.7 (CH3)	12.1 (CH3)	116.9 (CH2)	12.6 (CH3)	14.2 (CH3)
29	16.4 (CH3)	16.9 (CH3)	16.4 (CH3)	17.1 (CH3)	16.4 (CH3)	16.1 (CH3)
30	17.9 (CH3)	17.8 (CH3)	17.8 (CH3)	17.8 (CH3)	17.8 (CH3)	14.2 (CH3)
1’	174.2 (C)	--	--	174.3 (C)	174.3 (C)	174.2 (C)
2’-13’	29.2-29.7 (CH2)	--	--	29.2-29.7 (CH2)	29.2-29.7 (CH2)	29.2-29.7 (CH2)
14’	14.2 (CH3)	--	--	14.2 (CH3)	14.2 (CH3)	14.2 (CH3)
CH3O	--	--	--	--	54.5 (CH3)	--

The semi-synthetic allylic alcohols provide some SAR in this series, with all of the alcohols retaining bioactivity. Also, all with a free C3 alcohol were isolated as the myristate esters, and the C3 ester is not a requirement for activity, with the saponified derivative, compound **20,** retaining activity. However, partial hydrogenation of the side chain of **18** led to an inactive compound **23**, indicating that the C22, 23 alkene in the side chain is required for activity. All compounds were also tested against L6 (toxicity), *T. brucei* and the intracellular and extracellular forms of *T. cruzi*. Results are summarized in Table 4.

Table 4. Antitrypanosomal activity, toxicity, and selectivity of selected compounds.

	IC_{50} (µg/mL)[1]				Selectivity Multiple [5]		
Comp.	*T. brucei (BSF)*	*T. cruzi (TM)*	*T. cruzi (I)*	L6 Toxicity	Tb/L6	Tc (TM) / L6	Tc (I) / L6
16	3.6	NT	>50	136	37.78	ND	ND
17	5.42	>50	>50	49.07	9.05	ND	ND
18	5.4	>50	>50	>100	>18.52[4]	ND	ND
19	2.13	17.09	ND [2]	35.14	16.05	2.02	ND
20	6.21	22.39	ND [2]	22.71	3.66	0.16	ND
21	2.4	14.68	>50	26.27	10.95	0.75	ND
22	2	25.3	>50	36.043	18.02	0.71	ND
23	>50	>50	>50	>100	ND	ND	ND
Pent.	0.16	NT	NT	NT	ND	ND	ND

[1] Tb BSF = bloodstream form trypomastigotes . Tc TM = T. cruzi trypomastigotes (Tulahuen, 24h CellTiter Glo Assay) , Tc I = T. cruzi intracellular assay (96h CPRG Glo Assay), L6 (rat skeletal myoblasts, 72h PrestoBlue Assay). NT= not tested, ND = could not be determined. Mean of 2 or more independent trials. Standard error of the mean <3, except as noted. [2] Doses that produced > 50% inhibition of T. cruzi were excluded as false positives due to host cell interference (host toxicity >10%) [3] SEM=5.8. [4]Selectivity estimated using L6 IC_{50} = 100 ug/mL.

This is the first report of the possible use of *Iris domestica* extracts to treat trypanosomal diseases. Although iridals have previously been reported as having several types of bioactivity, there are no prior reports of antitrypanosomal activity of compounds in this family. The reported iridals have previously been isolated from *I. domestica*, however there are no reports of antitrypanosomal activity of these compounds. Limited SAR indicates that neither the aldehyde nor the ester are not required for activity, with the corresponding allylic alcohols **18**, **19**, **20**, **21** and **22** maintaining moderate activity against trypanosomes. However, the triene side chain seems to be required, with the partially saturated derivative **23** losing all activity against *T. brucei*. Seven of the compounds (**16-22**) produced strong activity against *T. brucei* with IC_{50} doses <10 µg/mL. Five of these (**16**, **18**, **19**, **21** and **22**) had therapeutically relevant selectivity multiplies (>10 compared with L6 toxicity). Although extracellular *T. cruzi* IC_{50} doses ranging from 14.68-25.30 µg/mL were produced by **19-22**, all failed to produce relevant selectivity multiples or activity in *T. cruzi* intracellular assays.

Materials and methods

Instrumentation and chromatography material

NMR data were obtained using a 500 MHz FT-NMR model ECA-500 JEOL (Peabody, MA) purchased with funding provided by the National Science Foundation through the NSF-MRI program (#0321211).

High resolution ESI-MS was performed at Notre Dame University, Notre Dame, Indiana.

Thin layer chromatograpy (TLC) was performed on glass plates coated with silica gel and UV active backing purchased from Fisher Scientific, Pittsburgh, PA. The TLC plates were analyzed with a short wavelength (254 nm) UV light and subsequently stained with phosphomolybdic acid (reagent grade, Aldrich, Milwaukee, WI) prepared as a 10% solution in ethanol. Gravity column chromatography was performed with silica gel, 63-200 micron 70-230 mesh ASTM (reagent grade, Fisher Scientific, Pittsburgh, PA). Flash column chromatography was performed with silica gel, 60 Å 230-400 mesh ASTM, reagent grade, Fisher Scientific, (Pittsburgh, PA). Methylene chloride, methanol, acetone, ethyl acetate, ethanol, and hexanes were purchased from Fisher Scientific, (Pittsburgh, PA). HPLC was performed using a Breeze Waters System with a normal phase Waters Spherisorb column (10 x 250 mm).

Plant material

The whole plant of *I. domestica* was collected at the Cultivation Center at Guangxi Botanical Garden of Medicinal Research, Nanning, Guangxi Autonomous Region, P.R. China, in Jun 2009, and identified by Dr. Xueyan Huang (Guangxi Botanical Garden of Medicinal Research, Nanning, P. R. China). A voucher specimen (No. 200906010) has been deposited in the natural product library at Guangxi Botanical Garden of Medicinal Research.

Cell lines and culture conditions

Trypanosoma brucei brucei 427 cells were maintained in 75 cm^2 tissue culture flasks (Corning, Corning, NY) by subculturing every 2-3 days. Cells were grown in HMI-9 medium supplemented with 10% heat inactivated fetal calf serum (FCS) and 50 IU/mL penicillin and 50 μg/streptomycin (HyClone, Logan, UT) with incubation at 37ºC and 5% CO_2. Stock cultures of *T. b. brucei* 427 were kindly provided by Dr. James Morris at Clemson University.

The rat skeletal myoblast cell line, L6 (ATCC CRL-1458, ATCC, Rockville, MD), was used as a mammalian toxicity model. Cells were maintained in 75 cm^2 tissue culture flasks (Corning, Corning, NY) by subculturing every 2-3 days. Cells were grown in DMEM (HyClone, Logan, UT) supplemented with 10% heat inactivated fetal calf serum (FCS, Atlanta Biological, Atlanta, GA) and 50 IU/mL penicillin and 50 μg/mL streptomycin solution (P/S, HyClone, Logan, UT) with incubation at 37°C and 5% CO_2.

Trypanosoma cruzi Tulahuen trypomastigotes expressing β-galactosidase (Buckner, 1996) were added to adherent L6 cells and incubated in DMEM without phenol red (HyClone, Logan, UT) supplemented with 10% heat inactivated FCS and 1% penicillin-streptomycin-glutamate solution (HyClone, Logan,UT) at 37°C and 5% CO_2. Trypomastigotes that burst from infected L6 cells were collected and used in assays or to infect new flasks of L6 cells. Initial stock cultures of *T. cruzi* were kindly provided by Dr. Ana Rodriguez at New York University School of Medicine.

Extraction and isolation

Dried and powdered plant material was extracted with petrol, and the solvent was evaporated. The extract was found to exhibit significant inhibitory activity against *Trypanosoma brucei* with 100% inhibition at 50 μg/mL.

The petrol extract (1g) was purified by gravity column chromatography on silica gel. The gravity column was eluted successively with hexanes, mixtures of hexanes and EtOAc, and pure EtOAc, respectively, to yield seven fractions (FI to FVII). FIV (392 mg) eluted with 45% EtOAc/hexanes. Flash column chromatography of FIV eluting successively with hexanes, mixtures of hexanes and EtOAc, and pure EtOAc afforded three fractions (FIVA, FIVB and FIVC). FIVC (70 mg) eluted with 10% EtOAc/Hex and was identified as isoiridogermanal **16** by NMR and MS. Attempts at further purification by HPLC led to decomposition. This compound has previously been reported as being unstable. ^{1}H-NMR and ^{13}C-NMR (C_6D_6) data were identical to that previously reported in the literature, and confirmed by HRMS. (Abe, et al., 1991). MS (C_{30} H_{76} O_5 Na, calculated, 707.5590, found, 707.5585).

Flash column chromatography of FVI (117 mg), eluting successively with hexanes, mixtures of hexanes and EtOAc, and pure EtOAc afforded two fractions (FVIA and FVIB). FVIA (53 mg) eluted with 15% EA/Hex as a white powder, was identified as anhydrobelachinal **17** by NMR and MS (C_{30} H_{45} O_4, calculated, 469.3318, found, 469.3328). R_f 0.72 [ethyl acetate-hexane 1:1]. $[\alpha]_D$ = + 70.6 ($CHCl_3$, c =0.002).

Reduction of iridals and extract fractions

Iso-iridogermanol -3-myristate (**18**)

To a solution of iso-iridogermanal, **16** (75.0 mg, 0.10 mmol) in 6 mL methanol was added sodium borohydride (43.0 mg, 1.13 mmol). The resulting solution was stirred at room temperature for 4h. The solution was poured into 1M HCl, and extracted twice with ethyl acetate. The organic layer was washed with aqueous sodium bicarbonate and brine and then dried over magnesium sulfate, filtered and the solvent was evaporated. The crude product was purified by flash column chromatography on silica gel, eluting with hexanes, 1:20, 1:10, and 1:5 ethyl acetate-hexane and ethyl acetate to afford 20.4 mg of the allylic alcohol, iso-iridogermanol **18** (27.2%). R_f 0.75 [ethyl acetate-hexane 1:1]. $[\alpha]_D$ = +6.6° ($CHCl_3$, c = 0.01); ^{1}H NMR (500 MHz, $CDCl_3$) δ 0.87 (3H, t, J=7.2 Hz), 1.00 (3H, s), 1.09 (3H, s), 1.24, 1.33 (2H, m), 1.25 (2H, m), 1.33 (3H, s), 1.61 (3H, s), 1.62 (3H, s), 1.64 (3H, s), 1.68 (2H, m), 1.95 (2H, m), 2.01 (2H, m), 2.03 (3H, s), 2.03 (2H, m), 2.05 (2H, m), 2.25 (2H, m), 2.27 (2H, m), 2.3, 1.2-1.3 (24H), 2.5 (1H, m), 3.98 (1H, dd, J=5.1 Hz), 4.01 (2H, t, J=6.6 Hz), 4.11 (2H, t, J=6.6 Hz), 5.07 (1H, m), 5.09 (1H, m), 5.28 (1H, t, J=6.9 Hz); ^{13}C NMR (125 MHz, CDCl3) δ 63.6 (C-1), 135.9 (C-2), 64.8 (C-3), 34.3 (C-4) 22.8 (C-5), 44.3 (C-6), 128.2 (C-7), 21.4 (C-8), 39.9 (C-9), 76.9 (C-10), 43.9 (C-11), 36.7 (C-12), 22.4 (C-13), 126.3 (C-14), 138.9 (C-15), 75.4 (C-16), 34.5 (C-17), 120.1 (C18), 136.9 (C-19), 37.1 (C-20), 25.1 (C-21), 124.2 (C-22), 131.8 (C-23), 25.8 (C-24), 16.1 (C-25), 26.6 (C-26), 17.8 (C-27), 12.1 (C-28), 16.4 (C-29), 17.9 (C-30), 174.2 (C-1'), 29.2-29.7 (C-2'-13'), 14.2 (C-14'); positive HR-ESI-MS at *m/z* [M + Na] for $C_{44}H_{78}O_5Na$, calculated, 709.5747, found, 709.5741.

Anhydrobelachinol (**5**)

To a solution of 245 mg of anhydrobelachinal**, 17** (245 mg, 0.52 mmol) in 30 mL methanol was added sodium borohydride (186.2 mg, 4.9 mmol). The resulting solution was stirred at room temperature for 4h. The solution was poured into 1M HCl, and extracted twice with ethyl acetate. The organic layer was washed with aqueous sodium bicarbonate and brine and then dried over magnesium sulfate, filtered and evaporated. The crude product was purified with preparative thin layer chromatography, eluting with 1:1 ethyl acetate-hexane to afford 14.9 mg of the corresponding alcohol anhydrobelachinol **19**. R_f 0.52 [ethyl acetate-hexane 1:1]; $[\alpha]_D$ = +30.77 ($CHCl_3$, c =0.03); ^{1}H NMR (500 MHz, $CDCl_3$) δ 1.28 (3H, s), 1.44 (2H, dd) 1.60 (3H, s),1.6-1.8 (2H, m), 1.68 (3H, s), 1.77 (3H, s), 1.77 (3H, s), 1.77 (3H, s), 2.08 (2H, m), 2.09 (2H, m), 2.27 (2H, m), 2.30 (1H, m), 2.8-3.0 (2H, m), 3.51 (2H, dt), 4.18 (2H, m), 4.86 (1H, q, J=8.02 Hz), 5.09 (1H, m), 5.39 (1H, s), 5.62 (1H, d, 8.54 Hz), 5.87 (1H, d, J= 10.9 Hz), 6.17 (1H, d, J=15.5 Hz), 6.38 (1H, dd, J=10.9 Hz, 15.5 Hz); ^{13}C NMR (125 MHz, CDCl3) δ ^{13}C NMR (500 MHz, CDCl3) δ 63.3 (C-1), 139.1 (C-2), 70.8 (C-3), 32.4 (C-4), 32.8 (C-5), 48.1 (C-6), 124.0 (C-7), 22.1 (C-8), 39.3 (C-9), 73.6 (C-10), 60.7 (C-11), 43.9 (C-12), 77.8 (C-13), 124.4 (C-14), 140.7 (C-15), 135.0 (C-16), 124.8 (C-17), 125.4 (C-18), 139.1 (C-19), 40.2 (C-20), 26.7 (C-21), 124.1 (C-22), 131.8 (C-23), 25.8 (C-24), 16.6 (C-25), 111.1 (C-26), 28.2 (C-27), 12.7 (C-28), 16.9 (C-29), 17.8 (C-30); positive HR-ESI-MS at *m/z* [M + Na] for $C_{30}H_{46}O_4Na$, calculated, 493.3294, found, 493.3288.

Iso-iridogermanol (**20**)

Iso-iridogermanol -3-myristate **(18)** (50.0 mg, 0.07 mmol) was dissolved in 5 mL NaOMe/methanol. The resulting solution was stirred at room temperature for 24h. The solution was poured into 1M HCl, and extracted twice with ethyl acetate. The organic layer was washed with aqueous sodium bicarbonate and brine and then dried over magnesium sulfate, filtered and evaporated. The crude product was purified by flash column chromatography on silica gel, eluting with 20%, 30%, 40%, 60% and 80% ethyl acetate-hexane and ethyl acetate to afford 25 mg of compound **20** (75%). R_f 0.18 [ethyl acetate-hexane 1:1]; $[\alpha]_D$ = +40.64 ($CHCl_3$, c =0.003); ^{1}H NMR (500 MHz, $CDCl_3$) δ 1.00 (3H, s), 1.09 (3H, s), 1.3 (2H,m), 1.3 (2H, m), 1.58 (3H, s), 1.60 (3H, s), 1.61 (3H, s), 1.67 (3H, s), 1.75 (2H, m), 1.83 (3H, s), 1.9 (2H, m), 1.95 (2H, m), 2.03 (2H, m), 2.07 (2H, m), 2.3 (2H, m), 2.54 (1H, m), 2.54 (2H, m), 3.56 (2H, t, J= 13.2 Hz), 3.93 (1H, t, J=13.9 Hz), 4.08, 4.16 (2H, ABq, J=11.7) , 5.06 (1H, m), 5.07 (1H, m), 5.24 (1H, t, J=6.9 Hz); ^{13}C NMR (125 MHz, $CDCl_3$) δ 63.1 (C-1), 136.1 (C-2), 63.4 (C-3), 32.7 (C-4), 26.6 (C-5), 44.0 (C-6), 127.9 (C-7), 22.4 (C-8), 36.7 (C-9), 76.9 (C-10), 44.3 (C-11), 37.1 (C-12), 22.8 (C-13), 126.3 (C-14), 136.8 (C-15), 75.4 (C-16), 34.3 (C-17), 120.1 (C-18), 138.8 (C-19), 39.9 (C-20), 25.3 (C-21), 124.2 (C-22), 131.8 (C-23), 25.8 (C-24), 16.1 (C-25), 26.6 (C-26), 17.8 (C-27), 12.1 (C-28), 16.4 (C-29), 17.8 (C-30); positive HR-ESI-MS at *m/z* [M + Na] for $C_{30}H_{52}O_4Na$, calculated, 499.3763, found, 499.3758.

26-Hydroxy-15-methylidene-spiroirid-16-enol-3 myristate (**21**)

To a solution of the impure extract fraction FIII (375.0 mg) in 30 mL methanol was added sodium borohydride (240.0 mg, 6.25 mmol). The resulting solution was stirred at room temperature for 4h. The solution was poured into 1M HCl, and extracted twice with ethyl acetate. The organic layer was washed with aqueous sodium bicarbonate and brine and then dried over magnesium sulfate, filtered and the solvent was evaporated. The crude product was purified by flash column chromatography on silica gel, eluting with hexanes, 5%, 10% ethyl acetate-hexane and ethyl acetate only afford 43.2 mg of crude product, which was purified by flash column chromatography on silica gel, eluting with hexanes, 5% and 10% ethyl acetate-hexane to afford three fractions. The alcohol (35.5 mg) eluted with 10% EA/Hex as an oily liquid. R_f 0.7 [ethyl acetate-hexane 2:3]; $[\alpha]_D$ = +54.16 ($CHCl_3$, c =0.005); ^{1}H NMR (500 MHz, $CDCl_3$) δ 0.87 (3H, m), 0.91 (3H, s), 1.5 (2H, m), 1.66 (3H,s), 1.6 (2H, m), 1.68 (3H,s), 1.79 (3H, s), 1.80 (3H, s), 2.08 (2H, m), 2.1 (2H, m), 2.2 (2H, m), 2.3, 1.2-1.3 (24H, m), 2.35 (2H, m), 2.79 (2H, m), 3.0 (1H, m), 4.0, 4.22 (2H, m), 4.20 (2H, br s), 4.33 (1H, d, J=4.0), 5.02 (1H, s), 5.09 (1H, m), 5.26 (1H, s), 5.5 (1H, d, J=8.6), 5.88 (1H, d, J=10.9 Hz), 6.2 (1H, d, J=16 Hz), 6.39 (1H, dd, J=10.9, 15.5 Hz); ^{13}C NMR (125 MHz, $CDCl_3$) δ 65.0 (C-1), 137.9 (C-2), 63.1 (C-3), 32.0(C-4), 29.5 (C-5), 44.9 (C-6), 127.5 (C-7), 22.8 (C-8), 38.3 (C-9), 74.9 (C-10), 57.9 (C-11), 34.5 (C-12), 25.1 (C-13), 49.3 (C-14), 144.1 (C-15), 131.9 (C-16), 124.8 (C-17), 125.7 (C-18), 141.0 (C-19), 40.2 (C-20), 26.6 (C-21), 123.9 (C-22), 131.9 (C-23), 25.8 (C-24), 14.2 (C-25), 73.3 (C-26), 27.8 (C-27), 116.9 (C-28), 17.1 (C-29), 17.8 (C-30); positive HR-ESI-MS at *m/z* [M + Na] for C_{44} H_{74} O_5 Na, found, 705.5428 calculated 705.5434.

Iridotectorol-3 myristate (**22**)

To a solution of the impure extract fraction FV, (300.0 mg) in 25 mL methanol, sodium borohydride (190.0 mg, 5.0 mmol) was added. The resulting solution was stirred at room temperature for overnight. The solution was poured into 1M HCl, and extracted twice with ethyl acetate. The organic layer was washed with aqueous sodium bicarbonate and brine and then dried over magnesium sulfate, filtered and the solvent was evaporated. The crude product was purified by flash column chromatography on silica gel, eluting with 10%, 20%, and 30%, 40% ethyl acetate-hexane and ethyl acetate to afford 43 mg of alcohol **22**. R_f 0.92[ethyl acetate-hexane 1:1]; $[\alpha]_D$ = +59.2° ($CHCl_3$, c = 0.003); ^{1}H NMR (500 MHz, $CDCl_3$) δ 0.87 (3H, m), 1.24 (3H, s), 1.28 (2H, m), 1.3 (2H, m), 1.60 (3H, s), 1.67 (3H,s), 1.67 (2H, m), 1.77 (3H,s), 1.79 (3H, s), 1.80 (2H, m), 1.81 (3H, s), 2.08 (2H, m), 2.09 (2H, m), 2.3, 1.2-1.3 (24H,m), 2.35 (2H, m), 2.9 (1H, m),3.98,4.08 (2H, m), 4.18, 4.22 (2H, m), 5.0 (3H, s), 3.34(CH_3O, s), 4.83 (1H, m), 5.09 (1H, m), 5.5 (1H, d, J=8.6), 5.88 (1H, d, J=11.5 Hz), 6.1 (1H, d, J=7.4 Hz), 6.40 (1H, dd, J=4.0 Hz, J=6.3 Hz); ^{13}C NMR (125 MHz, CDCl3) δ 64.9 (C-1), 139.4 (C-2), 62.8 (C-3), 34.5 (C-4), 29.3 (C-5), 45.3 (C-6), 127.6 (C-7), 25.1 (C-8), 38.2 (C-9), 73.4 (C-10), 60.4 (C-11), 42.8 (C-12), 76.1 (C-13), 125.2 (C-14), 134.8 (C-15), 135.2 (C-16), 134.9 (C-17), 135.2 (C-18), 135.6 (C-19), 40.2 (C-20), 26.7 (C-21), 124.0 (C-22), 131.8 (C-23), 25.8 (C-24), 16.3 (C-25), 106.2 (C-26), 16.9 (C-27), 12.6 (C-28), 16.4 (C-29), 17.8 (C-30), 174.3 (C-1'), 29.2-29.7 (C-2'-13'), 14.2 (C-14'), 54.5 (CH_3O); positive HR-ESI-MS at *m/z* [M + Na] for $C_{45}H_{76}NaO_6$ calculated, 735.5540, found, 735.5508.

22, 23-Dihydro-iso-iridogermanol-3-myristate (**23**)

Iso-iridogermanol -3-myristate **(18)** (50.0 mg, 0.07 mmol) was dissolved in 5 mL EtOAc and then added 50.0 mg of 10% palladium on carbon . The mixture was placed on a Parr shaker, and hydrogenated at 10psi for 18h. The mixture was filtered through Celite and washed with ethyl acetate. The filtrate was evaporated and the crude product was purified by flash column chromatography on silica gel, eluting with hexane only, 5%, 10%, 15%, ethyl acetate-hexane to afford 12.7 mg of compound **23** (10.4%). R_f 81.5% [ethyl acetate-hexane 1:1]. $[\alpha]_D$ = +29.29 ($CHCl_3$, c =0.004); ^{1}H NMR (500 MHz, $CDCl_3$) δ 0.87 (3H, m), 1.00 (3H,s), 1.10 (3H, s), 1.2-1.3, 2.3 (24H, m), 1.3 (2H, m), 1.3 (2H, m), 1.4 (2H, m), 1.61 (3H, d, J=13.1 Hz), 1.61 (3H,s),1.61 (3H, s), 1.61 (3H, d, J=13.1 Hz), 1.67 (3H, s), 1.7 (2H, m), 2.0 (2H, m), 2.03 (2H, m), 2.26 (2H, t, J=7.5 Hz), 2.3 (2H, m), 2.6 (1H, m), 3.92 (1H, m), 4.01 (2H, m), 4.13 (2H, m), 5.05 (1H, m), 5.06 (1H, m), 5.29 (1H, m); ^{13}C NMR (125 MHz, $CDCl_3$) δ 63.2 (C-1), 135.6 (C-2), 64.9 (C3), 32.0 (C-4), 26.1 (C-5), 44.3 (C-6), 128.2 (C-7), 21.4 (C-8), 38.2 (C-9), 75.0 (C-10), 43.9 (C-11), 37.0 (C-12), 22.4 (C-13), 128.6 (C-14), 141.0 (C-15), 77.3 (C-16), 34.5 (C-17), 120.0 (C-18), 136.0 (C-19), 37.1 (C-20), 25.1 (C-21), 22.8 (C-22), 26.1 (C-23), 14.2 (C-24), 17.9 (C-25), 26.6 (C-26), 17.9 (C-27), 14.2 (C-28), 16.1 (C-29), 14.2 (C-30), 174.2 (C-1'), 29.2-29.7 (C-2'-13'), 14.2 (C-14'); positive HR-ESI-MS at *m/z* [M + Na] for $C_{44}H_8NaO_5$ calculated, 711.5903, found, 711.5723.

Bioassays

Log phase bloodstream form *T. brucei* cultures were adjusted in fresh media to deliver $1x10^4$ cells per well in 90 μL into clear 96 well microtiter plates (Corning, Corning, NY). Extract samples were dissolved in DMSO and diluted in fresh media such that the addition of 10 μL would produce final test concentrations ranging from 3.125 μg/mL – 50 μg/mL. Maximum test concentrations of DMSO did not exceed 0.5%. Control wells were treated with pentamidine (Sigma-Aldrich, St. Louis, MO), DMSO, or media only. Each condition was plated in triplicate. Treated samples were incubated at 37°C and 5% CO_2 for 48 hours, at which time 11 μL of Presto Blue was added to each well. Plates were incubated for an additional 24 hours under the same conditions. At 72 hours, 60 μL of a 4% paraformaldehyde solution (Santa Cruz Biotechnology, Dallas, TX) was added to each well. Fluorescence was measured on a SpectraMax M5 plate reader (Molecular Devices, Sunnyvale, CA) using excitation and emission wavelengths of 560 and 590 nm, respectively. Percent inhibition was calculated based on the difference between fluorescent intensity levels of treated and untreated wells.

For toxicity assays, log phase L6 cells were trypsinized and adjusted in fresh media to deliver $5x10^3$ cells per well in 90 μL into black wall, clear bottom microtiter plates (Corning, Corning, NY). Extract samples were dissolved in DMSO and diluted in fresh media such that the addition of 10 μL would produce final well concentrations ranging from 6.25 μg/mL – 100 μg/mL. Maximum well concentrations of DMSO did not exceed 1%. Control wells were treated with podophyllotoxin (Sigma-Aldrich, St. Louis, MO), DMSO, or media only. Each condition was plated in triplicate. Treated samples were incubated at 37°C and 5% CO_2 for 71.5 hours, at which time 11 μL of the resazurin-based indicator, PrestoBlue (Invitrogen, Frederick, MD), was

added to each well. Plates were incubated for an additional 30 minutes under the same conditions. At 72 hours, fluorescent intensity was measured on a SpectraMax M5 plate reader (Molecular Devices, Sunnyvale, CA) using excitation and emission wavelengths of 560 and 590 nm, respectively. Toxicity was calculated based on the difference between fluorescent intensity levels of treated and untreated wells.

Freshly burst *T. cruzi* trypomastigotes were collected 5-7 days following infection. Separation of trypomastigote forms from amastigotes was accomplished by centrifugation at 2,700 rpm for 7 minutes, followed by incubation for 3 hours to allow trypomastigotes to swim out of the pellet. For extracellular assays, separated trypomastigotes were adjusted to deliver $4x10^4$ cells/well in 90 uL in clear 96 well plates. Extract samples were dissolved in DMSO and diluted in fresh media such that the addition of 10 µL would produce final well concentrations ranging from 0.39 – 50 µg/mL. Maximum test concentrations of DMSO did not exceed 0.5%. Control wells were treated with Amphotericin B (Sigma-Aldrich, St. Louis, MO), DMSO, or media only. Treated samples were incubated at 37°C and 5% CO_2 for 24 hours, at which time 45 µL of the luciferin-lucerase reagent, CellTiter Glo (Promega, Madison, WI), was added. Plates were shaken for 10 minutes, and incubated for an additional 15 minutes before transferring 100 uL from each well to an opaque microtiter plate (Corning, Corning, NY). Luminescence was measured using the aforementioned plate reader and inhibition calculated as described.

For intracellular assays, 45 µL of $1x10^6$ L6 cells/mL were plated in clear wall 96 well microtiter plates and allowed to adhere for 3 hours. Trypomastigotes were separated as described and 45 µL of $1x10^6$ cells/mL were added to wells along with 10 µL of test compounds. Controls included those detailed for extracellular assays with the addition of uninfected cell

controls. At 96 hours, 25 µL of a substrate solution containing 500 µM chlorophenol red β-galactopyranosidase (Sigma-Aldrich, St. Louis, MO) and 1% IPEGAL (Sigma-Aldrich, St. Louis, MO) was added and incubated for 4 hours. Absorbance readings were taken at 590 nm and percent inhibition was calculated as described.

The minimum dose that produced 50% inhibition (IC_{50}) was determined using a four parameter non-linear regression of log-transformed doses versus inhibition values with GraphPad Prism. Mean IC_{50} doses and selectivity for each compound tested against *T. brucei*, *T. cruzi*, and L6 were determined from two or more independent observations.

CHAPTER 4

CONCLUSION

Investigation of two different plant derived classes of compounds has identified compounds with both anticancer and anti-trypanosomal activity.

In one investigation, novel analogs of the plant metabolite podophyllotoxin were investigated. While podophyllotoxin acts as a microtubule inhibitor, isomerization at C4, and demethylation at C4' is known to provide useful cancer drugs such as etoposide, that act as topoisomerase II poisons. It has been proposed that the activity of etoposide requires two drugs to cleave DNA as part of its anticancer mechanism to carry out double strand DNA cleavage. To test this hypothesis, several novel flexible ether-linked dimers of demethylepipodophyllotoxin were designed and synthesized and compared to their corresponding monomers. The hypothesis is that the dimers, with two drugs connected through the linker, should exhibit higher levels of double strand DNA cleavage than the monomers. As predicted, all ether-linked dimers induced higher levels of double-stranded DNA cleavage than the monomers in the presence of human topoisomerase IIα. These results lend credence to the two drug model. In addition, both the dimers and monomers were tested for cancer cell cytotoxicity. All dimers were more cytotoxic against cancer cells than the corresponding monomers. Finally, the dimers and monomers were tested for toxicity to normal cells, and displayed better selectivity for cancer cells vs. normal cells.

Overall, a series of novel dimers of 4'-demethylepipodophyllotoxin were synthesized, along with their corresponding monomers. The goal was to provide

evidence for the two-drug model for activity of topoisomerase II poisons. The DNA cleavage patterns support this model. Also, all compounds displayed promising cancer cytotoxicity, with selectivity for cancer vs. normal cells.

In the other investigation, bioassay guided fractionation was used to identify novel anti-trypanosomal activity of known iridals from *I. domestica*. Bioassay guided fractionation led to the isolation of two known iridals, iso-iridogermanal (myristate ester) and anhydrobelachinal. Due to instability of the unsaturated aldehydes, they were reduced to the corresponding allylic alcohols, which maintained activity. Knowing that the aldehyde was not required for activity, two other impure fractions of the plant extract were reduced directly, affording two novel reduced bioactive iridals. To our knowledge, direct chemical modification of impure plant extracts has not been previously reported. Saponification of the myristate ester of reduced isoiridogermanal still maintained activity. These modifications show that neither the aldehyde nor the myristate ester group are required for antitrypanosomal activity. Further investigation of the structure-activity relationships of the isoiridogermanal series included partial hydrogenation of the triene side chain. In this case, the terminal alkene seems to be required, with the partially saturated derivative losing all activity against *T. brucei*.

While the parent iridal aldehydes were all known compounds, this is the first report of the possible use of iridals and their semi-synthetic derivatives from Iris domestica extracts to treat trypanosomal diseases. Although iridals have previously been reported as having several types of bioactivity, there are no prior reports of antitrypanosomal activity of compounds in this family.

REFERENCES

1. Koehn, F. E.; Carter, G. T. Rediscovering natural products as a source of new drugs. *Discov Med.* **2005**, *5(26)*, 159-164.

2. World Health Organization. Global status report on noncommunicable diseases 2010. http://www.who.int/nmh/publications/ncd report fullen.pdf (accessed April 29, 2016).

3. National Cancer Institute at the National Institutes of Health. http://www.cancer.gov/about-cancer/treatment/drugs. (Accessed June 10, 2016).

4. Gerber, D. E. Targeted Therapies: A New Generation of Cancer Treatments, *AAFP*, **2008**, *77(3)*, 311-319.

5. Bhattacharyya, P. K.; Medhi, C. Theoretical study on the mechanism of alkylation at N-7 of guanine by few nitrogen mustards. *Indian Journal of Chemistry*, **2005**, *44B*, 1319-1323.

6. Koster, D. A.; Crut, A.; Shuman, S.; Bjornsti, M. A.; Dekker, N. H. Cellular strategies for regulating DNA supercoiling: a single-molecule perspective. *Cell*, **2010**, *142(4)*, 519-530.

7. Pommier, Y. Topoisomerase I inhibitors: camptothecins and beyond. *Nat Rev Cancer.* **2006**, *6(10)*, 789-802.

8. Dunlap, N.; Salyard, T. L. J.; Liyana Pathiranage , A.; Stubblefield, J.; Pitts, S. L.; Ashley, R. E.; Osheroff, N. Synthesis and evaluation of ether-linked dimethyl epi-podophyllotoxin dimers. *Bioorg. & Med. Chem. Lett.* **2014**, *24(24)*, 5627-5629.

9. Van Amerongen, R.; Berns, A. TXR1-mediated thrombospondin repression: a novel mechanism of resistance to taxanes? *Genes Dev.* **2006**, *20(15)*, 1975-1981.

10. Keglevich, P.; Hazai, L.; Kalaus, G.; Szántay, C. Modifications on the basic skeletons of vinblastine and vincristine. *Molecules*, **2012**, *17*, 5893-5914.

11. Walsh, V.; Goodman, J. Cancer chemotherapy, biodiversity, public and private property: the case of the anti-cancer drug taxol. *Soc Sci Med.* **1999,** *49(9),* 1215-1225.

12. Tian, X.; Liu, Y. Q.; Yang, L. Podophyllotoxin: current perspectives. *Curr. Bioact. Compd.* **2007**, *3*, 37-66.

13. Utsugi, T.; Shibata, J.; Sugimoto, Y.; Aoyage, K.; Wierzbe, K.; Kobunai, T.; Terada, T.; Oh-hoar, T.; Tsuruo, T.; Yamada, Y. Antitumor activity of a novel podophyllotoxin derivative (TOP-53) against lung cancer and lung metastatic cancer. *Cancer Res*. **1996**, *56*, 2809-2814.

14. Richard, C.; Mendis. K. N. Evolutionary and historical aspects of the burden of malaria. *Clin Microbiol Rev*. **2002**, *15(4)*, 564–594.

15. Guo, Z. Artemisinin anti-malarial drugs in China. *Acta Pharm Sin B.* **2016**, *6(2),* 115–124.

16. Delfino, R. T.; Santos-Filho, O. A.; José D.J.; Figueroa-Villar. Type 2 Antifolates in the chemotherapy of falciparum Malaria. J. *Braz. Chem. Soc.* **2002**, *13*, 727-741.

17. Laura Vargas-Parada, L. Kinetoplastids and their networks of interlocked DNA, *Nature Education*, **2010**, *3(9)*, 63.

18. Brennand, A.; Rico, E.; Michels, P. A. M. Autophagy in Trypanosomatids. *Cells*, **2012**, *1(3)*, 346-371.

19. Barrett, M. P.; Boykin, D. W.; Brun, R.; Tidwell, R. R. Human African trypanosomiasis: pharmacological re-engagement with a neglected disease. *Br J Pharmacol.* **2007,** *152(8)*, 1155-1171.

20. Croft, S. L.; Sundar, S.; Fairlamb, A. H. Drug resistance in leishmaniasis. *Clin Microbiol Rev.* **2006,** *19(1)*, 111-126.

21. Wink, M. Medicinal plants: A source of anti-parasitic secondary metabolites. *Molecules***,** **2012**, *17*, 12771-12791.

22. Hoet, S.; Opperdoes, F.; Brun , R.; Quetin-Leclercq, J. Natural products active against African trypanosomes: a step towards new drugs. *Nat.Prod. Rep.* **2004**, *21*, 353-364.

23. May, J. D.; Cassels. B, K,; Iturriaga-Vásquez, P.; Ferreir, J.; Faúndez, M.; Galanti, N.; Ferreira, A.; Morello, A. Mode of action of natural and synthetic drugs against Trypanosoma cruzi and their interaction with the mammalian host. *Com. Biochem Phys*, **2007**, *146*, 601–620.

24. MacRae, W. D.; Hudson, J. B.; Towers, B. H. N. The antiviral action of lignans. *Planta Med.* **1993**, *55*, 531-535.

25. Kuhn, M.; von Wartburg, A. [On a new glycoside synthesis process. II. Glycosides of 4'-demethylepipodophyllotoxins]. *Helv. Chim. Acta.* **1969**, *52*, 948-955.

26. Desbéne, S.; Giorgi-Renault, S. Drugs that inhibit tubulin polymerization: the particular case of podophyllotoxin and analogues. *Curr. Med. Chem. – Anti-Cancer Agents.* **2002**, *2*, 71-90.

27. Tian, X.; Liu, Y. Q.; Yang, L. Podophyllotoxin: Current Perspectives. *Curr. Bioact. Compd.* **2007**, *3*, 37-66.

28. Baikar, S.; Malpathak, N. Secondary metabolites as DNA topoisomerase inhibitors: A new era towards designing of anticancer drugs. *Pharmacogn. Rev*. **2010**, *4*, 12-26.

29. Gordaliza, M.; Castro, M. A.; del Corral, J. M.; Feliciano, A. S. Antitumor properties of podophyllotoxin and related compounds. *Curr. Pharm. Des*. **2000,** *6*, 1811-1839.

30. Islam, M. N.; Iskander, M. N. Microtubulin binding sites as target for developing anticancer agents. *Mini. Rev. Med. Chem.* **2004,** *4*, 1077-104.

31. Desbène, S.; Giorgi-Renault, S. Drugs that inhibit tubulin polymerization: the particular case of podophyllotoxin and analogues. *Curr. Med. Chem. Anticancer Agents.* **2002,** *2*, 71-90.

32. Lee, K. S.; Beer, A. S.; Wang, Z. Q.; Mori, M.; Kuo, Y. H.; Liu, S. Y.; Chang, J. Y.; Han, F. S.; Cheng, Y. C. Antitumor Agents. 111. New 4'-hydroxylated anailino derivatives of 4-demethyl *epi*-podophyllotoxin as potent inhibitors of human DNA topoisomerase II. *J. Med. Chem*. **1990**, *33*, 1364-1368.

33. Utsugi, T.; Shibata, J.; Sugimoto, Y.; Aoyage, K.; Wierzbe, K.; Kobunai, T.; Terada, T.; Oh-hoar, T.; Tsuruo, T.; Yamada, Y. Antitumor activity of a novel podophyllotoxin derivative (TOP-53) against lung cancer and lung metastatic cancer. *Cancer Res*. **1996**, *56*, 2809-2814.

34. Burden, D. A., Osheroff, N. Mechanism of action of eukaryotic topoisomerase II and drugs targeted to the enzyme. *Biochim. Biophys. Acta*, **1998**, *1400*, 139-154.

35. Koster, D. A., Crut, A.; Shuman, S.; Bjornsti, M. A, Dekker, N. H. Cellular strategies for regulating DNA supercoiling: A Single-Molecule Perspective *Cell*, **2010**, *142(4)*, 519-530.

36. Burden, D.A.; Kingma, P.S.; Froelich-Ammon, S. J.; Bjornsti, M. A.; Patchan, M. W.; Thompson, R. B.; Osheroff, N. Topoisomerase II. Etoposide interactions direct the formation of drug-induced enzyme-DNA cleavage complexes. *J Biol Chem*. **1996**, *271(46)*, 29238-29244.

37. Bromberg, K.D.; Burgin, A. B.; Osheroff, N. A two-drug model for etoposide action against human topoisomerase IIalpha. *J Biol Chem*. **2003**, *278(9)*, 7406-7412.

38. Kamal, A.; Laxman, E.; Khanna, G. B.; Reddy, P. S.; Rehana, T.; Arifuddin, M.; Neelima, K.; Kondapi, A. K.; Dastidar, S. G. Design, synthesis, biological evaluation and QSAR studies of novel bisepipodophyllotoxins as cytotoxic agents. *Bioorg Med Chem*. **2004**, *12(15)*, 4197-209.

39. Woźniak, D.; Matkowski, A. Belamcandae chinensis rhizome--a review of phytochemistry and bioactivity. *Fitoterapi*, **2015**, *107*, 1–14.

40. Le Zhang, L.; Wei. K.; Xu, J.; Yang, D.; Zhang, C.;Wang, Z.; Li, M. *Belamcanda chinensis (L.)* DC-An ethnopharmacological, phytochemical and pharmacological review. *J. Ethnopharmacol*, **2016**, *186*, 1–13.

41. Xin, R.; Zheng, J.; Cheng, L.; Peng, W.; Luo, Y. *Belamcanda chinensis (l.)* Dc: Ethnopharmacology, phytochemistryand pharmacology of an important traditional Chinese medicine. *AJOL*, **2015**, *12*.

42. Seki, K.; Haga, k.; Kaneko, R. Belamcandones A-D, dioxotetrahydrodibenzofurans from *Belamcanda chinensis. Phytochem*, **1995**, *38*, 703-709.

43. Krick, W.; Marner, F. J.; Jaenicke, L. Isolation and Structure Determination of the Precursors of α- and γ-irone and homologous compounds from *Iris pallida* and *Iris florentina*. *Z. Naturforsch*. **1983**, *38c*, 179- 184.

44. Jaenicke, L.; Marner, F. J. The Irones and Their Precursors, Fortchritte der Cheie organischer Naturstoffe/ Progress in the Chemistry of Organic Products. Springer-Verlag/ Wien **1986**.

45. Domingo, V.; Arteaga, J. F.; Quílez Del Moral, J. F.; Barrero, A. F. Unusually cyclized triterpenes: occurrence, biosynthesis and chemical synthesis. *Nat Prod Rep*. **2009,** *26(1)*, 115-134.

46. Ito, H.; Onoue, S.; Miyake, Y.; Yoshida, T. Iridal-type triterpenoids with ichthyotoxic activity from *belamcanda chinensis. J Nat Prod*. **1999**, *62(1)*, 89-93.

47. Takahashi, K.; Hano , Y.; Suganuma, M.; Okabe, S.; Nomura, T. 28-Deacetylbelamcandal, a tumor-promoting triterpenoid from *Iris tectorum. J. Nat. Prod.*, **1999**, *62 (2)*, 291–293.

48. Takahashi, K.; Suzuki, S.; Hano, Y.; Nomura, T. Protein kinase C activation by iridal type triterpenoids. *Biol Pharm Bull.* **2002,** *25(4)*, 432-436.

49. Zhang, C. L.; Wang, Y.; Liu, Y. F.; Ni, G.; Liang, D.; Luo, H.; Song, X. Y.; Zhang, W. Q.; Chen, R. Y.; Chen, N. H.; Yu, D. Q. Iridal-type triterpenoids with neuroprotective activities from Iris tectorum. *J Nat Prod.* **2014,** *77(2)*, 411-415.

50. Abe, F.; Chen, R.-F.; Yamauchi, T. Iridals from *Belamcanda chinensis* and *Iris japonica*. *Phytochemistry*, **1991**, *30*, 3379-3382.

51. Marner, F.-J.; Karimi-Nejad, Y.; Jaenicke, L. 47. Structure determinaion of a new spirobicyclictriterpenoid from *Iris foetidissima*. *Helv. Chim. Acta*. **1990**, *73*, 4.

APPENDICES

APPENDIX A

NMR spectra of new compounds

Figure 1: ^{1}H-NMR compound 18

Figure 2: ^{13}C-NMR compound 18

Figure 3: HMBC correlations compound 18

Figure 4: ^{1}H-NMR compound 19

Figure 5: ^{13}C-NMR compound 19

Figure 6: HMBC correlations compound 19

Figure 7: ^{1}H-NMR compound 20

Figure 8: ^{13}C-NMR compound 20

Figure 9: HMBC correlations compound 20

Figure 10: ^{1}H-NMR compound 21

Figure 11: ^{13}C-NMR compound 21

Figure 12: HMQC correlations compound 21

Figure 13: HMBC correlations compound 21

Figure 14: ^{1}H-NMR compound 22

Figure 15: ^{13}C-NMR compound 22

Figure 16: ^{1}H-NMR compound 23

Figure 17: ^{13}C-NMR compound 23

Figure 1: Compound **16**

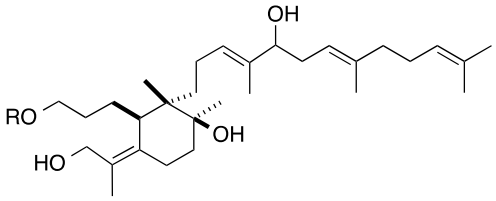

4: R = myristoyl

^{1}H-NMR (500MHz, CDCl3)

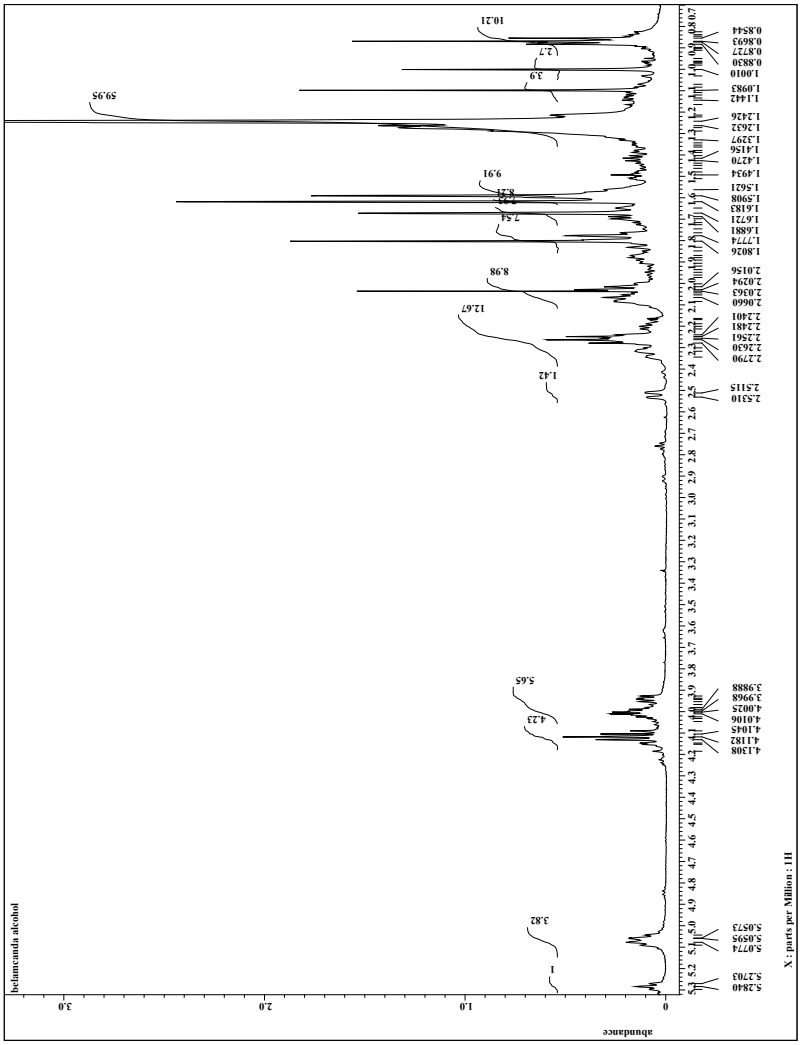

Figure 2: Compound **16**

^{13}C NMR (125MHz, CDCl3)

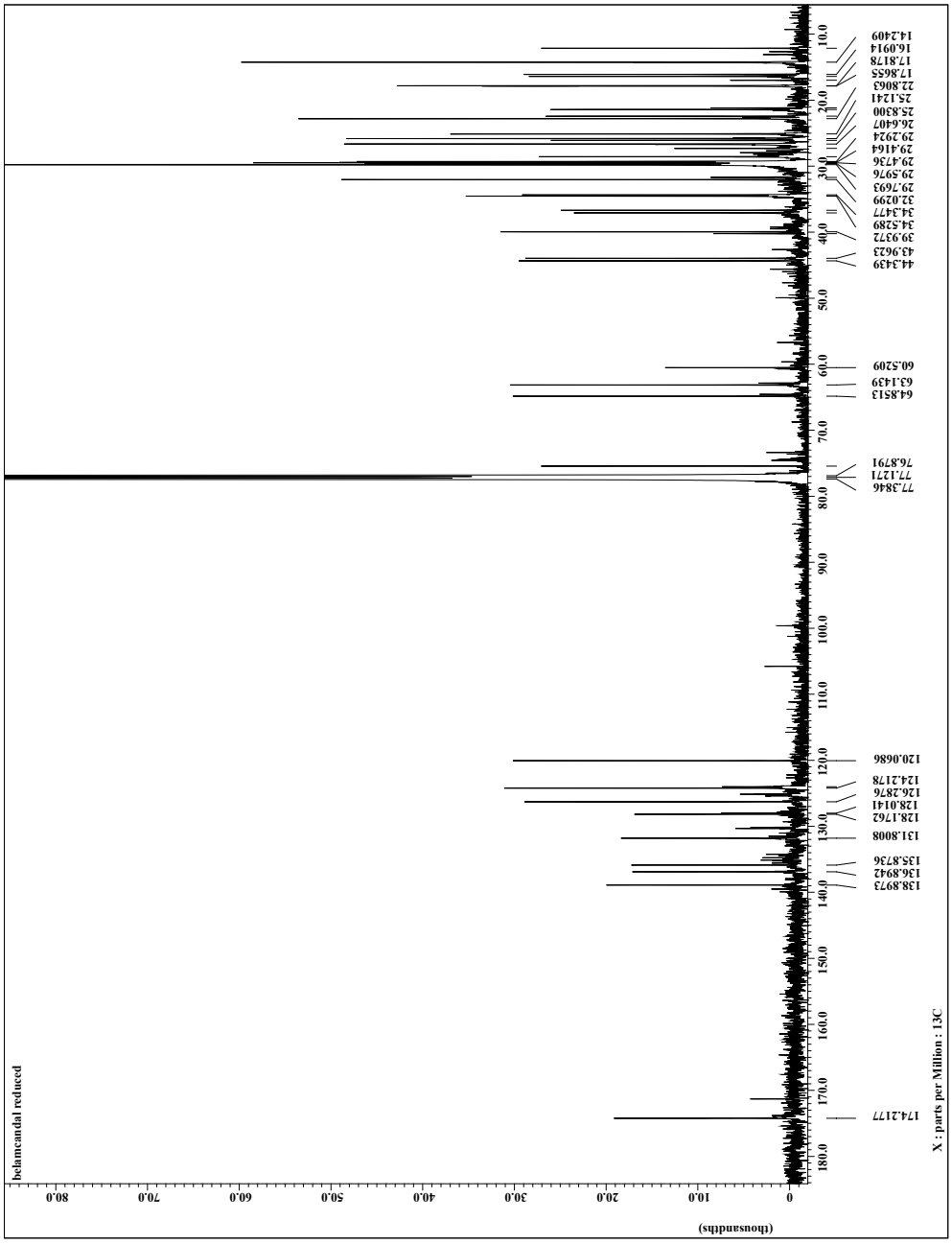

Figure 3: Compound **16**

HMBC correlations

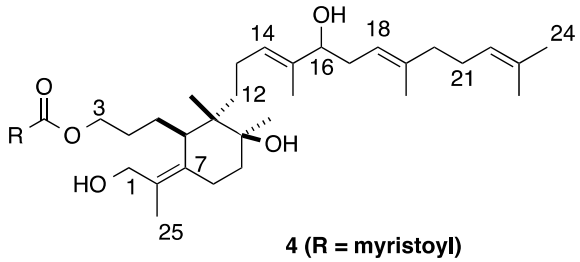

4 (R = myristoyl)

HMBC:
H1–> C25, C2, C7
H3–> ester C=O
H14--> C12
H16 --> C18, C14
H18 --> C16, C21
H22 --> C24

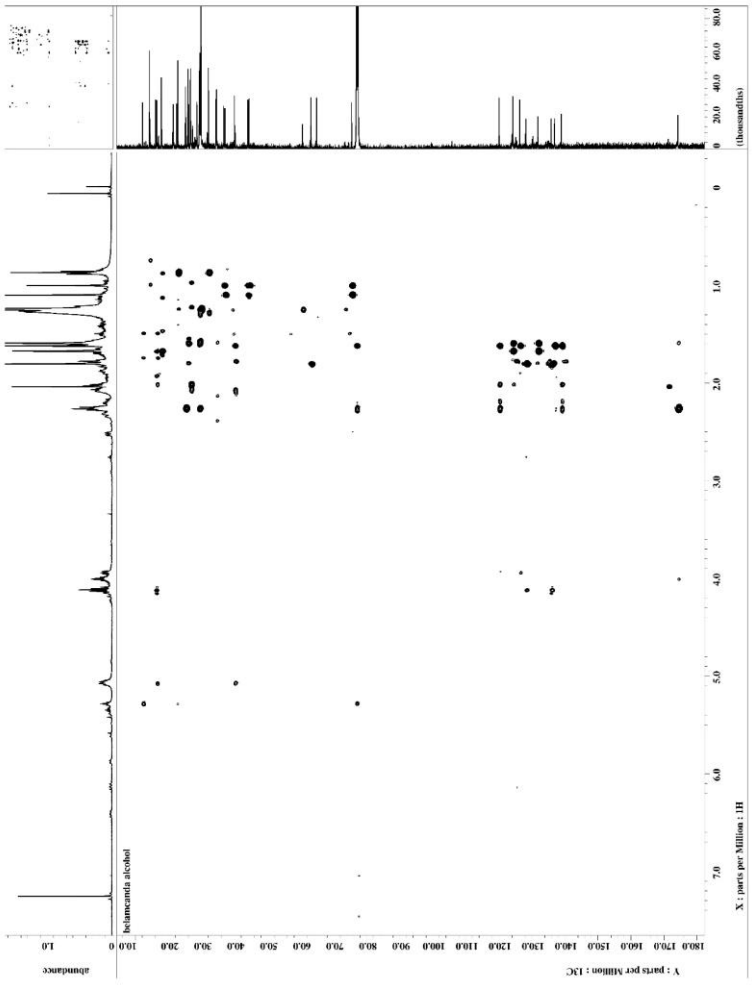

Figure 4 : Compound **19**

1H-NMR (500MHz, CDCl3)

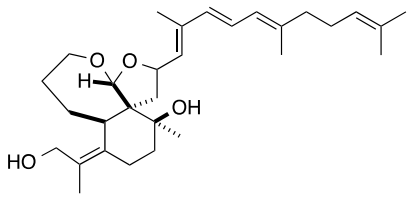

5

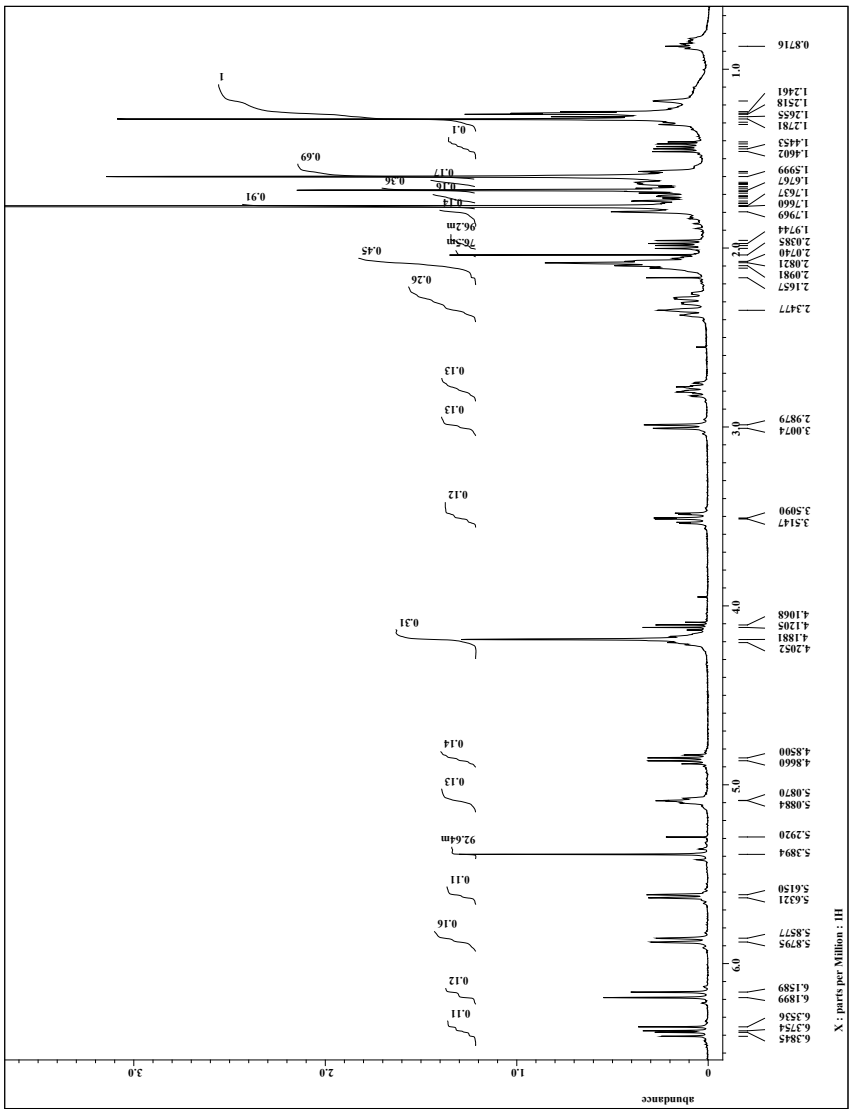

Figure 5: Compound **19**

13C-NMR (125MHz, CDCl3)

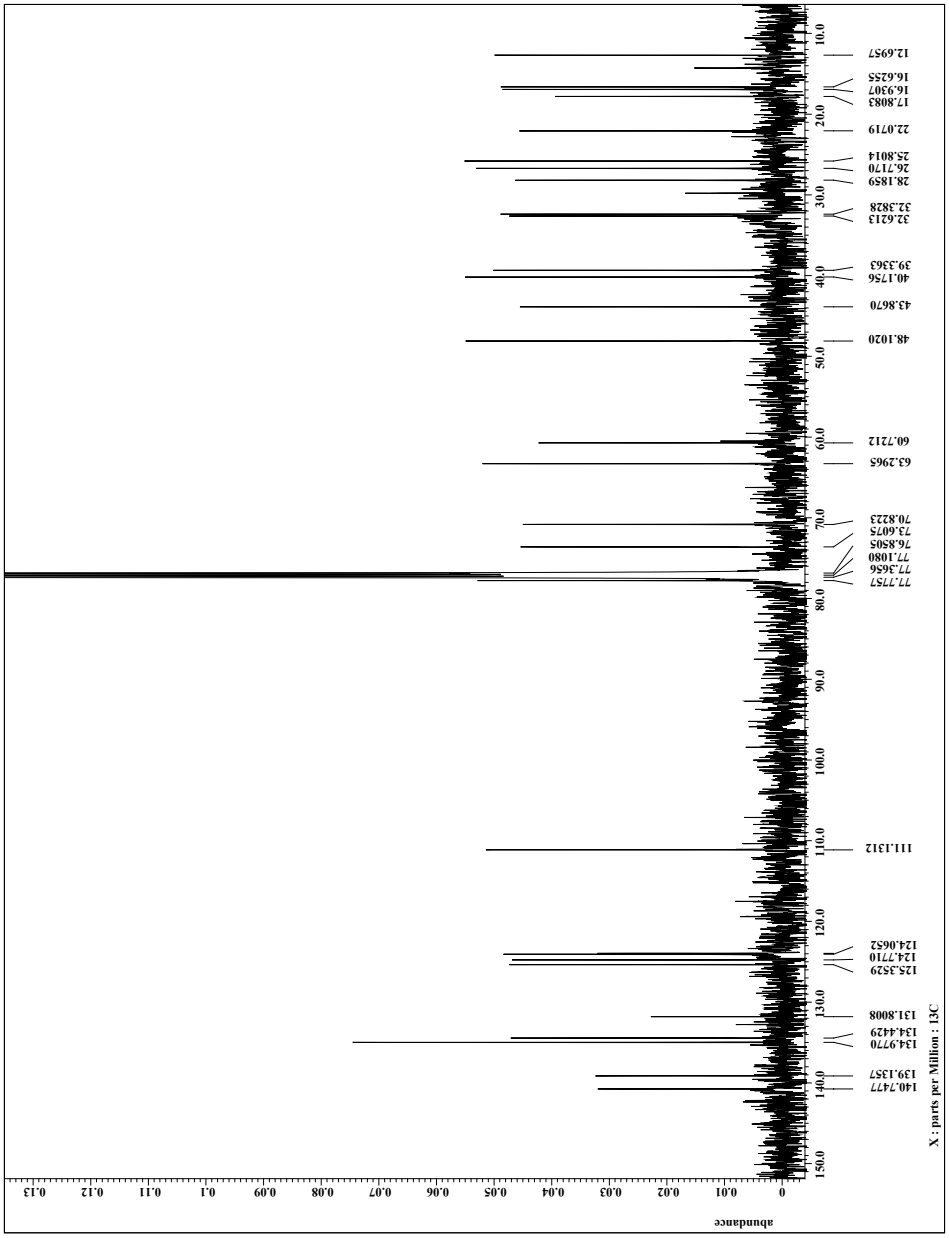

Figure 6: Compound 19

HMBC correlations

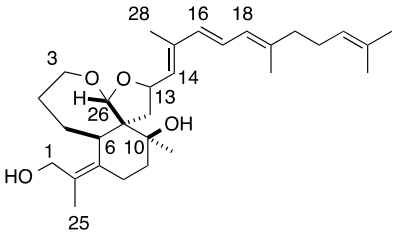

HMBC:
H1–> C25
H3–> C26
H26--> C12, C6, C13, C10, C3
H16 –> C28, C18, C14
H14 –> C16, C28

5

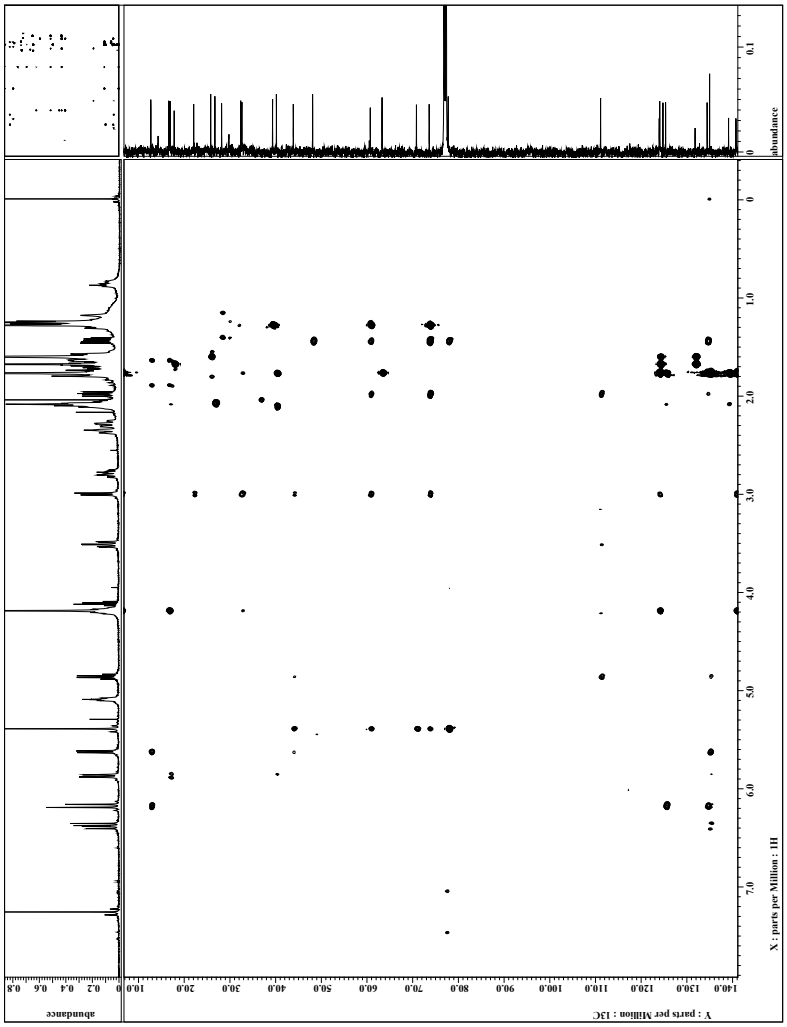

Figure 7: Compound **20**

^{1}H-NMR (500MHz, CDCl3)

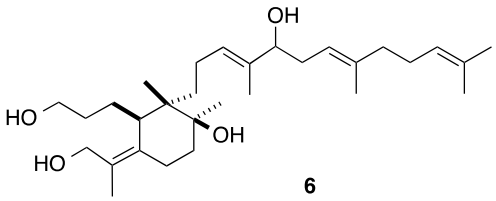

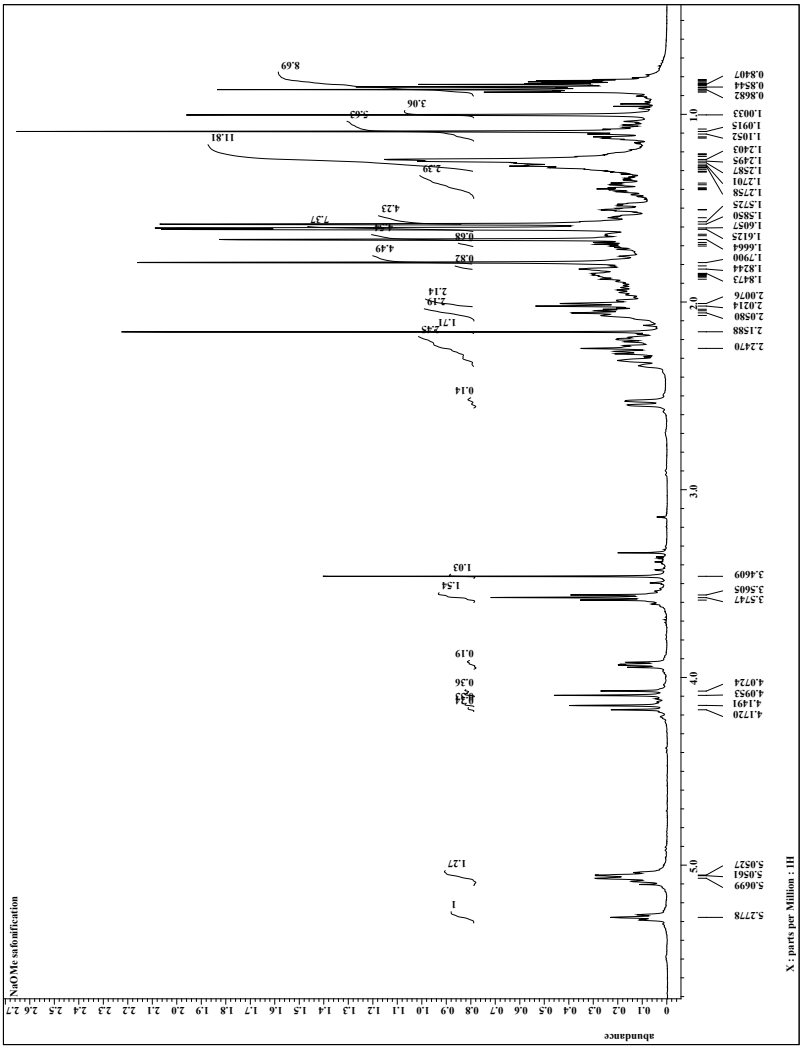

Figure 8: Compound **20**

^{13}C NMR (125MHz, CDCl3)

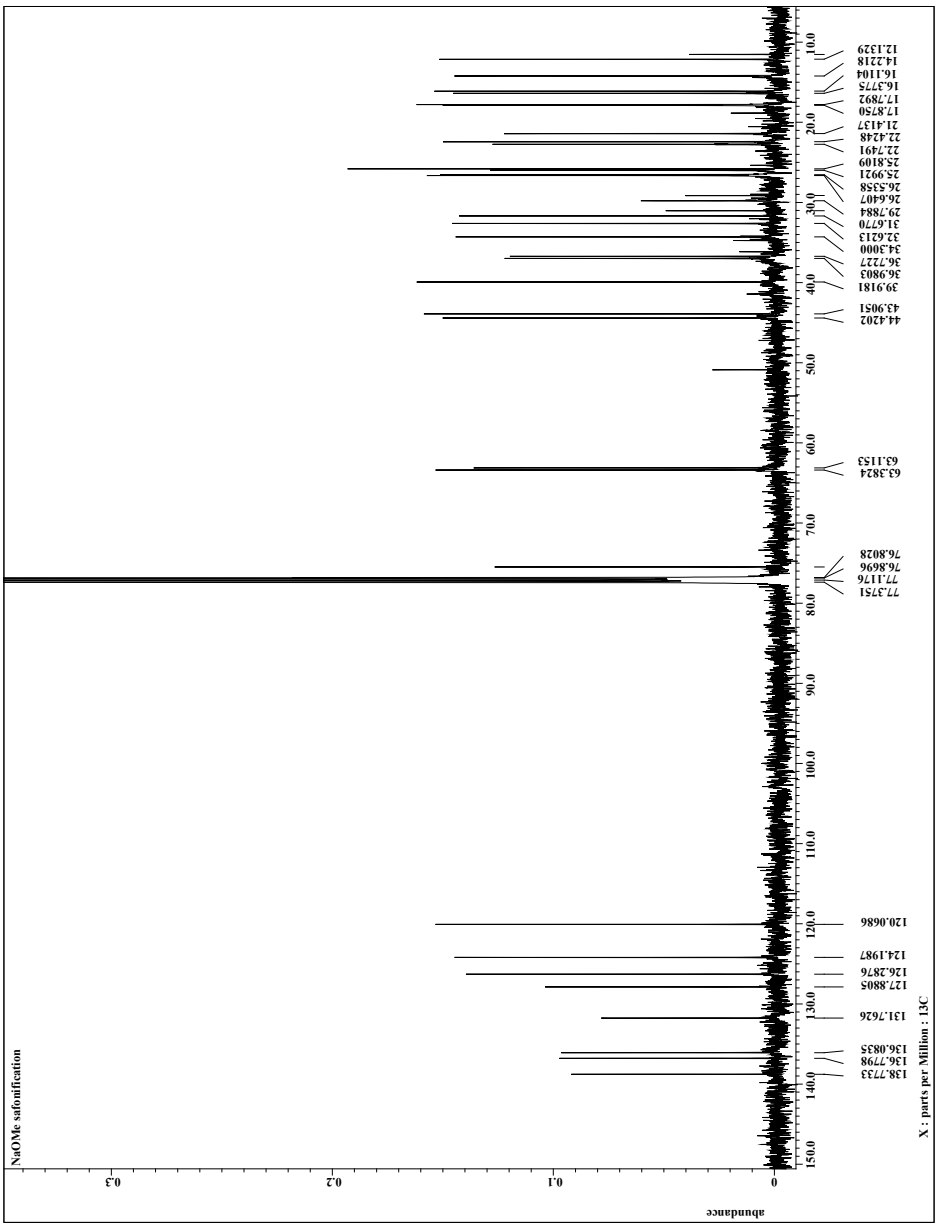

Figure 9: Compound **20**

HMBC

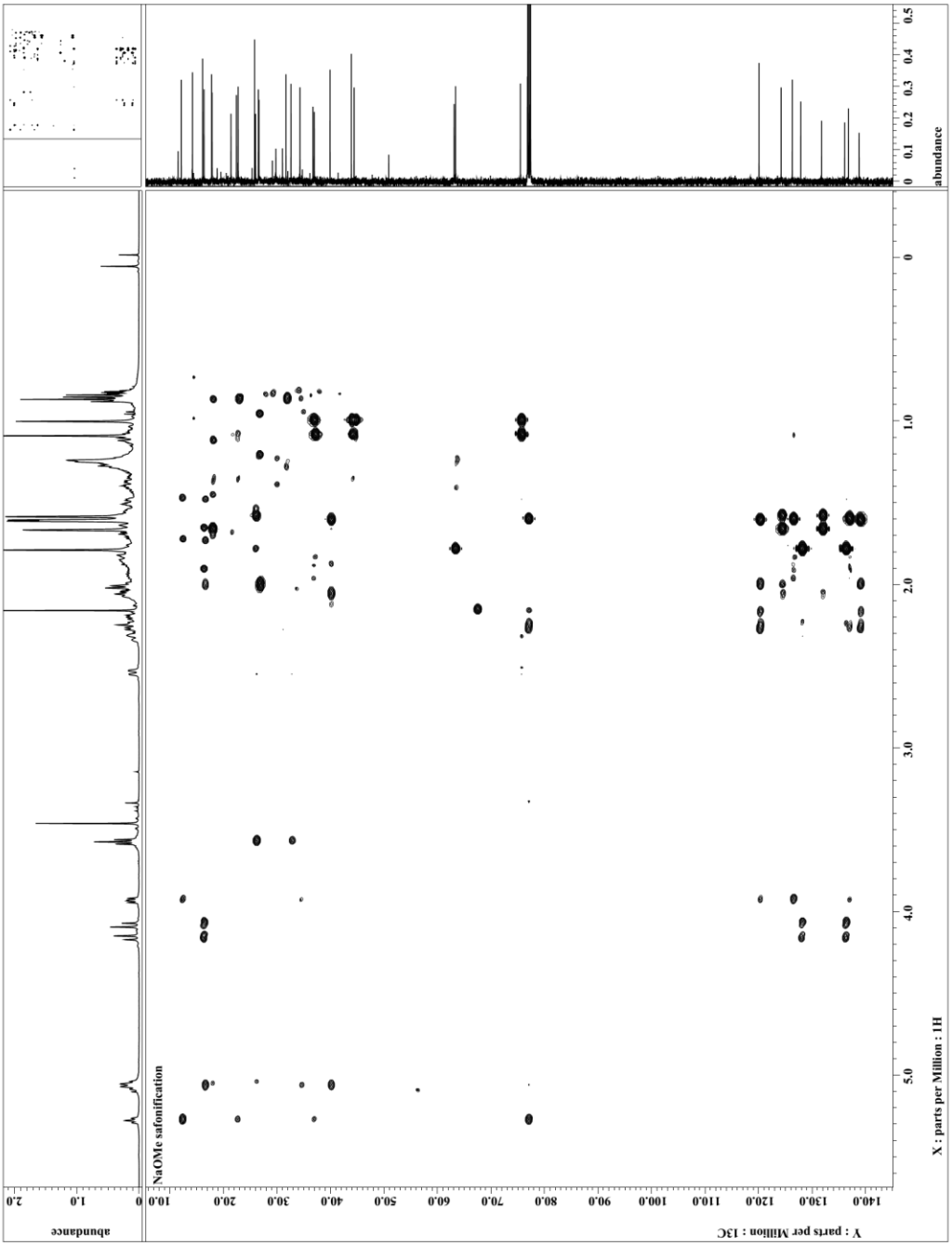

Figure 10: Compound **21**

^{1}H-NMR (500MHz, CDCl3)

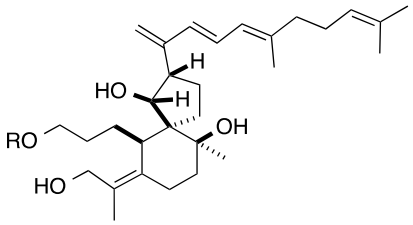

7: R = myristoyl

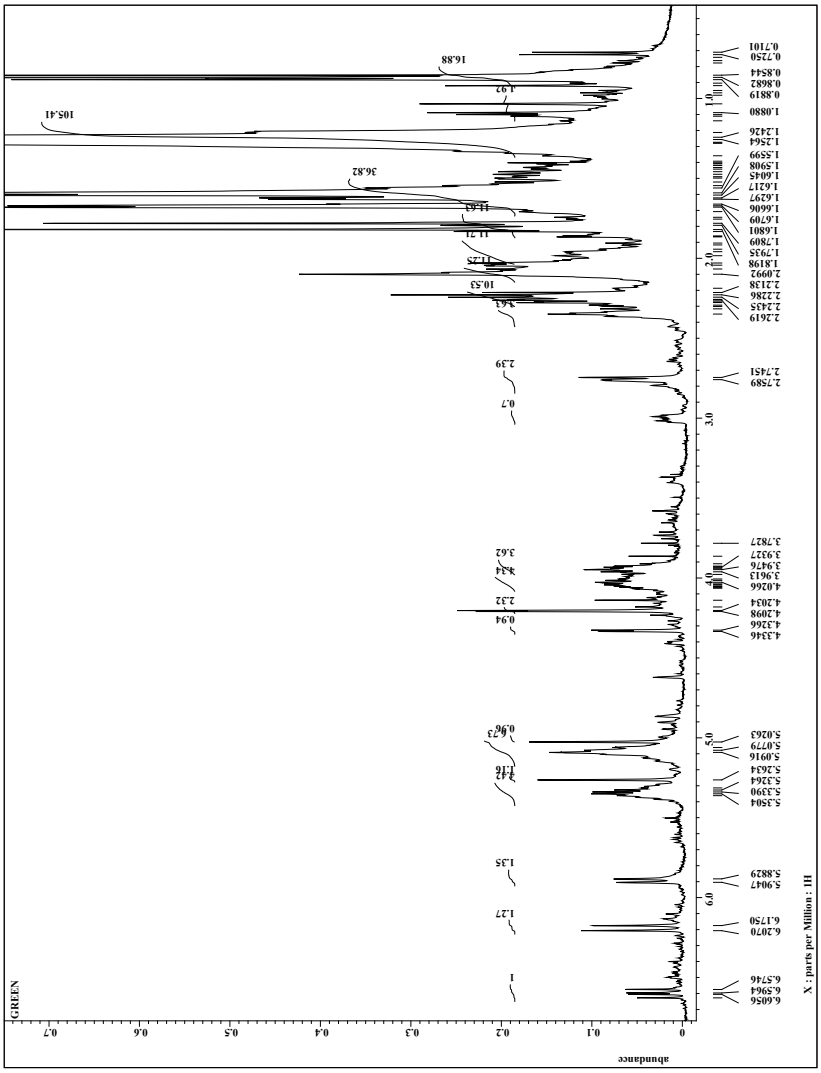

Figure 11: Compound **21**

^{13}H-NMR (125MHz, CDCl3)

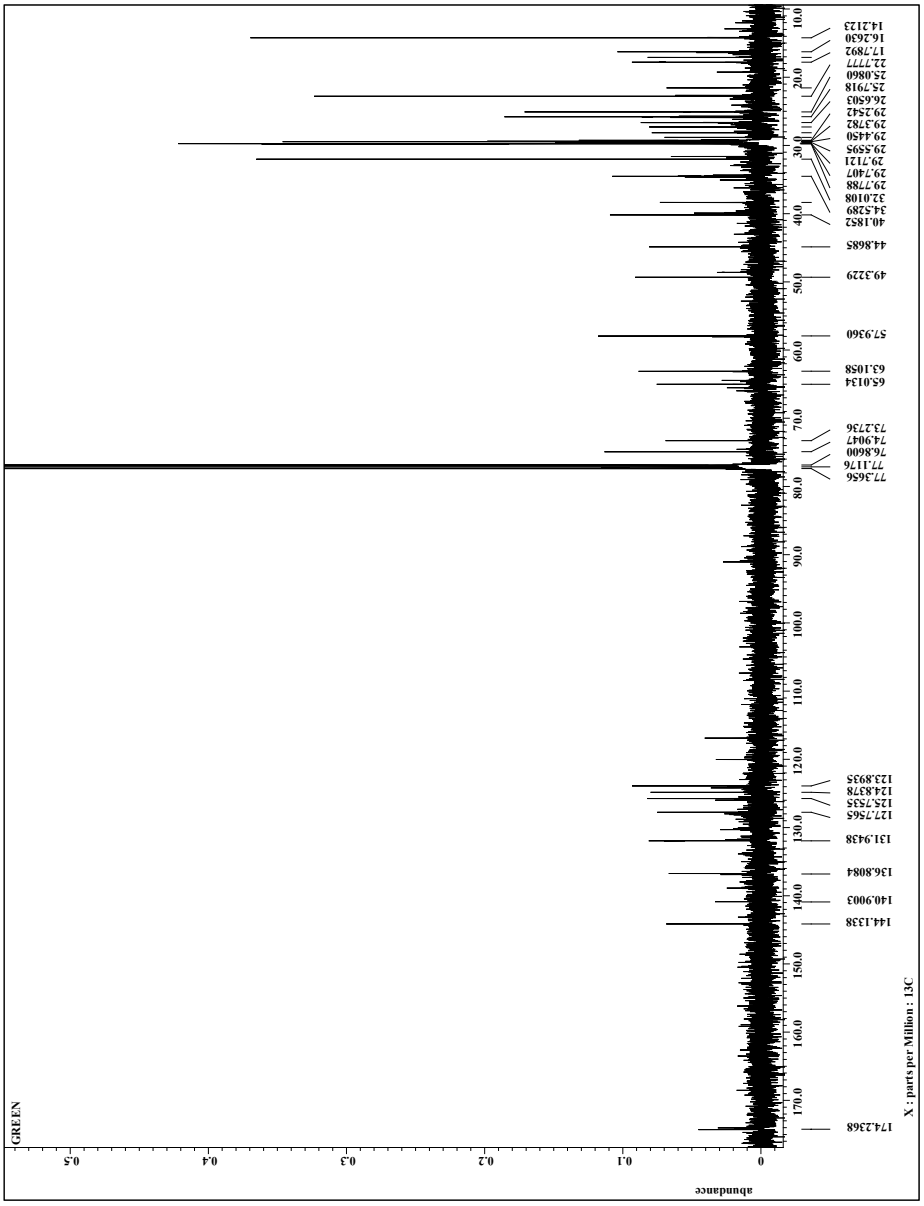

Figure 12: Compound **21**

HMQC

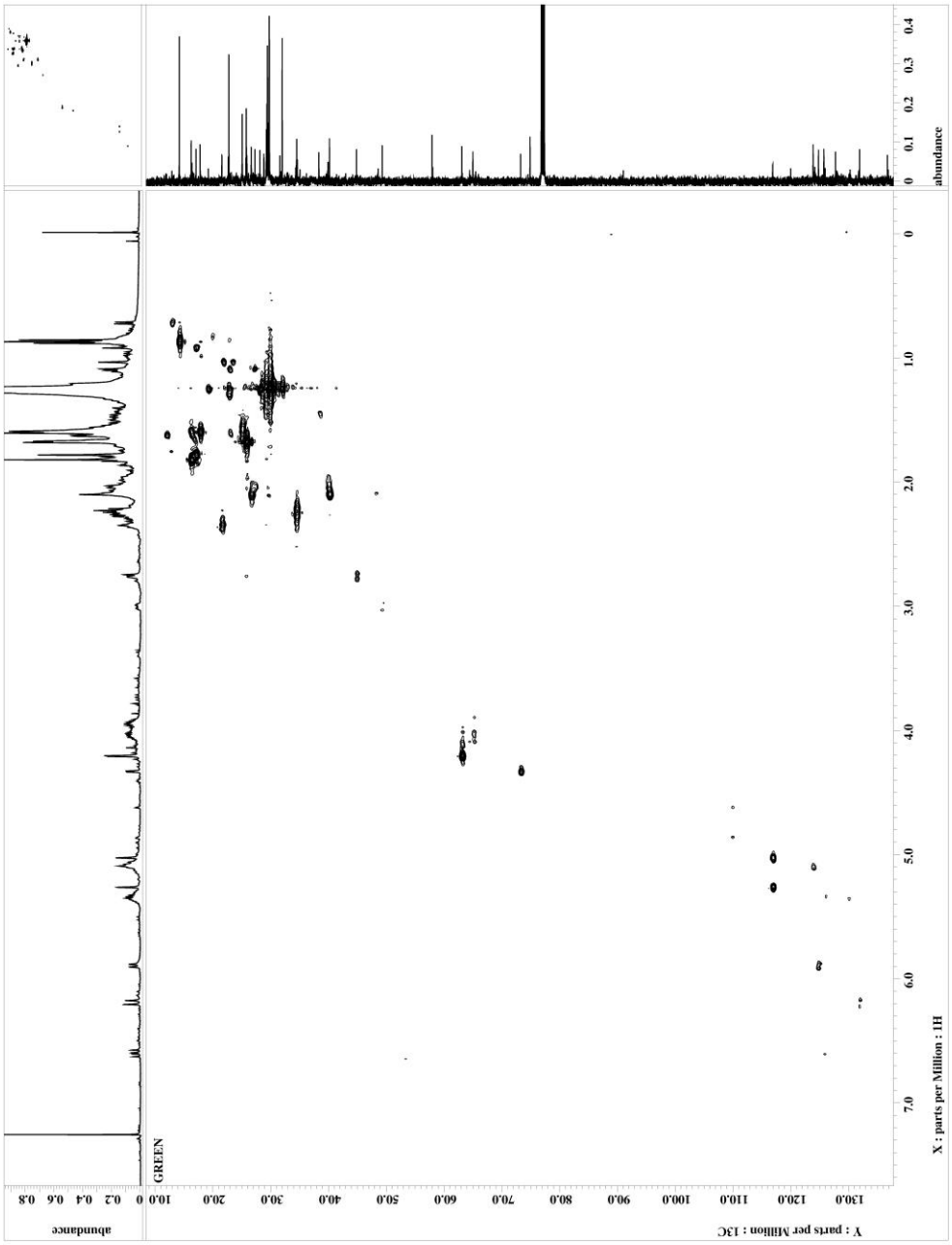

Figure 13: Compound **21**

HMBC

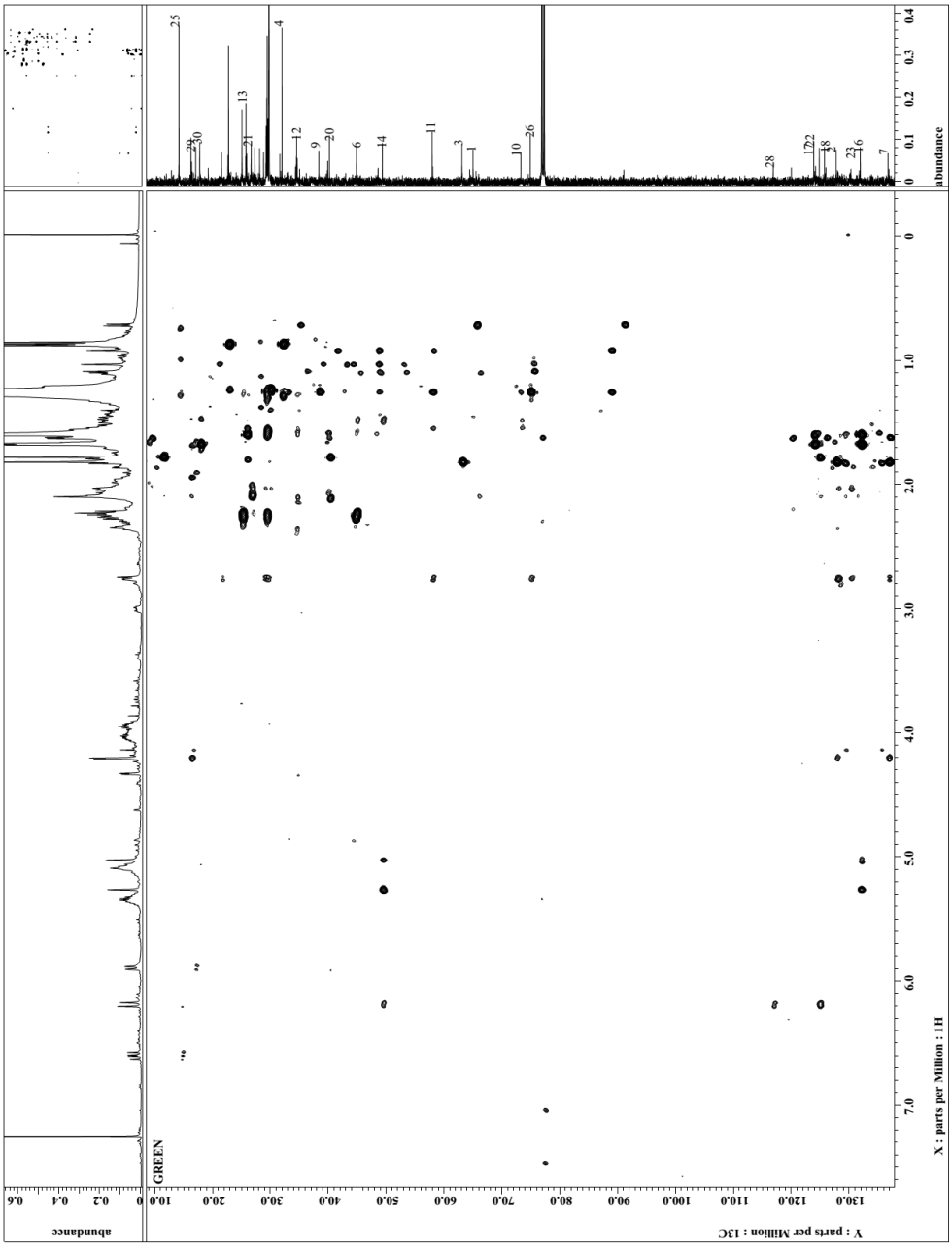

Figure 14: Compound **22**

^{1}H-NMR (500MHz, CDCl3)

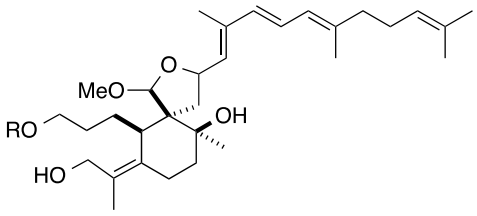

8: R = myristoyl

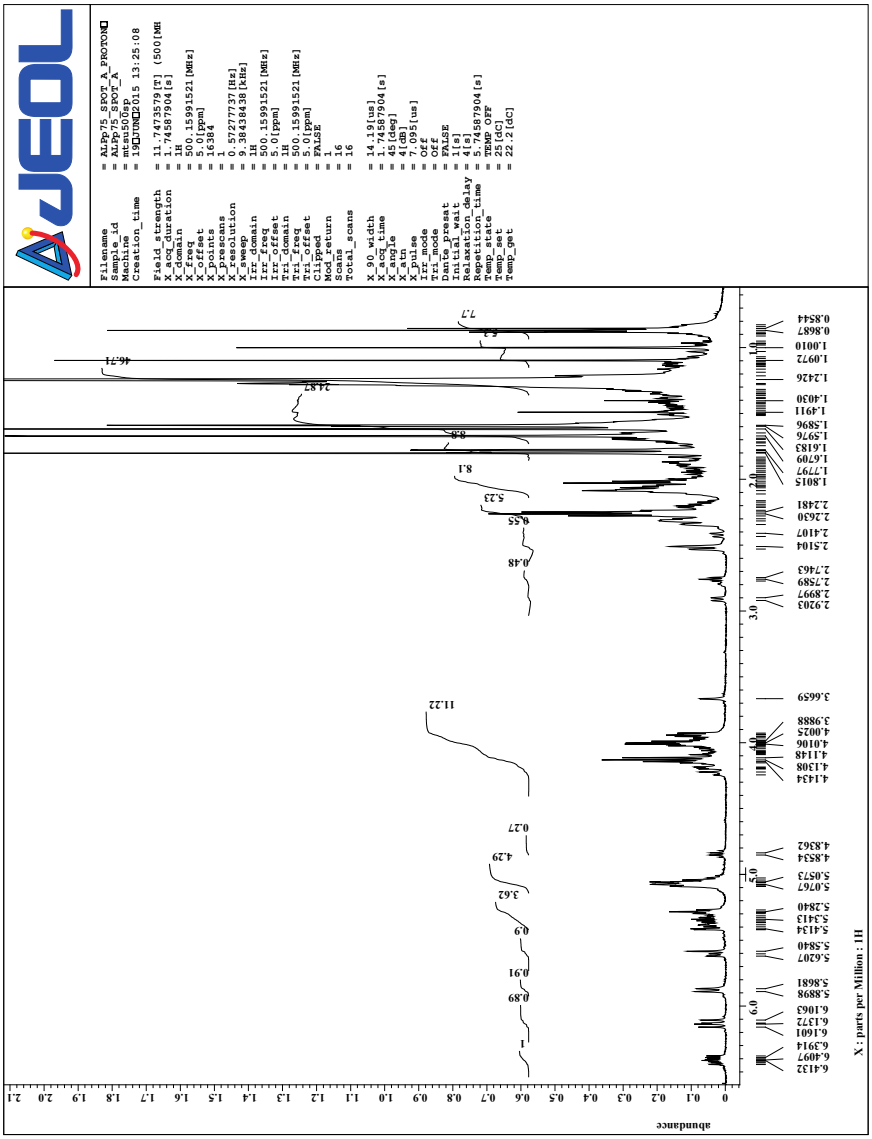

Figure 15: Compound **22**

^{13}C-NMR (125 MHz, CDCl3)

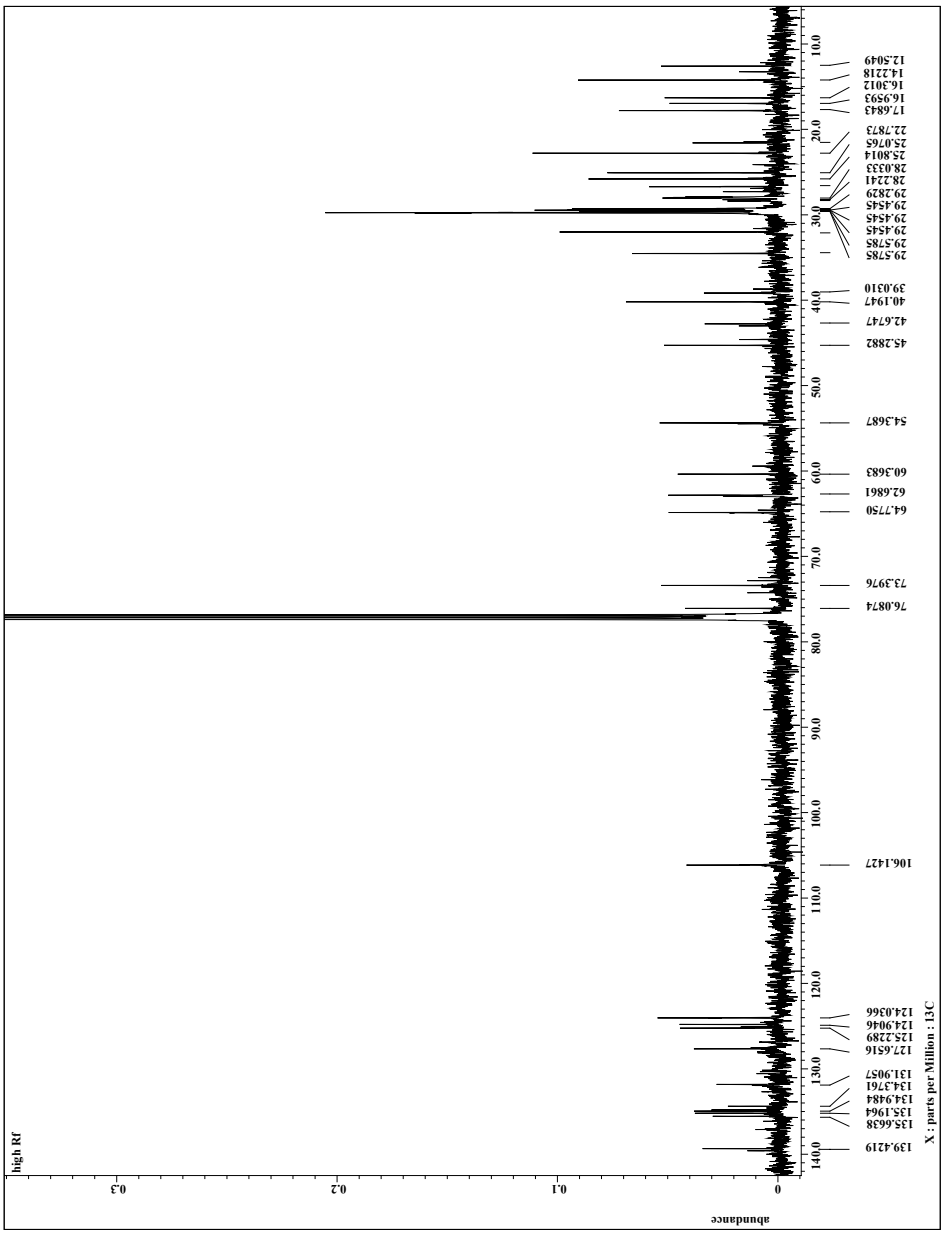

Figure 16: Compound **23**

^{1}H-NMR (500MHz, CDCl3)

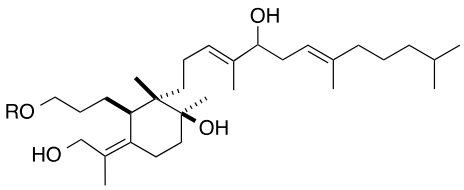

9: R = myristoyl

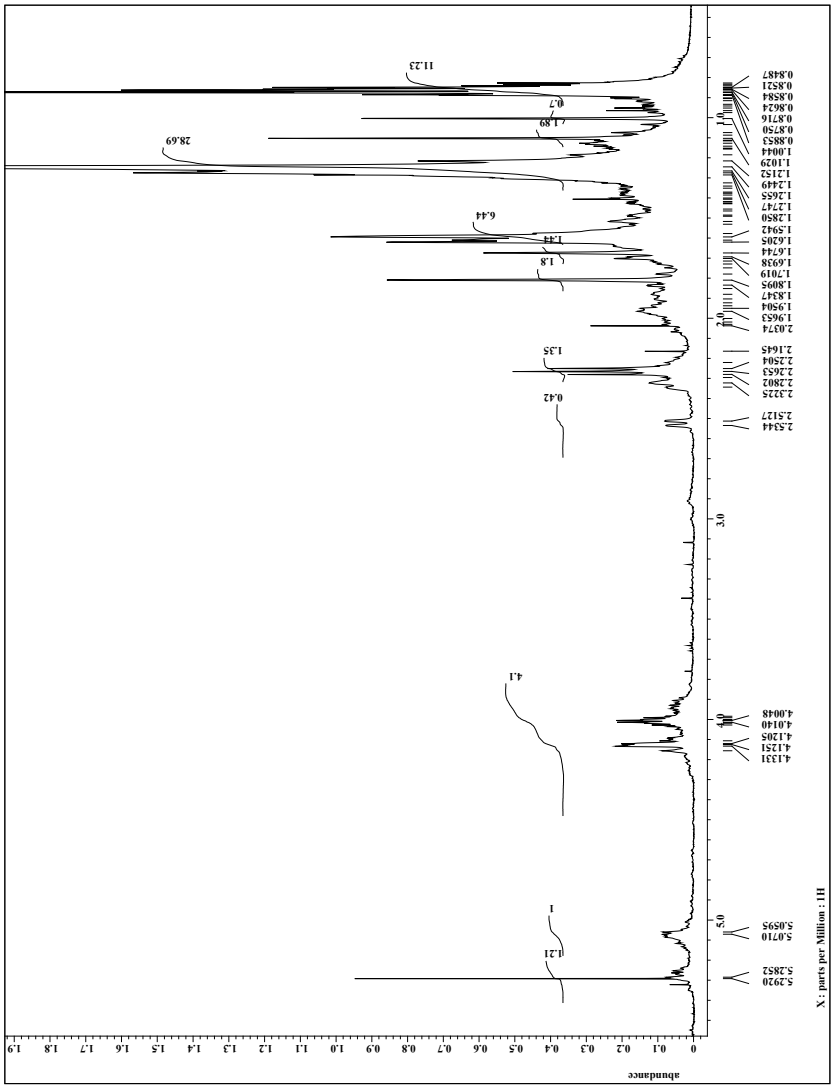

Figure 17: Compound **23**

^{13}C-NMR (500 MHz, CDCl3)

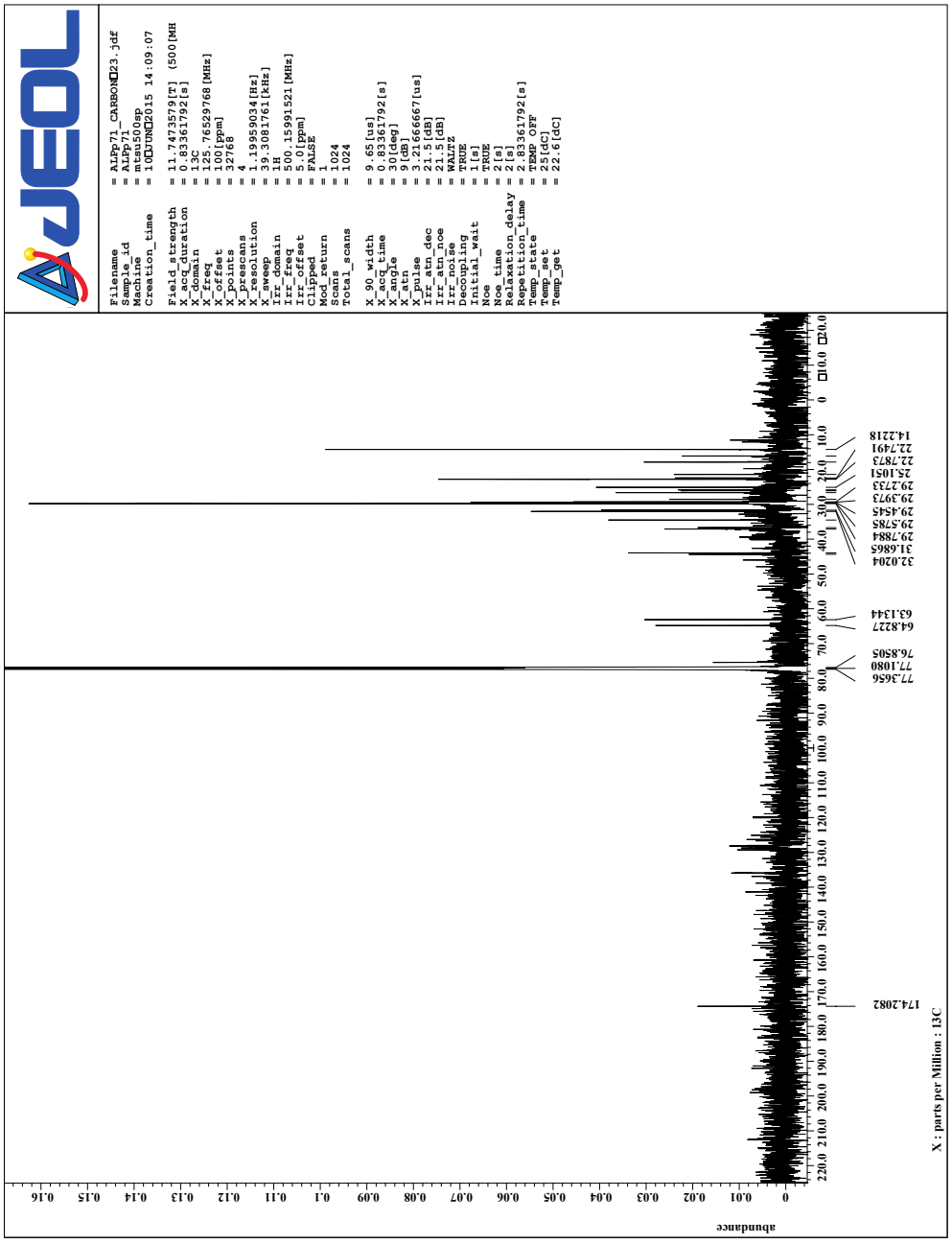

APPENDIX B

Permission request approvals

Permission Request

Date: Friday, April 29, 2016

ILLUSTRATION OR SELECTION DESIRED

AUTHOR Gerber
DESCRIPTION Figure 1

JOURNAL OR BOOK TITLE *American Family Physician 2004*

IF JOURNAL, ARTICLE TITLE A New Generation of Cancer Treatments.

VOL., PAGE & FIG. NO 2008;77(3):311-319

PUBLISHER & YEAR OF COPYRIGHT Renee Cannon 2007

RE: A New Generation of Cancer Treatments. Am Fam Physician 2008; 77(3):311-319.

To Whom It May Concern: Renee L. Cannon

Anuradha Liyana Pathiranage: Requests your permission for a one time U.S. right to reproduce the above mentioned illustration to be printed in her dissertation for submission to the PhD board of Middle Tennessee State University. This permission allows Ms. Pathiranage to reproduce this image specifically for this publication only.

Ms. Cannon retains full copyrights to all subsequent and additional publications including: further editions of this publication, all foreign publications in any language, and any other publication. Further publication rights must be requested in writing, and approved by Ms.Cannon.

Furthermore, Ms. Cannon reserves all rights to all modifications and derivative work.
If permission is granted, please sign this form in the space provided below.

Ms. Pathiranage, will give full acknowledgment to the source.
Please sign below to indicate your consent to this request.

Sincerely,

Anuradha Liyana Pathiranage.
Middle Tennessee State University
Molecular Biosciences Program
Dept. of Chemistry
Email: al2u@mtmail.mtsu.edu

I (WE) HAVE THE RIGHT TO GRANT PERMISSION FOR THE USE OF THE MATERIAL DESCRIBED ABOVE AND HEREBY GRANT SUCH PERMISSION. THE RE-USE FEE (IS WAIVED) FOR THIS ONE TIME U.S PUBLICATION.

Name: Renee Cannon Date: April 29, 2016

ELSEVIER LICENSE
TERMS AND CONDITIONS

May 19, 2016

This is a License Agreement between Anuradha Liyana Pathiranage ("You") and Elsevier ("Elsevier") provided by Copyright Clearance Center ("CCC"). The license consists of your order details, the terms and conditions provided by Elsevier, and the payment terms and conditions.

All payments must be made in full to CCC. For payment instructions, please see information listed at the bottom of this form.

Supplier	Elsevier Limited The Boulevard,Langford Lane Kidlington,Oxford,OX5 1GB,UK
Registered Company Number	1982084
Customer name	Anuradha Liyana Pathiranage
Customer address	Department of Chemistry, P.O. Box 68 , MURFREESBORO, TN 37130
License number	3858381224760
License date	Apr 29, 2016
Licensed content publisher	Elsevier
Licensed content publication	Cell
Licensed content title	Cellular Strategies for Regulating DNA Supercoiling: A Single-Molecule Perspective
Licensed content author	Daniel A. Koster,Aurélien Crut,Stewart Shuman,Mary-Ann Bjornsti,Nynke H. Dekker
Licensed content date	20 August 2010
Licensed content volume number	142
Licensed content issue number	4
Number of pages	12
Start Page	519
End Page	530
Type of Use	reuse in a thesis/dissertation
Portion	figures/tables/illustrations
Number of figures/tables/illustrations	1
Format	both print and electronic

Are you the author of this Elsevier article?	No
Will you be translating?	No
Original figure numbers	Figure 4 Types of topoisomerases
Title of your thesis/dissertation	Introduction to medicinal plants as a drug source
Expected completion date	May 2016
Estimated size (number of pages)	50
Elsevier VAT number	GB 494 6272 12
Permissions price	0.00 USD
VAT/Local Sales Tax	0.00 USD / 0.00 GBP
Total	0.00 USD
Terms and Conditions	

Genes & Development

From: Anuradha Liyana Pathiranage <al2u@mtmail.mtsu.edu>
Sent: Friday, April 29, 2016 1:23 PM
To: Genes & Development
Subject: Permission

Dear publisher,

I am a graduate student at Middle Tennessee state university. I am in the process of preparing my dissertation and am seeking permission to include the following figure in my dissertation. This figure is really important and very valuable for me to include in the introduction chapter. in my dissertation.

(1) The author's full name(s)- Renée van Amerongen and Anton Berns

(2) The title, edition and volume- TXR1-mediated thrombospondin repression: a novel mechanism of resistance to taxanes?

Genes Dev. 2006 20: 1975-1981

(3) The exact image I wish to use for my introduction- Figure 1. Microtubules are instrumental in maintaining cell viability

I would be very grateful for your permission. If you require any additional information, please do not hesitate to contact me.
Thank you.
Sincerely,

Anuradha LiyanaPathiranage.
Middle Tennessee State University
Molecular Biosciences Program
Email: al2u@mtmail.mtsu.edu

Permission granted by the copyright owner, contingent upon the consent of the original author, provided complete credit is given to the original source and copyright date.

By Lauren Connell, Ph.D. 5/20/16
Date

COLD SPRING HARBOR LABORATORY PRESS

11200 Rockville Pike
Suite 302
Rockville, Maryland 20852

August 19, 2011

American Society for Biochemistry and Molecular Biology

To whom it may concern,

It is the policy of the American Society for Biochemistry and Molecular Biology to allow reuse of any material published in its journals (the Journal of Biological Chemistry, Molecular & Cellular Proteomics and the Journal of Lipid Research) in a thesis or dissertation at no cost and with no explicit permission needed. Please see our copyright permissions page on the journal site for more information.

Best wishes,

Sarah Crespi

American Society for Biochemistry and Molecular Biology
11200 Rockville Pike, Rockville, MD
Suite 302
240-283-6616
JBC | MCP | JLR

11200 Rockville Pike
Suite 302
Rockville, Maryland 20852

August 19, 2011

American Society for Biochemistry and Molecular Biology

To whom it may concern,

It is the policy of the American Society for Biochemistry and Molecular Biology to allow reuse of any material published in its journals (the Journal of Biological Chemistry, Molecular & Cellular Proteomics and the Journal of Lipid Research) in a thesis or dissertation at no cost and with no explicit permission needed. Please see our copyright permissions page on the journal site for more information.

Best wishes,

Sarah Crespi

American Society for Biochemistry and Molecular Biology
11200 Rockville Pike, Rockville, MD
Suite 302
240-283-6616
JBC | MCP | JLR